April 2005 • NREL/TP-550-34830

Technical Report

# Analysis of the Energy Performance of the Chesapeake Bay Foundation's Philip Merrill Environmental Center

B. Griffith, M. Deru, P. Torcellini, and P. Ellis

**National Renewable Energy Laboratory**
**1617 Cole Boulevard, Golden, Colorado 80401-3393**
**303-275-3000 • www.nrel.gov**

Operated for the U.S. Department of Energy
Office of Energy Efficiency and Renewable Energy
by Midwest Research Institute • Battelle

Contract No. DE-AC36-99-GO10337

April 2005 • NREL/TP-550-34830

# Analysis of the Energy Performance of the Chesapeake Bay Foundation's Philip Merrill Environmental Center

B. Griffith, M. Deru, P. Torcellini, and P. Ellis

Prepared under Task No. BEC3.4001

**National Renewable Energy Laboratory**
**1617 Cole Boulevard, Golden, Colorado 80401-3393**
**303-275-3000 • www.nrel.gov**

Operated for the U.S. Department of Energy
Office of Energy Efficiency and Renewable Energy
by Midwest Research Institute • Battelle

Contract No. DE-AC36-99-GO10337

**NOTICE**



Available electronically at http://www.osti.gov/bridge

Available for a processing fee to U.S. Department of Energy and its contractors, in paper, from:

U.S. Department of Energy
Office of Scientific and Technical Information
P.O. Box 62
Oak Ridge, TN 37831-0062
phone: 865.576.8401
fax: 865.576.5728
email: mailto:reports@adonis.osti.gov

Available for sale to the public, in paper, from:

U.S. Department of Commerce
National Technical Information Service
5285 Port Royal Road
Springfield, VA 22161
phone: 800.553.6847
fax: 703.605.6900
email: orders@ntis.fedworld.gov
online ordering: http://www.ntis.gov/ordering.htm

Printed on paper containing at least 50% wastepaper, including 20% postconsumer waste

## Acknowledgments

This work was made possible by the U.S. Department of Energy's Office of Energy Efficiency and Renewable Energy through its High Performance Building's initiative (HPBi). We appreciate the support and guidance of Dru Crawley, program manager, HPBi. The authors would also like to thank Roger Perry, building operations manager at the Philip Merrill Environmental Center, for his gracious assistance to researchers. In addition, the authors want to recognize the contributions by NREL researchers Nicholas Long (he processed and managed the data from the monitoring systems) and Kris Lasnik (he helped with revisions for the final version). Finally, we would like to thank the following people for their careful review and thoughtful comments: Dr. Michael McCabe of Navigant Consulting and Ed Hancock of Mountain Energy Partnership. Ed Hancock also designed and implemented the data acquisition system.

# Contents

## Figures

## Tables

# Executive Summary

## Introduction

The Chesapeake Bay Foundation (CBF) is dedicated to restoring and protecting the resources of the Chesapeake Bay, North America's largest estuary and a seriously threatened ecosystem. In 2000, CBF built the 31,000-ft$^2$ (2,880-m$^2$) Philip Merrill Environmental Center on a 31-acre (12.5-ha) site in Annapolis, Maryland, to serve as foundation headquarters. CBF incorporated numerous high-performance energy-saving features (including a ground-source heat pump system to heat the building in winter and help cool it in summer) into the building to minimize its environmental effects on the bay. Large, south-facing windows provide additional passive solar heating and reduce lighting loads by allowing more use of natural light (daylighting). Building daylighting is monitored by sensors that automatically dim some lights when daylighting is sufficient to displace electric lighting. Manually and motor-operated windows attempt to use the Chesapeake Bay's breezes for natural ventilation. An energy management system tracks the outdoor temperature and humidity and uses this information to control the building's heating, ventilation, and air-conditioning system. The National Renewable Energy Laboratory (NREL) selected the Merrill Center as a technical case study after being contacted by CBF to provide an unbiased energy performance evaluation. Because the center has attracted much attention in the sustainable design community, an unbiased evaluation was necessary to help designers replicate successes and identify and correct problem areas. This report focuses on the monitoring and analysis of the building's overall energy performance.

## Research Goals and Approach

This report is part of a series of six case studies to develop, document, analyze, and evaluate the processes by which highly energy-efficient buildings can be reliably produced. NREL established the Merrill Center evaluation with the following goals:

- Study the overall energy performance of a Leadership in Energy and Environmental Design™ Platinum certified building.
- Analyze the integration of energy-efficient features, such as natural ventilation, daylighting, ground-source heat pumps, and a photovoltaic (PV) system, into an office building.
- Apply the International Energy Agency/Solar Heating and Cooling (IEA/SHC) Task 21 Daylighting monitoring protocol.
- Determine how the building performance matches the design expectations.

NREL collected energy data via monitoring meters and computer simulation to assess the energy performance of the building. Electronic data acquisition systems were designed to measure the important electrical and thermal flows and local weather conditions. Measurements were collected continuously beginning in August 2001; analysis focused on the period from November 7, 2001 through November 6, 2002. In addition, NREL used computer modeling to develop a benchmark for energy savings. Baseline energy modeling determines how the building would perform if it had been built according to the minimum code standards of the American Society of Heating, Refrigerating and Air-Conditioning Engineers (ASHRAE) under standard ASHRAE/IESNA 90.1-2001. NREL also applied a new informational Appendix G contained in Addendum E of the ASHRAE standard. NREL also performed error analysis of the baseline energy model that accounted for errors in input, ambiguities in determining geometry of baseline buildings, and potential errors in the weather file. NREL used EnergyPlus, a whole-building energy analysis software program sponsored by the U.S. Department of Energy, to perform

computer simulations. Data from an entire year of monitoring measurements were used to assemble an annual weather file with 15-minute resolution. Monitoring data were also used to calibrate receptacle and other miscellaneous electrical loads.

## Results

Results of the performance monitoring and baseline analysis are summarized in Table ES-1. Error margins and percentage savings are also shown.

On-site energy production from the PV system makes it important to distinguish between net and total energy use. Net energy use is the difference between the total energy use and the energy produced by the system. Energy performance is characterized by three categories of annual performance metrics:

- Annual total or net site energy is the measure of energy use in the building (both net and total).
- Annual source energy is the measure of energy consumed to produce and deliver the net energy.
- Annual energy cost is the measure of the annual energy operating expense.

Results for individual end uses are provided elsewhere in the report.

**Table ES-1 Annual Performance Metrics**

| | **Total Site Energy Use Intensity** kBtu/ft$^2$·yr *(MJ/m$^2$·yr)* | **Net Site Energy Use Intensity** kBtu/ft$^2$·yr *(MJ/m$^2$·yr)* | **Net Source Energy Use Intensity** kBtu/ft$^2$·yr *(MJ/m$^2$·yr)* | **Energy Cost Intensity** $/ft$^2$·yr *($/m$^2$·yr)* |
|---|---|---|---|---|
| Baseline Model | 53.3 ±7.3 *(604.8 ±82.8)* | 53.3 ±7.3 *(604.8 ±82.8)* | 159.6 ±20.0 *(1,812 ±227)* | 1.20 ±0.17 *(12.87 ±1.8)* |
| Monitoring | 40.2 ±0.3 *(456.8 ±2.9)* | 39.9 ±0.3 *(453.2 ±2.9)* | 124.3 ±0.7 *(1,412 ±8)* | 1.05 ±0.003 *(11.31 ±0.03)* |
| Savings | (24.5 ±14.1)% | (25.0 ±14.1)% | (22.1 ±12.8)% | (12.1 ±14.1)% |

As these percentages show, the Merrill Center performs well relative to the baseline energy model. This work identified specific recommendations that would improve the building's energy performance (see Section 7). Some recommendations are related to the design; some involve possible changes to the Merrill Center's systems and operation; others relate to research methods.

The analysis of monitored data and computer simulation models culminates in conclusions (see Section 8) about the performance of the Merrill Center, building monitoring, and the baseline analysis. Conclusions drawn in this study include:

- During cooling, the temperature of water returning from the ground heat exchanger, which supplies the water-to-air heat pumps, is often warmer than expected (and sometimes warmer than ambient), which indicates a need for additional research on the performance of ground-source heat pumps.
- Daylight is not harvested as well as it could be on the second floor.
- The Merrill Center is a good candidate for follow-on research.
- A long-term monitoring effort can succeed in collecting detailed annual data sets for energy use and weather that are suitable for evaluating energy performance.
- The new Appendix G for standard ASHRAE/IESNA 90.1-2001 is helpful for defining baseline energy models.

- An analysis of error in the baseline building energy models shows that such models have considerably more uncertainty than actual measurements that establish a true energy balance.
- Significant differences were found between the actual energy performance and predictions made for rating purposes. These differences indicate that there is a need to improve protocols for rating and to continue efforts to study actual buildings so that design models can better predict performance.

# 1 Introduction

In 1964 a group of Baltimore businessmen who were dissatisfied with the polluted state of the Chesapeake Bay, founded the Chesapeake Bay Foundation (CBF), a privately funded organization whose primary goal is to restore this seriously threatened ecosystem. The bay has lost to pollution approximately 98% of its oysters, 90% of its underwater grasses, 60% of its wetlands, and 50% of its forests, according to CBF statistics. CBF built the Philip Merrill Environmental Center in Annapolis, Maryland, to serve as its headquarters for the promotion of environmental issues associated with the bay. Because the Merrill Center promoted sustainable commercial building design by using high-performance energy features, it helped to augment CBF's mission.

Among the Merrill Center's high-performance energy-saving features are a good thermal building envelope, passive solar technology and ground-source heat pumps for heating and cooling, natural ventilation to reduce energy consumption from the air-conditioning system, and natural light to reduce lighting loads. Daylighting controls automatically dim some interior electric lights when natural, exterior daylight is sufficient. Other noteworthy features include a 4.2-kW photovoltaic (PV) system that helps to offset electrical loads and an array of evacuated-tube solar collectors that provides all the domestic hot water (DHW) needs.

The National Renewable Energy Laboratory (NREL) selected The Merrill Center as a technical case study because the building integrates several high-performance energy-saving features into its design. NREL staff monitored the building for one year. This report focuses on monitoring results from electronic data acquisition systems specified and installed by NREL researchers. NREL was not involved in the design phase of the project. Computer modeling was used in the evaluation to establish a benchmark for determining energy savings.

## 1.1 Energy Use in Commercial Buildings in the United States

The operation of commercial buildings accounts for approximately 18% of the total primary energy consumption in the United States. The total for all buildings is more than one-third of the primary energy consumption and more than 70% of the electricity consumption. The operation of buildings in the United States results in 38% of U.S. and 9% of global carbon dioxide ($CO_2$) emissions. Electricity consumption in the commercial building sector doubled between 1980 and 2002, and it is expected to increase another 50% by 2025 (DOE 2004). Reducing site energy consumption in commercial buildings through energy-efficient and renewable building technologies would significantly reduce primary energy consumption in the United States. Site energy is also a concern for the building owner or those responsible for paying the utility bills.

Typical site energy consumption by end use for office buildings is shown in Figure 1-1 (DOE 2004). The building's site energy use intensity (EUI) is 97.2 kBtu/ft$^2$·yr (1,104 MJ/m$^2$·yr). These numbers are based on 1995 data collected by the Energy Information Administration (EIA). Most of the space heating, water heating, and cooking are by natural gas; the rest of the energy consumption is electricity. The primary energy consumed to generate and distribute the electricity is approximately three times the energy used on site. Lighting is the largest primary energy end use; therefore, a primary objective in office buildings should be to reduce lighting loads.

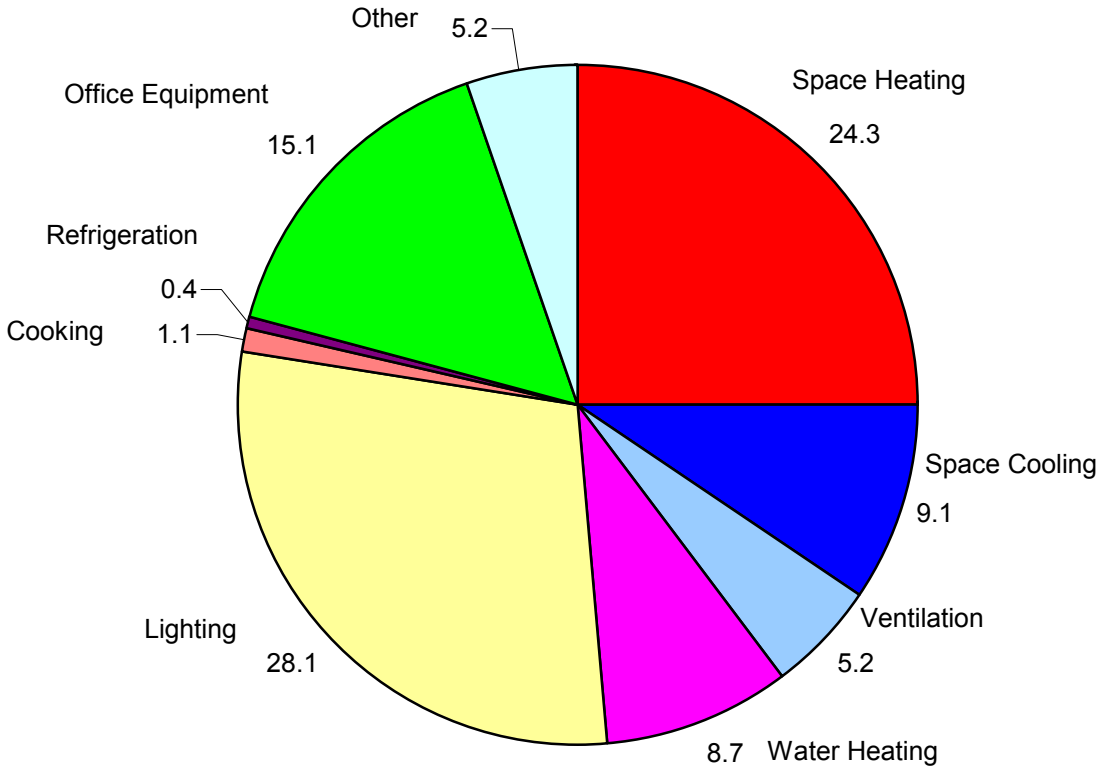


**Figure 1-1 Typical site EUIs by end use for office buildings (kBtu/ft$^2$·yr) (DOE 2004)**

## 1.2 High-Performance Buildings Research Objectives

The High-Performance Buildings Research project at NREL evaluates commercial building design from a whole-building perspective for the U.S. Department of Energy (DOE). NREL's whole-building perspective seeks to understand the integration issues of design and building operation to substantially reduce energy costs in commercial buildings and improve other attributes such as occupant satisfaction. Documenting the high performance of research-level buildings supplies examples that help to transform the marketplace. In addition, documenting common threads and analysis methodologies provides direct assistance to industry. The objectives of the research are to:

- Develop high-performance building design, construction, and operation processes.
- Provide the tools needed to replicate the processes and design strategies for creating high-performance buildings.
- Research new technologies for high-performance buildings.
- Develop standardized metrics and procedures for measuring building energy performance.
- Measure and document building performance in high-profile examples.

## 1.3 Building Evaluation Scope

NREL collaborated with CBF staff to monitor, evaluate, and document the energy performance of the Merrill Center from November 2001 through November 2002. NREL staff did not participate in the design process, but performance issues related to design decisions are discussed in this report. The Merrill Center has attracted a lot of attention in the sustainable design community, so an unbiased, real-world evaluation of the energy performance was made available so that designers can better learn from the project. In addition, problems with building equipment and operations can be identified and perhaps be corrected or otherwise be changed to improve the performance of the building.

Before monitoring began, a plan was developed to measure the overall building energy use and some individual energy end uses. The intent of the monitoring was to assess how the building performs as a whole system rather than to focus on individual aspects of the design or operation. Designing a monitoring project always requires balancing the extra cost and complexity of additional measurements with the usefulness of the expected results. For the Merrill Center, the focus was on the whole-building performance. The plan specifically did *not* call for detailed evaluation of several interesting subsystems and features of the Merrill Center, including natural ventilation, solar DHW, potable and nonpotable water systems, nor all the various sustainability measures that do not directly relate to energy performance. Subsystems that were evaluated to some extent include the PV system power, daylighting, and ground-source heat pumps.

## 1.4 Report Organization

This report contains an executive summary, eight primary sections, a list of references, and appendices. Section 2 provides background information. Section 3 describes the design process. Section 4 details the physical components of the Merrill Center. Section 5 contains whole-building energy evaluation methods and results. Section 6 discusses the evaluation of specific subsystems. Sections 7 and 8 present recommendations and conclusions drawn from this study. The appendices contain a selection of detailed data from the monitoring effort, weather data and calibration schedules for the building energy modeling, and a description of the error analysis.

# 2 Background

## 2.1 Energy Comparison Data

To fully evaluate the Merrill Center's energy performance, NREL needed comparison data. NREL began its analysis by examining data EIA collected on thousands of U.S. commercial buildings. In 1999, EIA conducted the Commercial Buildings Energy Consumption Survey (CBECS), a national survey that collected information, including building characteristics, energy consumption, and energy expenditures for all types of commercial buildings, on thousands of building types in the United States. CBECS concluded that office buildings account for 19% of all energy and 25% of all electrical energy used in commercial buildings. The survey also showed that all commercial buildings in the Northeast Census Region had an average site EUI of 90.3 kBtu/ft$^2$·yr (1026 MJ/m$^2$·yr). Office building site energy intensity averaged 90.7 kBtu/ft$^2$·yr (1030 MJ/m$^2$·yr), as shown in Figure 2-1.

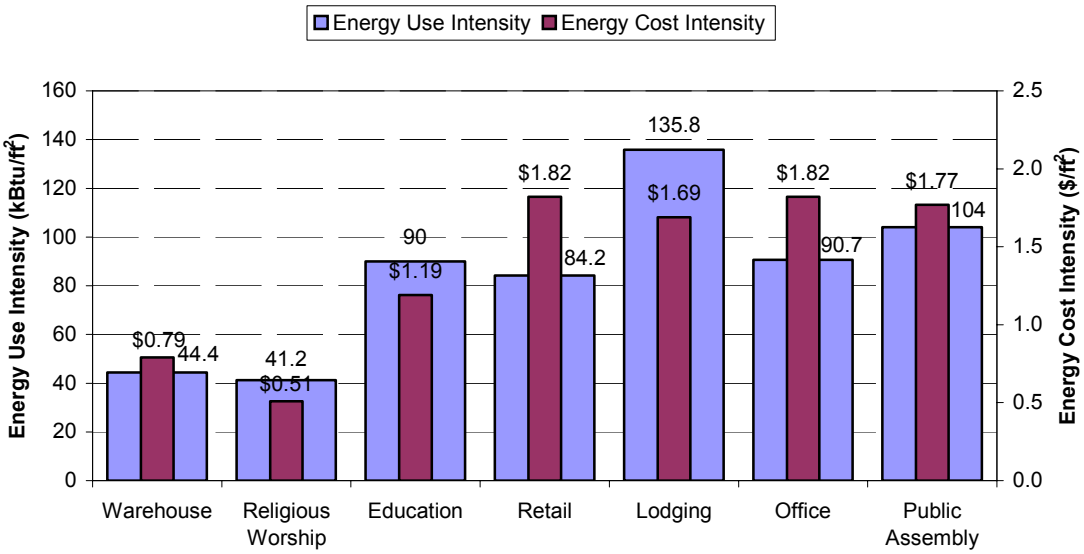


**Figure 2-1 1999 Northeast site energy intensity by building type**

Overall, CBECS found that office buildings consumed 1,089 trillion Btu (1,149 million GJ) of combined site electricity, natural gas, fuel oil, and district steam or hot water, which makes them the top energy consumer of all the commercial building types. Figure 1.1 shows the national end-use distribution. The survey also found that most site energy use was for space heating; lighting and cooling are the two next most energy-intensive end uses.

Various categories from the CBECS database were then considered. Similar-sized office buildings had an average energy intensity of 83.1 kBtu/ft$^2$·yr (944 MJ/m$^2$·yr) and recently constructed office buildings had an average energy intensity of 78.0 kBtu/ft$^2$·yr (886 MJ/m$^2$·yr). Although the CBECS survey provided data for national and regional comparisons, a local comparison was not established as local data are limited.

## 3 Design Process

Because NREL was not involved in the design of this building, this section presents only a brief overview of the design process. The design of the Merrill Center was led by the Washington, D.C. office of the architecture firm SmithGroup, Inc. Early in the design process, CBF's design team established a goal of achieving a Gold or Platinum rating under the U.S. Green Building Council's (USGBC) Leadership in Energy and Environmental Design (LEED™) certification program. The LEED certification goal had a strong influence on the building design; however, conserving the Chesapeake Bay was the organization's first priority, which meant that energy features were not optimized when they conflicted with conservation features.

The Sustainable Building Industries Council organized a peer review of the concept design (funded by DOE) that included reviewers from the Maryland Energy Administration, Maryland Department of Natural Resources, and the World Wildlife Fund. One of these reviewers, Greg Franta, used the Energy-10 computer program to conduct an early-phase design analysis. He used an integrated approach to design, and in-house engineers worked closely with architects. Benchmarking tours of other green projects and CBF's other educational centers were influential to the final design.

The team architect, who was already familiar with the design and project goals, administered the construction. Unfortunately, the contractor was not equally invested in the project goals had limited experience with high-performance building systems.

After the Merrill Center was built, CBF did reach its goal; the Merrill Center was the first building to be awarded a LEED Platinum certification from USGBC under version 1.0 of the LEED program (USGBC 2003). However, this report focuses on the energy use of the building, which is just one part of the LEED rating and CBF's goals for the building.

As part of the design process, the design team performed initial energy predictions for the building that were used as part of the documentation for the LEED certification. These predictions, along with the actual performance of the building, are shown in Section 5.4.2.

## 4 As-Built Building Description

The Merrill Center is a 31,000-ft$^2$ (2,880-m$^2$) building that serves as office space for 80 to 90 people, provides areas for training and education, and includes a small conference pavilion. The conference pavilion is separate from the main building and is connected by an enclosed walkway on the second floor. A kitchen and dining area for the staff are located in the conference pavilion. The south wall is mostly glass to provide a view of the bay, daylighting, and passive solar heating. North-facing clerestory windows provide additional daylighting and are operable for natural ventilation. Individual heating, ventilation, and air-conditioning (HVAC) systems are controlled by an energy management system (EMS). The EMS allows the building operator to monitor and control the HVAC and lighting (HVAC&L) systems from a desktop computer. Figure 4-1 shows a picture of the Merrill Center's entrance as viewed from the north. Figure 4-2 shows the plans of the first and second floors. The second floor is open to the first floor along the south wall of the main building. The overall length of the building in the east-west direction is 220 ft (67 m).

The design philosophy of the Merrill Center was sustainability from cradle to grave, wherein all materials used in construction are environmentally safe or recyclable throughout the lifetime of the building. In addition, resources were chosen from local suppliers to reduce vehicle pollution from unnecessary transportation. Many of these materials are also considered rapidly renewable, given their relatively quick rate of replenishment (< 10 years). Forest materials used in building construction were either drawn from sustainable forests or certified by the Forest Stewardship Council.

CBF's commitment to protecting the bay extends beyond the building; CBF also promotes environmentally sound transportation options for its employees. Showers, lockers, and bicycle storage areas enable employees to walk, bike, or kayak to work. CBF also provides natural gas and hybrid vehicles for errands. Videoconferencing and a telecommuting policy minimize transportation, and CBF arranges carpooling and has lunch delivered daily.

Figure 4-3 depicts the Merrill Center and highlights many of the energy design measures. Located at grade level under the first floor are a storage area, mechanical rooms, and an open air parking area, which prevents polluted runoff from entering the bay.

**Figure 4-1 Merrill Center north entrance shows rainwater storage tanks and north clerestories**

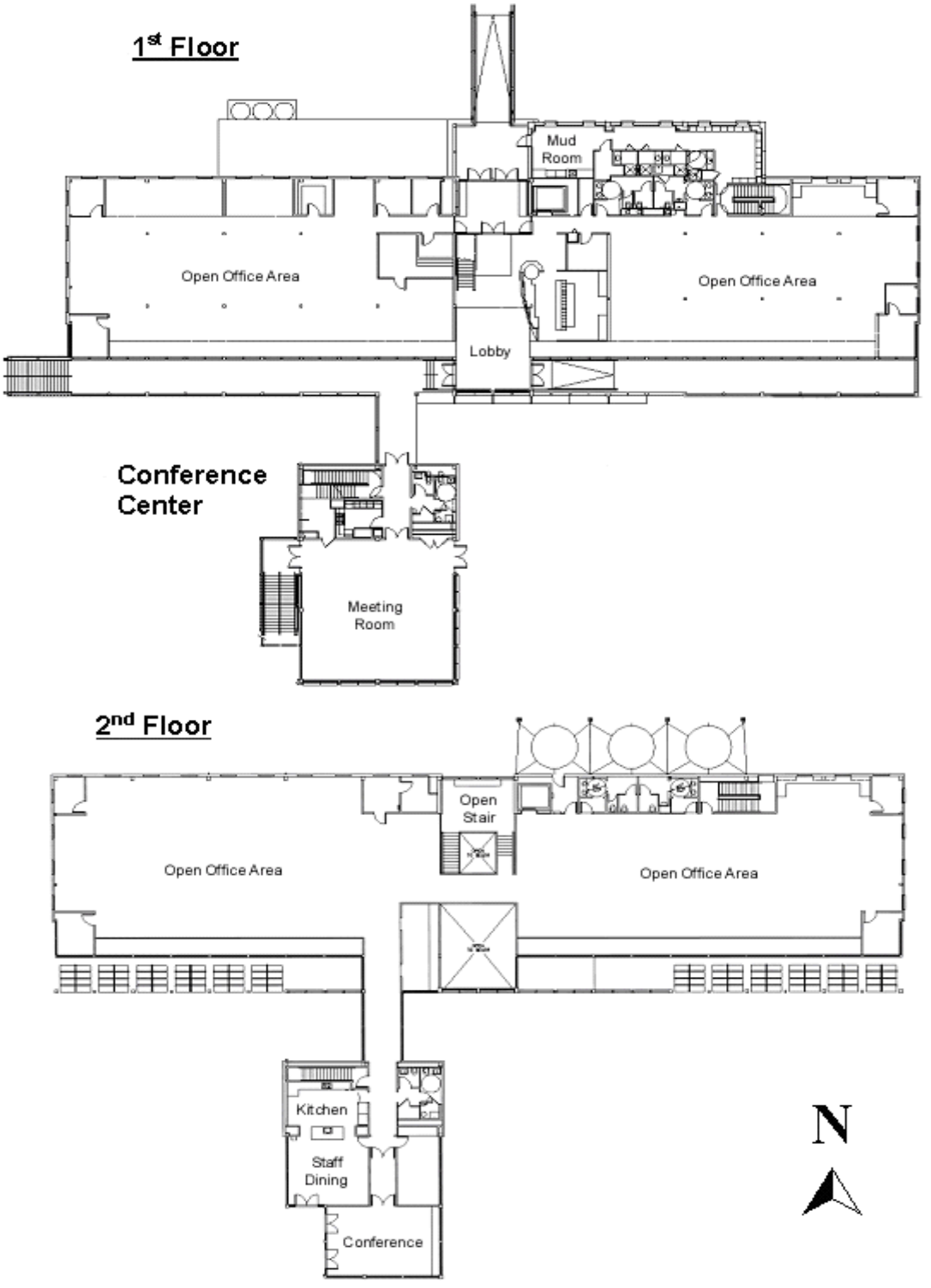


**Figure 4-2 First- and second-floor plans for the Merrill Center**

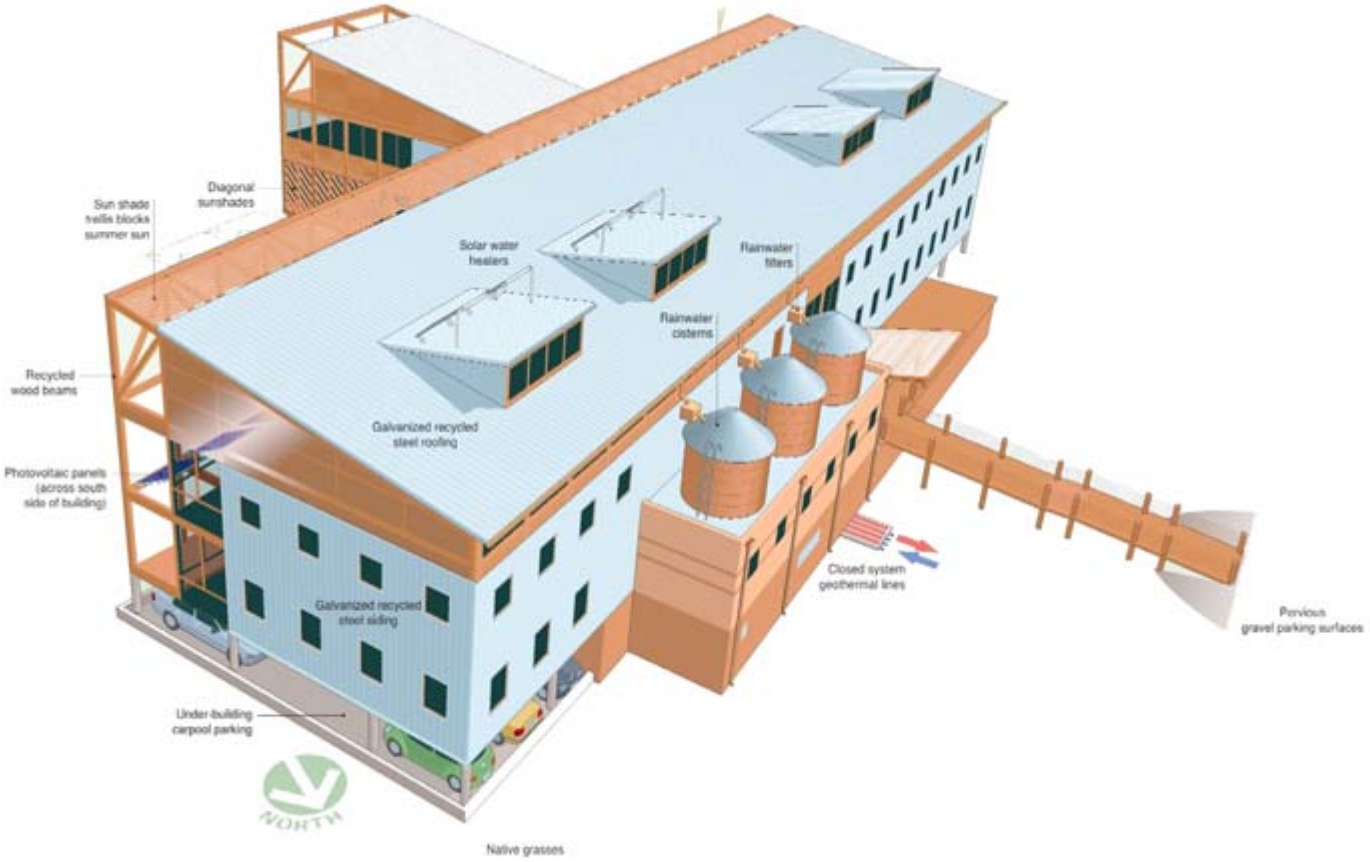


**Figure 4-3 Isometric sketch of the Merrill Center shows building features**

## 4.1 Building Envelope

Table 4-1 summarizes the high-performance thermal envelope used in the Merrill Center. The roof and most of the walls use structural insulated panels (SIPs). The SIPs are composed of oriented strand board (OSB) panels that sandwich expanded polystyrene foam. SIPs have foam cores with a thickness of either 5.5 in. (0.14 m) or 7.5 in. (0.19 m). In many places the interiors are left unfinished, and the OSB is exposed to the inside. Windows use spectrally selective, low-e glazing with wood frames.

**Table 4-1 Building Envelope Construction and Nominal Thermal Properties**

| Envelope Component | Construction (Outside to Inside) | $R_{\text{-factor}}$ h·ft²·°F/Btu *(m²·K/W)* |
|---|---|---|
| 6.5-in. (165-mm) Exterior Wall | ½-in. (13-mm) plywood, 5½-in. (140-mm) SIP foam, ½-in. (13-mm) plywood, ½-in. (13-mm) gypsum sheathing board | 28 *(4.9)* |
| 8.5-in. (216-mm) Exterior Wall and Built-Up Roof | ½-in. (13-mm) plywood, 7½-in. (191-m) SIP foam, ½-in. (13-mm) plywood, ½-in. (13-mm) gypsum sheathing board | 38 *(6.7)* |
| Interior Wall | ½-in. (13-mm) gypsum sheathing board, insulated metal frame, ½-in. (13-mm) gypsum sheathing board | 9.3 *(1.6)* |
| Interior Floor | 6-in. (152-mm) sound absorption blanket, ¾-in. (19-mm) wood subfloor, ¼-in. (6 mm) Masonite underlayment, ¼-in. (6 mm) tile finish flooring | 19 *(3.3)* |
| Exterior Floor | 2-½-in. (64-mm) dense insulation, ¾-in. (19-mm) wood subfloor, ¼-in. (6 mm) tile finish flooring | 10 *(1.8)* |
| Windows | Double-pane, 0.7-in. (18-mm) Argon-filled insulating glass with low-e coating. Shading Coef = 0.47 | 4.1 *(0.7)* |

South-facing windows form a passive part of the lighting and HVAC systems. In the summer, overhangs shade the glass from the high summer sun and shield the facility from unnecessary solar gains. (See Figure 4-7.)

## 4.2 Lighting and Daylighting

The first-floor office lighting is provided by indirect T-8 lamps with electronic ballasts. The first row of lights on the south side of the building near the windows is dimmable and controlled by photocells. Figure 4-4 shows the building interior when the first row of lights is off. The second-floor office luminaires are 50% direct and 50% indirect. The first two rows of lamps on the south side are controlled by photocells. Figure 4-5 shows the overhead fixtures for the second floor. Installed lighting power densities (LPDs) for the offices and conference lighting zones are shown in Table 4-2. Task lighting is provided at all workstations. The lights in the normally occupied areas and the exterior lights are controlled by the building automation system and have manual/timed override switches. These controls are in parallel, such that if one is on, the lights are on. The timed override switches are push buttons—when the button is pushed, the switch enables the lights for a set time interval. The restroom lights are compact fluorescent lamps on occupancy sensors. Daylighting provides considerable natural light to the second-floor offices, the conference pavilion, and the lobby.

**Figure 4-4 T-8 overhead lighting on the first floor (100% indirect)**

**Figure 4-5 T-8 overhead lighting and task lighting on the second floor (50% direct/50% indirect)**

**Table 4-2 LPD by Zone**

| Lighting Zone | LPD W/ft$^2$ (W/*m*$^2$) |
|---|---|
| First-Floor Offices | 1.2 (12.9) |
| Second-Floor Offices | 1.6 (*17.2)* |
| Conference Room | 1.4 (15.1) |

## 4.3 Description of Photovoltaic System

A 4.2-kW, thin-film PV system is mounted on the south side of the building. The panels are inclined at an angle of 30° and face approximately south. Three inverters feed the energy into one of the building electrical panels on the second floor, as shown in Figure 4-6. There is no storage or net metering[1] because loads connected to these panels immediately use all the electricity generated. The building structure and conference pavilion partially shade the PV panels during the summer, which reduces the system production (see Figure 4-7). The system production improves in the winter because of the low sun angle, the large amount of reflection off the bay, and the bright diffuse southern sky.

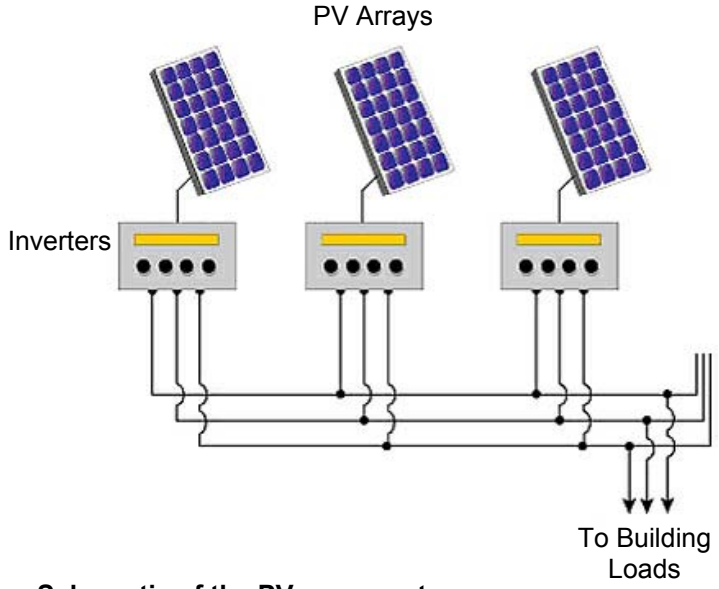


**Figure 4-6 Schematic of the PV array system**

[1] Many utility companies give building owners credit for excess power produced by their PV systems through a net-metering program.

**Figure 4-7 PV array and shading caused by building structure**

## 4.4 Hybrid Natural Ventilation

Figure 4-8 shows the design intent for natural ventilation in the Merrill Center, which uses operable windows and a geometry that is designed to take advantage of the breezes off the bay for natural ventilation. Low- and mid-height windows on the south side are grouped in banks of four and operated with hand cranks. Windows located high on the north side have motorized operators that are controlled by the building's EMS. Figure 4-9 shows a photograph of one of the signs in the office areas that reads "Open Windows." It is used to inform occupants when conditions are appropriate to open the manually operated windows. The natural ventilation system is a hybrid or mixed-mode system in that fans are often used to help move ventilation air. These fans exhaust air on the north side. A fan on the second floor exhausts air at a rate of 2,800 cfm (1.32 $m^3/s$). A fan on the first floor exhausts air at a rate of 5,600 cfm (2.64 $m^3/s$). This ventilation system represents an air change rate of about one air change per hour (ACH). Control of the hybrid natural ventilation is discussed in Section 4.4.1 and listed in Table 4-3. Control is based on sensor data for interior temperatures, interior humidity, and outdoor temperature. The north, motorized windows also have moisture sensors that detect when it is raining so that the windows can be automatically closed.

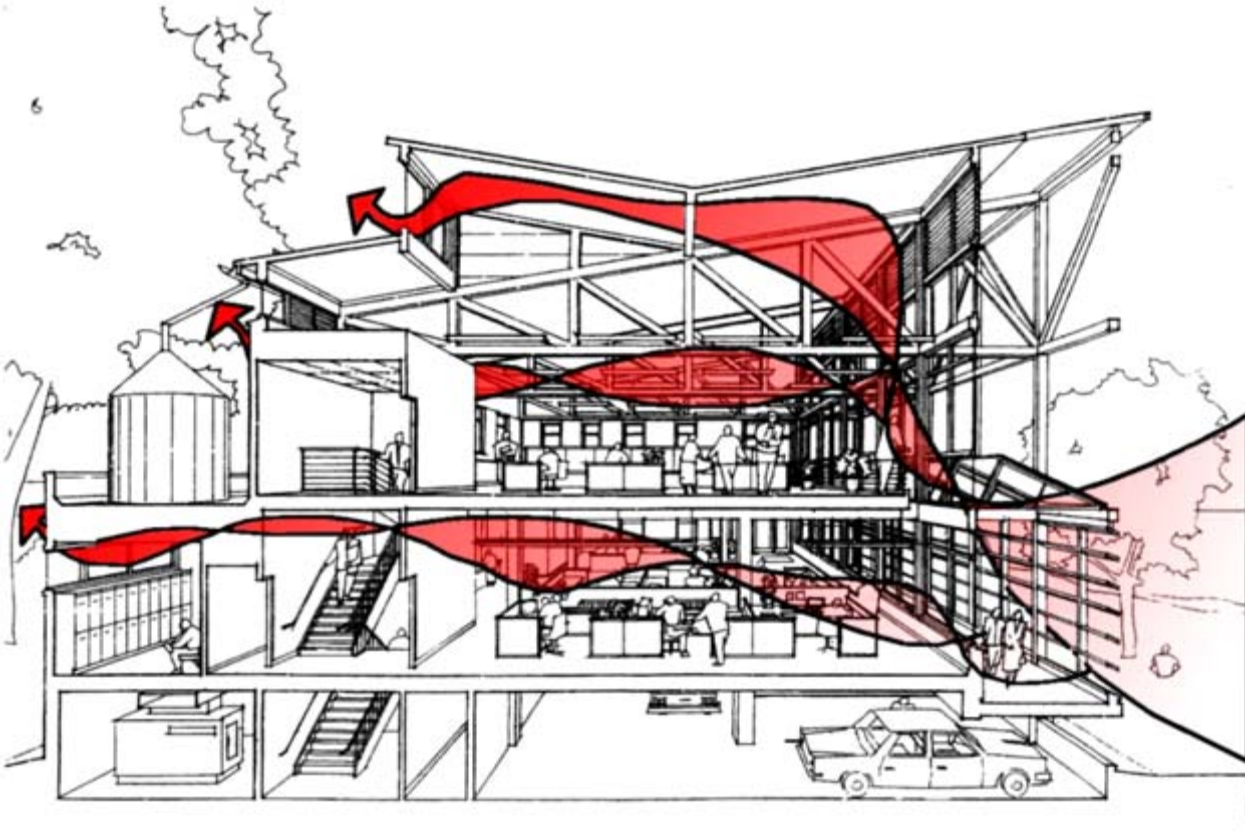

**Figure 4-8** **Intended airflow pathways for natural ventilation from the design phase**


**Figure 4-9 Signage directs occupants to operate windows**

### *4.4.1 Hybrid Natural Ventilation – Prior Research*

Chang (2002) studied the natural ventilation of the Merrill Center. He used monitoring equipment, simplified modeling, and occupant surveys for his evaluation. Chang concluded that the mixed-mode ventilation approach used at the Merrill Center shows good promise for application in commercial buildings in the eastern United States. He found that occupants were content with the natural ventilation. His monitoring results indicated that from May 16, 2001 to December 31, 2001, natural ventilation was used 34% of weekday working hours. Chang's study occurred during the first year of occupation and found problems with the control system; he helped the building manager improve natural ventilation controls and predicted that operation would improve over the second year. Chang found that the original design natural ventilation set point, when outdoor temperatures were below 77°F (25°C), was too high. Table 4-3 provides a summary of building operation strategies developed by Chang (as of December 2001).

**Table 4-3 Natural Ventilation System Control Set Points (Chang 2002)**

| Condition | Strategy |
|---|---|
| Natural Ventilation | Outside air between 46° and 72°F (7.7° and 22.1°C), natural ventilation is available. During this period, assist fans may or may not be turned on. Occupants open manually operated windows at their own discretion. |
| Assist Fans | Interior temperatures > 72°F (22.1°C), fans are turned on. When temperature < 68°F (19.9°C), fans are turned off. |
| Summer Cooling | The heat pump set point lies between 77° and 78°F (24.9° and 25.4°C). Humidity is controlled to 50% with a 10% range. |
| Winter Cooling | Allow interior to reach 81°F (27.1°C) before A/C heat pumps or natural ventilation is used. Once interior temperatures drop to 78°F (25.4°C), system is turned off. Once interior relative humidity reaches 65%, humidification is turned off. Once interior drops to 50% relative humidity, humidification is turned on. [2] |

Chang noted that winds tend to flow from the northwest when outdoor conditions are good for natural ventilation and contrasted this with the designer's intent to take advantage of winds that blow off the bay from south to north. Chang also noted that the electric lights were often on when daylighting was sufficient. He also tested a technique that uses a low-cost, Web-based camera to monitor the manual operation of windows. He indicated that, despite some difficulties, the approach showed promise.

## 4.5 Mechanical Systems

The Merrill Center uses ground-source heat pumps as the primary source of heating and cooling. Fin and tube radiators connected to a propane boiler provide supplementary heating in the entryways, middle landing of the main stairway, and along the glazed south wall of the main building. This section describes these systems.

### *4.5.1 Ground-Source Heat Pumps*

Table 4-4 lists the characteristics of the individual air-handling units served by a single groundwater loop. Figure 4-10 shows the locations of thermal zones served by heat pumps in the main occupied areas of the building. Eighteen heat pumps and one air conditioner are connected in parallel to the ground loop. The heat pumps are packaged water-to-air units with integral, constant volume air systems. The cooling only air conditioner (ACU-1) cools a computer server room. Two small heat pumps (HP-1 and HP-18) serve unoccupied areas on the ground floor and are not shown in Figure 4-10.

Figure 4-11 diagrams the ground heat exchanger (although only half the wells are drawn). The ground loop is connected to four circuits; each circuit has 12 vertical geothermal wells or boreholes. Each heat pump package is plumbed in parallel with the ground loop. Water is circulated with redundant parallel pumps. The loop pumps are variable speed and are controlled to maintain a pressure set point determined by the EMS. The operator manually adjusts the pressure set point to achieve a high temperature difference across the wells. As various heat pump packages cycle on or off, that portion of the water loop is opened or closed, which affects the pressure. Outside air is introduced via two air handlers, one in the main building and one in the conference pavilion. The air handlers provide the supply and return air streams for outside and relief air; they contain a heat recovery wheel and a desiccant wheel. (The heat recovery and desiccant systems are not being used.) Fresh outdoor air is introduced to the individual heat

[2] The building operator has since adopted a fan assist mode for winter cooling when windows are left closed, but the assist fans are run to introduce outside air from infiltration.

pump air units at the maximum rates shown in Table 4-4. The constant volume outdoor air system has two stages (in addition to off) and a $CO_2$ sensor determines which stage is needed. The total nominal cooling capacity is 115 tons (404 kW) or 270 $ft^2$/ton (7 $m^2$/kW).

**Table 4-4 Water-to-Air Heat Pump Design Data**

| Heat Pump | Water Loop Flow Rate gal/min; gpm *(L/s)* | Air System Flow Rate $ft^3$/min; cfm *($m^3$/s)* | Design Outside Air Ventilation $ft^3$/min; cfm *($m^3$/s)* | Nominal Cooling Power kBtu/h *(kW)* | Nominal Heating Power kBtu/h *(kW)* |
|---|---|---|---|---|---|
| HP-1 | 2.5 *(0.16)* | 339.0 *(0.16)* | 106.0 *(0.05)* | 10.9 *(3.19)* | 9.8 *(2.86)* |
| HP-2 | 16.0 *(1.01)* | 1,865.0 *(0.88)* | 360.0 *(0.17)* | 63.5 *(18.61)* | 63.4 *(18.58)* |
| HP-3 | 28.0 *(1.77)* | 3,814.0 *(1.80)* | 360.0 *(0.17)* | 129.3 *(37.91)* | 115.0 *(33.69)* |
| HP-4 | 16.0 *(1.01)* | 1,865.0 *(0.88)* | 381.0 *(0.18)* | 63.5 *(18.61)* | 63.4 *(18.58)* |
| HP-5 | 28.0 *(1.77)* | 3,836.0 *(1.81)* | 360.0 *(0.17)* | 129.3 *(37.95)* | 115.0 *(33.72)* |
| HP-6 | 16.0 *(1.01)* | 1,865.0 *(0.88)* | 848.0 *(0.40)* | 63.5 *(18.61)* | 63.4 *(18.58)* |
| HP-7 | 16.0 *(1.01)* | 1,865.0 *(0.88)* | 805.0 (0.38) | 63.5 *(18.61)* | 63.4 *(18.58)* |
| HP-8 | 13.0 *(0.82)* | 2,161.0 *(1.02)* | 339.0 *(0.16)* | 60.3 *(17.67)* | 59.2 *(17.34)* |
| HP-9 | 28.0 *(1.77)* | 3,984.0 *(1.88)* | 339 *(0.16)* | 130.5 *(38.24)* | 115.7 *(33.92)* |
| HP-10 | 28.0 *(1.77)* | 4,026.0 *(1.90)* | 0.0 *(0.0)* | 130.6 *(38.29)* | 115.8 *(33.95)* |
| HP-11 | 16.0 *(1.01)* | 2,458.0 *(1.16)* | 191 *(0.09)* | 80.2 *(23.52)* | 83.1 *(24.36)* |
| HP-12 | 28.0 *(1.77)* | 4,047.0 *(1.91)* | 0.0 *(0.0)* | 130.8 *(38.35)* | 116.0 *(33.99)* |
| HP-13 | 28.0 *(1.77)* | 3,475.0 *(1.64)* | 254.0 *(0.12)* | 121.5 *(35.61)* | 113.5 *(33.28)* |
| HP-14 | 15.0 *(0.95)* | 1,611.0 *(0.76)* | 403.0 (0.19) | 49.4 (14.47) | 61.1 (17.91) |
| HP-15 | 9.0 (0.57) | 1,102.0 (0.52) | 445.0 (0.21) | 37.3 (10.93) | 39.2 (11.49) |
| HP-16 | 12.0 (0.76) | 1,208.0 (0.57) | 275.0 *(0.13)* | 40.6 *(11.89)* | 45.2 *(13.26)* |
| HP-17 | 14.0 *(0.88)* | 1,547.0 *(0.73)* | 403.0 *(0.19)* | 45.3 *(13.29)* | 51.3 *(15.04)* |
| HP-18 | 2.5 *(0.16)* | 381.0 *(0.18)* | 0.0 *(0.0)* | 13.5 *(3.96)* | 14.6 *(4.27)* |
| ACU-1 | 3.8 *(0.24)* | 509.0 *(0.24)* | 0.0 *(0.0)* | 14.8 *(4.34)* | none |
| **Total** | **320.0 *(20.2)*** | **42,000.0 *(19.8)*** | **5,870.0 *(2.77)*** | **1,378.0 *(404)*** | **1,308.0 *(383)*** |

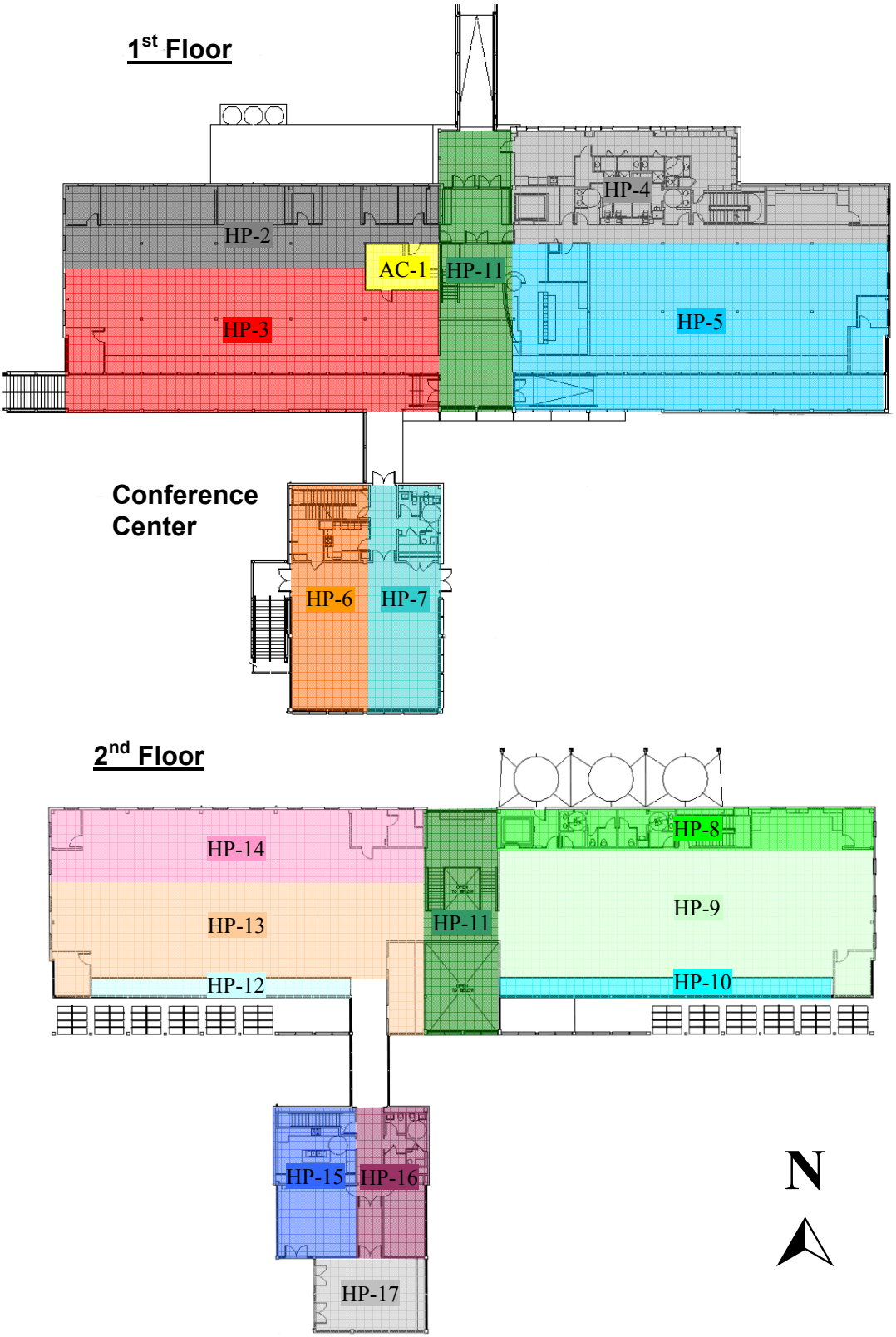


**Figure 4-10 Location of heat pump thermal zones**

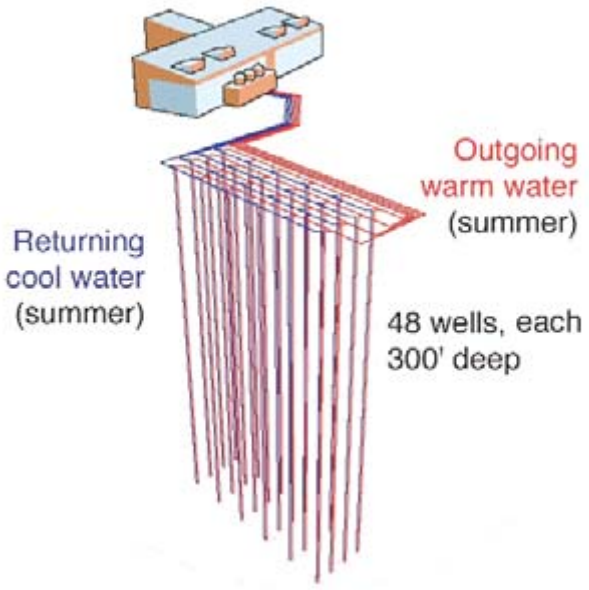


**Figure 4-11 Ground heat exchanger**

### *4.5.2 Desiccant System*

The outdoor air handlers for the building include a solid, wheel desiccant dehumidification system (see Figure 4-12). The desiccant wheel is regenerated by heating air with a hot-water coil that uses boiler-fired hot water. There is also a thermal wheel for energy exchange.

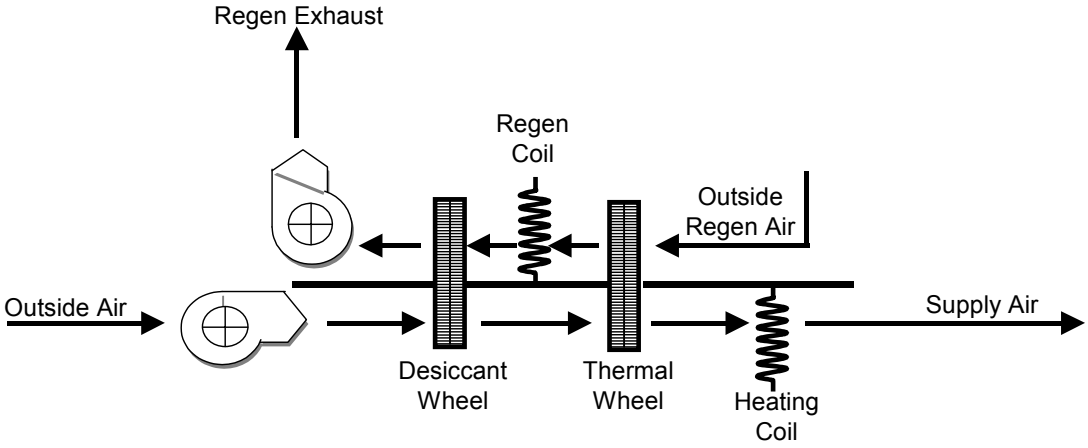


**Figure 4-12 Desiccant dehumidification system**

### *4.5.3 Water Heating*

There are two water heating systems in the Merrill Center: a solar thermal system for DHW and a propane boiler system for backup space heat, cistern freeze protection, and desiccant regeneration.

### *Domestic Hot Water*

The solar hot-water system consists of four arrays of 30 evacuated-tube solar collectors on the roof of the main building (see Figure 4-13). The collectors are inclined at an angle of 39° from the horizontal and face approximately south. A glycol loop circulates fluid from the roof to two hot water tanks that are plumbed in parallel. One tank is for potable and the other for nonpotable water. The tanks have electric backup heaters. The system provides DHW for sinks, showers, two dishwashing machines, and a clothes washing machine. Because the overall water use is very low, all the DHW needs of the building are met by the solar collectors; the backup heating coils have never come on.

**Figure 4-13 Evacuated-tube solar collector arrays**

### *Auxiliary Space Heating*

Figure 4-14 diagrams the boiler and pumping configuration; diagrams the terminal units and shows nominal heating capacities. This system is used in addition to space heating by the ground-source heat pumps. A propane-fired boiler heats water. The unit has a nominal thermal efficiency of 90%. Its rated input is 860 kBtu/h (252 kW). Hot water serves a combination of passive finned tube radiators and unitary heaters. The finned tube heaters are mostly located on the first floor along the south wall underneath the expansive windows. The enclosed walkway on the second floor, which connects the main building with the conference pavilion, also has finned tube radiators. The unitary heaters are used in vestibule entry areas, a mudroom, ground-floor storage and mechanical rooms, and restrooms in the conference pavilion. A heat exchanger arrangement allows the boiler to protect the rainwater cisterns against freezing. Freeze protection has not yet been necessary. The boiler-fired hot water is also configured to regenerate desiccant wheels in the outdoor air handler.

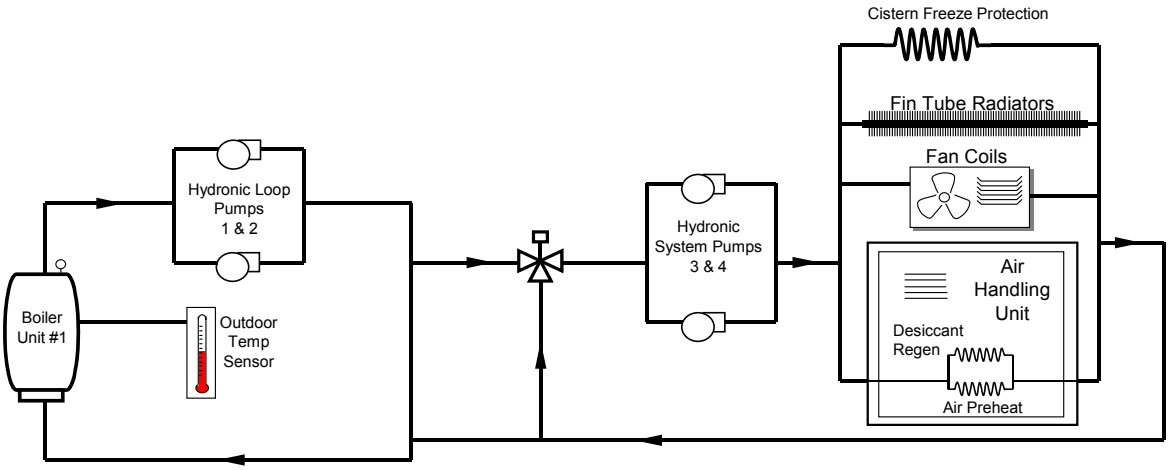


**Figure 4-14 Water heating boiler configuration**

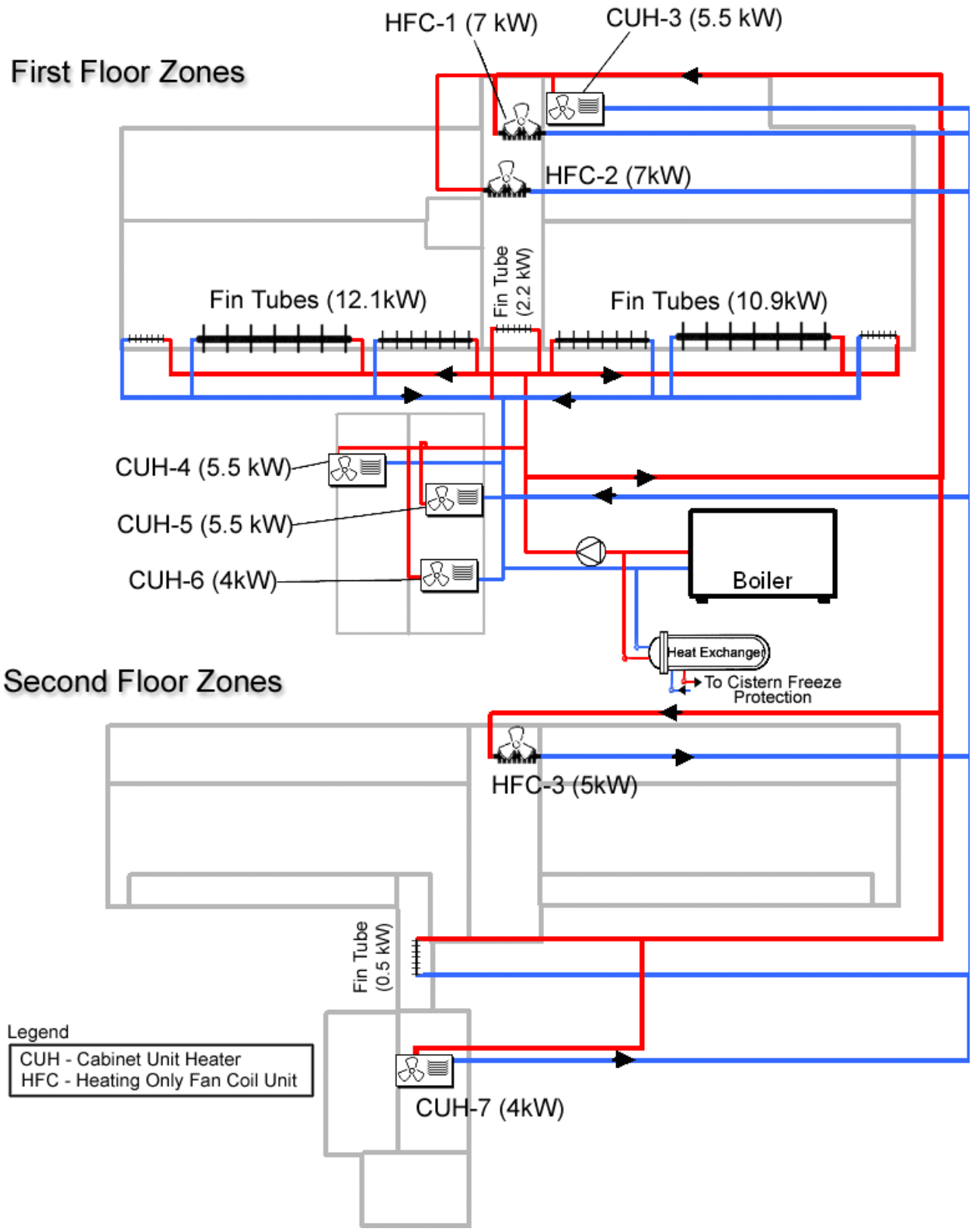


**Figure 4-15 Water heating equipment schematic**

## 4.6 Equipment and Water Systems

Equipment includes all connected plug loads that are not associated with heating, cooling, ventilation, or lighting HVAC&L. Potable and nonpotable water systems are also included in the equipment loads.

### *4.6.1 Potable Water System*

The potable water system provides water that is safe for drinking. The source of potable water is an on-site well with a residential-size pumping arrangement; no city water is available. The water is filtered and metered before being supplied to the kitchens and drinking fountains. Potable water is used quite a bit in the kitchens because lunch is served daily to encourage building occupants to stay on-site to reduce the environmental costs of transportation. All the lunch dishes are washed in the kitchen with potable water.

### *4.6.2 Nonpotable Water System*

The nonpotable water system supplies water for fire protection, clothes and body washing, and landscape watering. Nonpotable water for washing is supplied to the restroom sinks, locker room showers, clothes washing machine, laundry tub, and hose bibs on the outside of the building. A residential-size pump provides pressure for this system. Using large cisterns with rainwater collection eliminated the need to install a large water main for fire protection.

Several water conservation devices help minimize nonpotable water use. The restroom sinks are equipped with low-flow faucets and infrared control sensors for automatic operation. Composting toilets, which were purchased for all the restrooms, use minimal water to maintain appropriate levels of moisture for decomposition. The clothes washing machine is horizontal axis.

### *4.6.3 Rainwater Collection Systems*

Three rainwater collection systems serve all the nonpotable water needs of the building. The largest system collects rainwater from the roof of the main building. The rainwater passes through a particulate and organic matter reduction filter before being stored in three, 6,500-gal (24.6-$m^3$) cisterns on the north side of the building, as shown in Figure 4-1 and Figure 4-3. After the storage tanks, the water is chlorinated and carbon filtered. A minimum water level is maintained for the fire protection system. If the water falls below the minimum required for fire protection, it is made up with well water. Under normal operating and weather conditions, there is an ample supply of rainwater. Excess rainwater flows off as stormwater through an overflow drain. A heat exchanger, which is controlled by the EMS and connected to the boiler hot-water system, protects the cistern water from freezing. This freeze protection system did not operate during the monitoring period. Two smaller systems collect rainwater from the downspouts of the main building and conference pavilion for landscape watering and for washing boots and equipment.

### *4.6.4 Water Conservation and Resource Protection*

Potable and nonpotable water systems are part of the building's water conservation measures. Water is designated at its point of use as either potable or nonpotable, and in combination with water conservation devices such as waterless composting toilets, provides a successful strategy for conserving water resources. Another important feature is the parking design that reduces harmful runoff from surfaces into Chesapeake Bay by placing parking under the building and using gravel surfacing for parking outside the building. Remaining stormwater runoff flows through a bioretention stormwater treatment system designed to treat oils, and then flows through a constructed wetland.

# 5 Whole-Building Energy Evaluation

## 5.1 Whole-Building Evaluation Methodology

NREL used detailed energy metering and compared collected data with the monthly metering of utilities to evaluate the Merrill Center. NREL has monitored the building continuously since August 2001. This section discusses measurement procedures, data processing, and results. Figure 5-1 details a timeline of the monitoring effort.

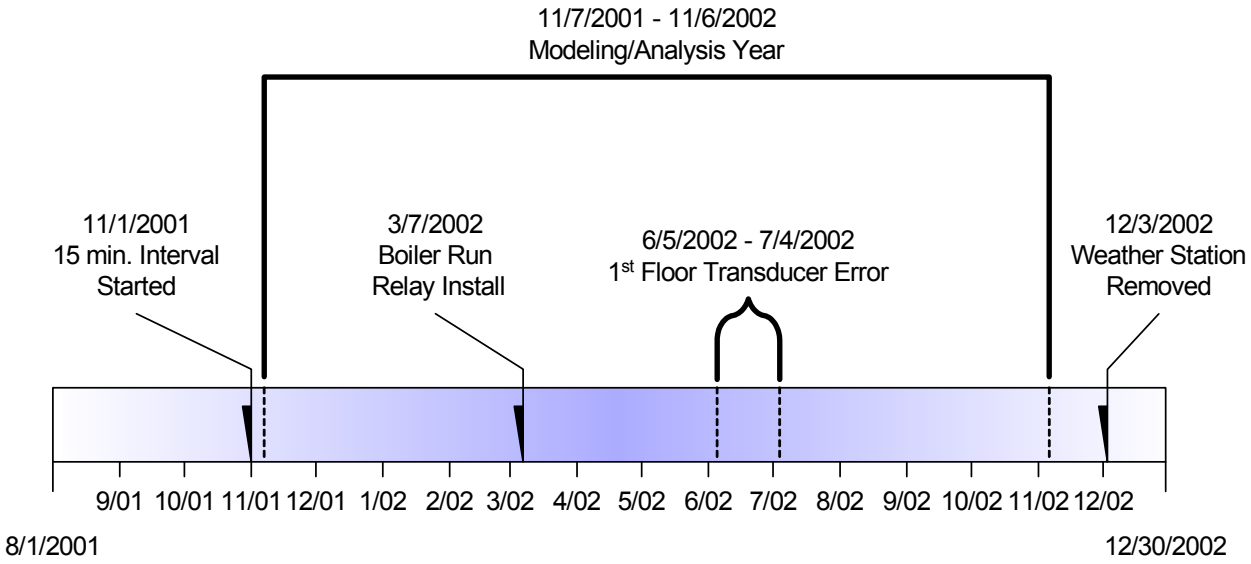


**Figure 5-1 Timeline of monitoring system and postoccupancy evaluation**

NREL used monitoring data for weather and operational schedules to develop a computer-simulated baseline model of a conventional energy code-compliant building. An as-built model of the building could not be developed for this project because of the complexity of the HVAC systems and the late addition of water source heat pumps in EnergyPlus. Developing an as-built model and comparing it to a baseline model would have been helpful, but we were only able to compare the actual measurements to a well-calibrated baseline model. The objective of the monitoring was to measure the performance of the building over the course of an entire year. For reference purposes, we used the actual measured weather data to compare this information with a base-case simulation of a typical code-compliant building.

Performance metrics analyzed include site energy savings, source energy savings, and energy cost savings. The flow chart in Figure 5-2 shows how the measured data were used in the models and the process used to obtain the simulation results.

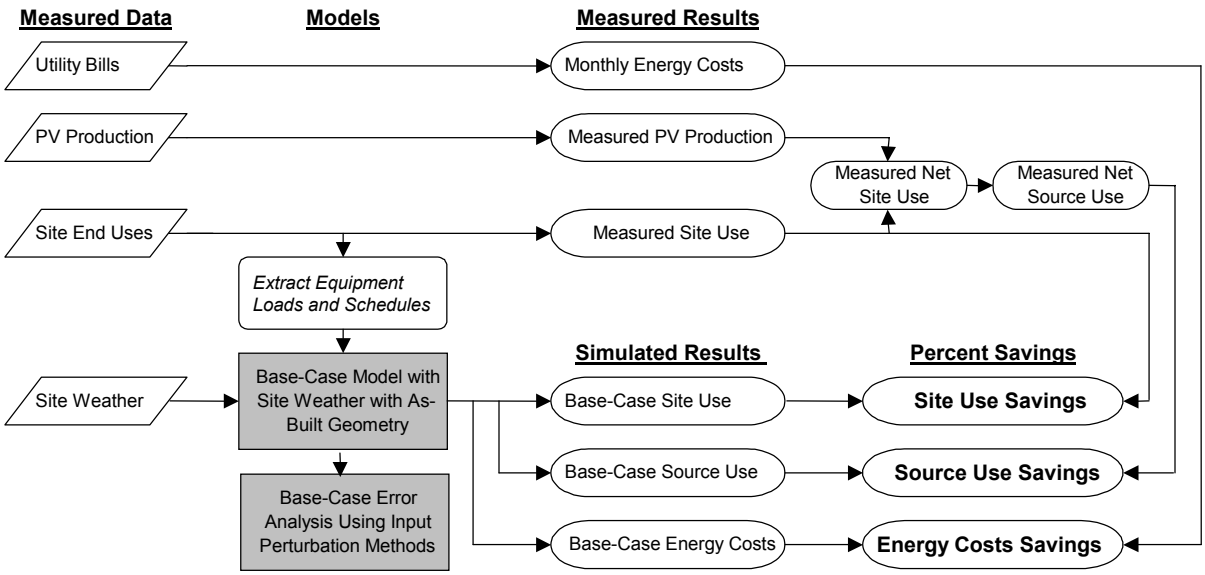


**Figure 5-2 Whole-building evaluation flowchart**

## 5.2 Whole-Building Monitoring

This section discusses the instrumentation and data collection techniques related to the data acquisition system that was installed in the Merrill Center.

### *5.2.1 Measurement Procedure*

NREL focused on a measurement and verification plan that included a task schedule, a summary of the building, a list of objectives, a list of equipment needed, and measurement points. The system was designed to measure the important electrical and thermal flows in the buildings and local weather conditions. NREL specified and installed all the equipment, but it was purchased by CBF. The plan included specifying that electrical services be designed and wired so that key end uses, such as lighting and plug loads, are served by separate electrical panels.

### *5.2.2 Instrumentation*

There are two separate components of the data acquisition system: one for the main building and a second for the conference pavilion. Figure 5-3 shows the individual points where electrical energy was monitored. Table 5-1 lists the points measured in the main building and Table 5-2 lists the points measured in the conference pavilion. The weather data were measured on top of the conference pavilion. The selection of sensors was based on successful application of such instruments on previous NREL building monitoring projects. NREL used watt-hour transducers to measure electrical energy.

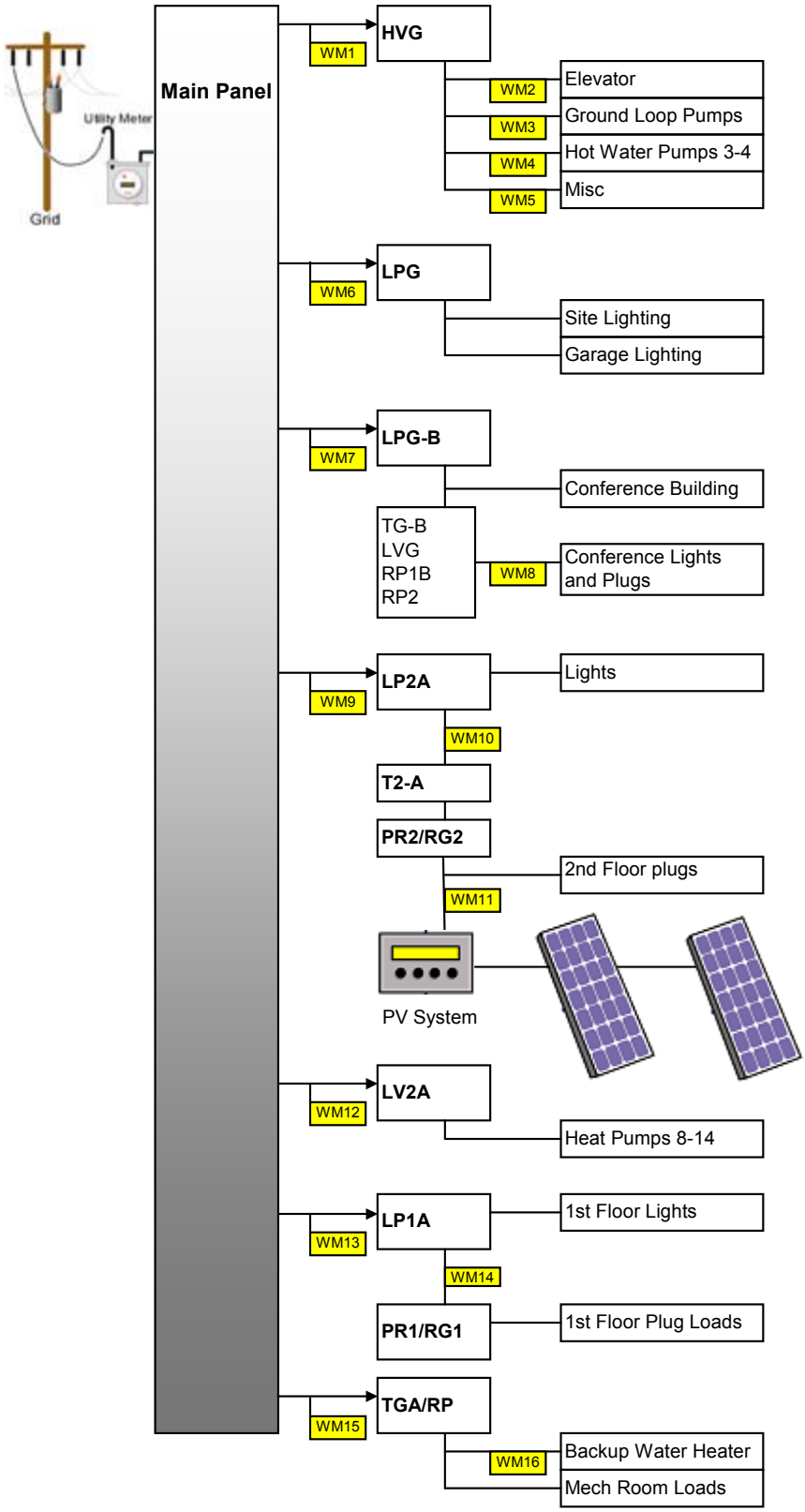


**Figure 5-3 Electrical monitoring points**

**Table 5-1 Measurement Points and Sensors: Main Building**

| Description | Units | Sensor | Sensor Accuracy | Notes |
|---|---|---|---|---|
| Ground-Loop Water Supply Temperature | °C | Type-T thermocouple | ±0.54°C | |
| Ground-Loop Water Return Temperature | °C | Type-T thermocouple | ±0.54°C | |
| Heat Pumps 4 and 5 Return Air Temperature | °C | Type-T thermocouple | ±0.54°C | Installed 03-07-03 |
| Heat Pump 4 Mixed Air Temperature | °C | Type-T thermocouple | ±0.54°C | Installed 03-07-03 |
| Heat Pump 4 Supply Air Temperature | °C | Type-T thermocouple | ±0.54°C | Installed 03-07-03 |
| Heat Pump 5 Mixed Air Temperature | °C | Type-T thermocouple | ±0.54°C | Installed 03-07-03 |
| Heat Pump 5 Supply Air Temperature | °C | Type-T thermocouple | ±0.54°C | Installed 03-07-03 |
| AH1 Process Out to Building Air Temperature | °C | Type-T thermocouple | ±0.54°C | Installed 03-07-03 |
| Boiler Relay On Status | On/Off | Relay/Pulse count | | Installed 03-07-02 |
| 1st-Floor Zone Air Temperature | °C | Vaisala Humitter 50Y | ±0.45°C | Shielded |
| 1st-Floor Relative Humidity | % | Vaisala Humitter 50Y | ±6% | ±3%: 10%–90% RH<br>±6%: 90%–100% RH |
| 2nd-Floor Zone Air Temperature | °C | Vaisala Humitter 50Y | ±0.45°C | Shielded |
| 2nd-Floor Relative Humidity | % | Vaisala Humitter 50Y | ±6% | ±3%: 10%–90% RH<br>±6%: 90%–100% RH |
| Heat Pumps 8–14 | kWh | WattNode P-series | ±0.45% read. | Add ±0.05% full scale |
| 2nd-Floor Lights and Receptacles | kWh | WattNode P-series | ±0.45% read. | Add ±0.05% full scale |
| 1st-Floor Lights and Receptacles | kWh | WattNode P-series | ±0.45% read. | Add ±0.05% full scale |
| Heat Pumps 2–5, Pumps, Compressor | kWh | WattNode P-series | ±0.45% read. | Add ±0.05% full scale |
| Site and Garage Lights | kWh | WattNode P-series | ±0.45% read. | Add ±0.05% full scale |
| Mechanical Room Loads | kWh | WattNode P-series | ±0.45% read. | Add ±0.05% full scale |
| Conference Building (HP = this – lights + plugs) | kWh | WattNode P-series | ±0.45% read. | Add ±0.05% full scale |
| 1st-Floor Receptacles | kWh | WattNode P-series | ±0.45% read. | Add ±0.05% full scale |
| 2nd-Floor Receptacles Minus PV | kWh | WattNode P-series | ±0.45% read. | Add ±0.05% full scale |
| PV Production | kWh | WattNode P-series | ±0.45% read. | Add ±0.05% full scale |
| Backup Water Heaters | kWh | WattNode P-series | ±0.45% read. | Add ±0.05% full scale |
| Elevator | kWh | WattNode P-series | ±0.45% read. | Add ±0.05% full scale |
| Ground-Loop Water Pumps | kWh | WattNode P-series | ±0.45% read. | Add ±0.05% full scale |
| Hot-Water Pumps 3–4 | kWh | WattNode P-series | ±0.45% read. | Add ±0.05% full scale |
| Reference Temperature | °C | Campbell AM25T | ± 0.2°C | |

**Table 5-2 Measurement Points and Sensors: Conference Building**

| Description | Units | Sensor | Sensor Accuracy | Notes |
|---|---|---|---|---|
| Outside Air Dry-Bulb Temperature | °C | Type-T, wire | ±0.54°C | Shielded |
| 1st-Floor Zone Air Temperature | °C | Vaisala Humitter 50Y | ±0.45°C | Shielded |
| 1st-Floor Relative Humidity | % | Vaisala Humitter 50Y | ±6% | ±3%: 10%–90% RH<br>±6%: 90%–100% RH |
| 2nd-Floor Zone Air Temperature | °C | Vaisala Humitter 50Y | ±0.45°C | Shielded |
| 2nd-Floor Relative Humidity | % | Vaisala Humitter 50Y | ±6% | ±3%: 10%–90% RH<br>±6%: 90%–100% RH |
| Horizontal Solar Radiation | $W/m^2$ | Li-Cor LI200X | ±5% | ±3% typical |
| Vertical (South-Facing) Solar Radiation | $W/m^2$ | Li-Cor LI200X | ±5% | ±3% typical |
| Outside Air Thermister Temperature | °C | Vaisala Humitter 50Y | ±0.5°C | Shielded |
| Outside Relative Humidity | % | Vaisala Humitter 50Y | ±6% | ±3%: 10%–90% RH<br>±6%: 90%–100% RH |
| Wind Speed | m/s | R.M. Young Wind Sentry 03001 | ±0.5 m/s | Threshold 0.5 m/s |
| Wind Direction | degrees | R.M. Young Wind Sentry 03001 | ±5° | Threshold 0.8 m/s |
| Conference Lights and Plugs | kWh | WattNode P-series | ±0.45% reading | Add ±0.05% of full scale |
| Thermocouple Reference Temperature | °C | Campbell AM25T | ±0.2°C | |

We determined some electrical end uses by calculating the differences between other meters rather than metering them directly, which reduced the number and redundancy of sensors. For example, we determined the energy use of the heat pumps that serve the conference pavilion (HP-6, HP-7, HP-15, HP-16, and HP-17) by subtracting the conference lights and plug readings from the aggregated readings for the entire conference pavilion. Other examples are first-floor lighting that was calculated from the difference between the first-floor plugs, and the combined first-floor plugs and lights. Three minor heat pumps that do not serve occupied areas were not metered. These included HP-1 and HP-18, which are combined with the miscellaneous mechanical room loads, and ACU-1, which is combined with the first-floor receptacles.

### *5.2.3 Data Acquisition*

The sensors are continuously monitored by two dataloggers. One datalogger measures sensors in the main building; the other collects data from the conference pavilion and weather station. The dataloggers take measurements every 20 seconds and report totaled or averaged results every 15 minutes. A telephone modem allows the 15-minute data to be retrieved automatically every day. The data are stored as text files.

### 5.2.4 Measured Data Processing

This section discusses additional processing of the raw data from the data acquisition system. In many cases, the data sought are not measured directly, but are obtained indirectly by using direct measurements to perform calculations. This section also provides additional detail on how monitored data were handled and processed for daylight saving time (DST), filling missing data, generating inputs for modeling, and calculating uncertainty.

### 5.2.5 Data Handling

Figure 5-4 diagrams the steps involved in retrieving and processing data from the Merrill Center. Data are automatically retrieved from each datalogger daily. These raw data files are held on NREL servers with daily backup. Another program ensures that the data were received properly and without errors. If errors are discovered, the program sends an e-mail to NREL for attention.

After the data are checked, a custom computer program called SortData[3] reads the raw text files, cleans the data to remove duplicates, and outputs clean new text data for an integer number of days. These text files are then read by a custom program called HPBAnalyzer.pro[4], where results are analyzed and visualized.

[3] SortData is a custom data analysis application written by Nicholas Long (NREL) in the Delphi programming language.

[4] HPBAnalyzer is a custom data analysis application written by Brent Griffith (NREL) in an interpreted language called Interactive Data Language by Research Systems Incorporated, Boulder, CO.

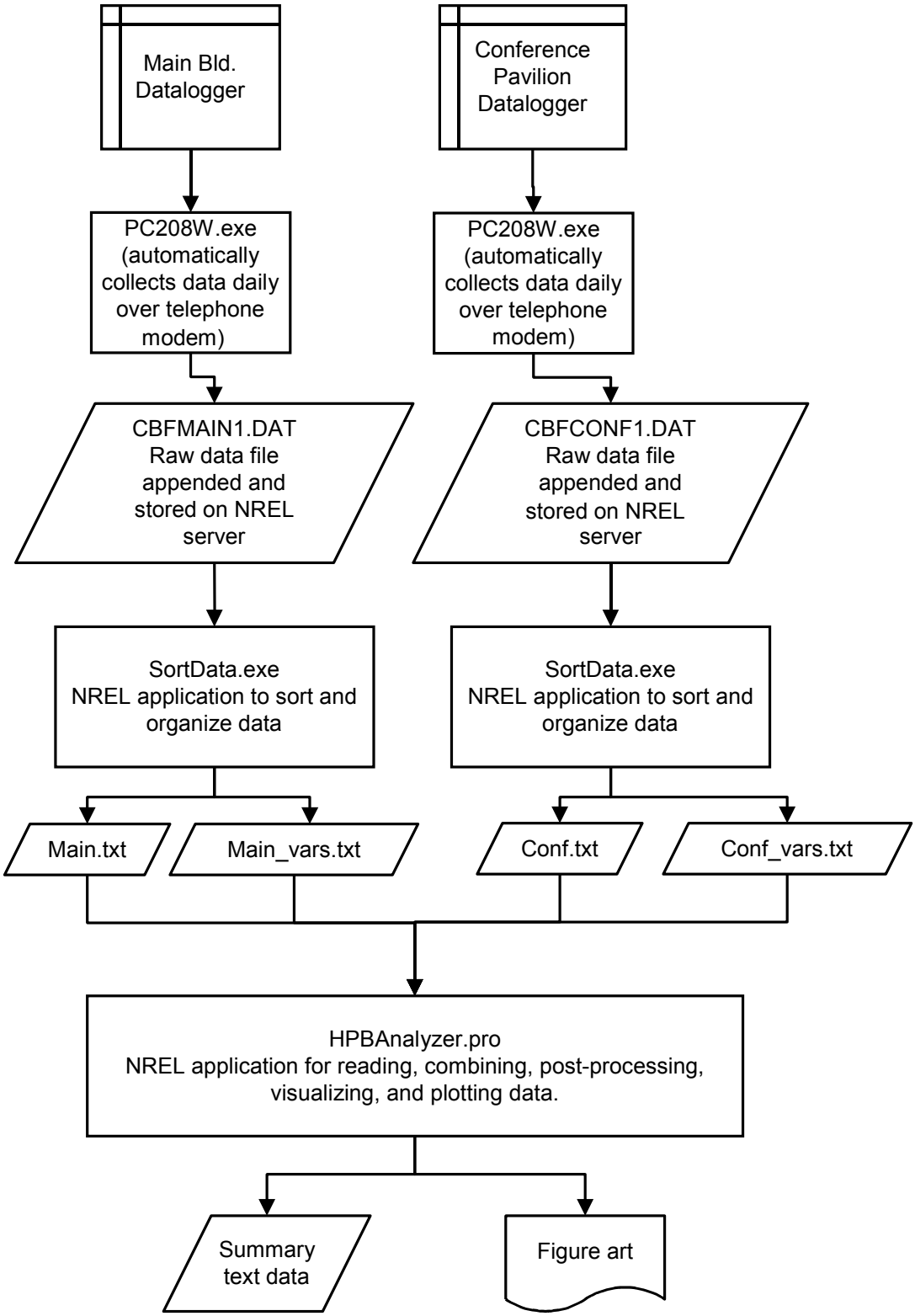


**Figure 5-4 Data collection, storage, and processing**

### 5.2.6 Daylight Saving Time

This section describes how NREL handled DST in the data monitoring analysis. The measured data are in Eastern Standard Time for the entire year; however, real behavior of the occupants and building operation follows DST in the summer. EnergyPlus (see Section 5.3.1) uses weather and scheduling data in Standard Time, but it allows for DST modeling when the schedules are input in Standard Time by automatically adjusting Standard Time to DST. Therefore, measured data related to schedules for modeling were processed in Standard Time (as if there were no DST).

To simplify scheduling data sets and computing average daily profiles, some data were rearranged (very slightly) to give the appearance of no DST. Data that were obtained when DST was in effect were shifted backward by 1 hour. The shifting of data involves corrupting 2 hours of data per year. For the spring DST shift (forward), an hour's worth of data are truncated, and for the fall DST shift (backward), an hour's worth of data are generated by replicating the values measured just before the new hour. This shifted data are referred to as DST data sets.

The DST data sets were used to generate results for daily profiles and schedules for modeling input. The use of monitored data in simulations is discussed in Section 5.3.2, but developing schedules without concern for DST is much more convenient. EnergyPlus was run with its own corrections for DST, which correct schedules, so that during the modeling, the shifting described in this section is essentially undone.

The DST data sets were not used for weather data because these were recorded in Standard Time. Weather does not adhere to the social convention, and EnergyPlus weather data are not in DST.

### 5.2.7 Filling Missing Data

The reality of experimental research is that measured data are often incomplete. The measurements at the Merrill Center have been reliable with no periods where data were lost or uncollected. Because the data set is very nearly complete, it is appropriate to correct the remaining problems. There are two main problem areas: (1) the electricity used for the first-floor receptacles and lights and (2) boiler operation.

#### *First-Floor Receptacles and Lights*

The transducer that measures the electrical loads for the first-floor receptacles (plugs) experienced intermittent malfunctions during two separate periods and resulted in lost data. The exact cause of the problem was not determined. The first period extended from about 8:00 p.m. on June 5, 2002 through about 9:00 a.m. on July 4, 2002. The second extended from about 11:00 a.m. on November 23, 2002 through about 12:00 noon on February 21, 2003. The loss of these data also affects the first-floor light loads because the loads for lights and plugs are measured together and the lighting load is determined by subtracting the plug loads.

To extrapolate values for plugs and lights, NREL analyzed periods of good data to develop typical daily profiles. Averaged curves were developed that describe the ratio of the plug loads to the combination of plug *and* light loads. Three separate curves were formulated for weekdays, Saturdays, and Sundays. Holidays were grouped with Sundays. Figure 5-5 shows the average curves used to correct the data.

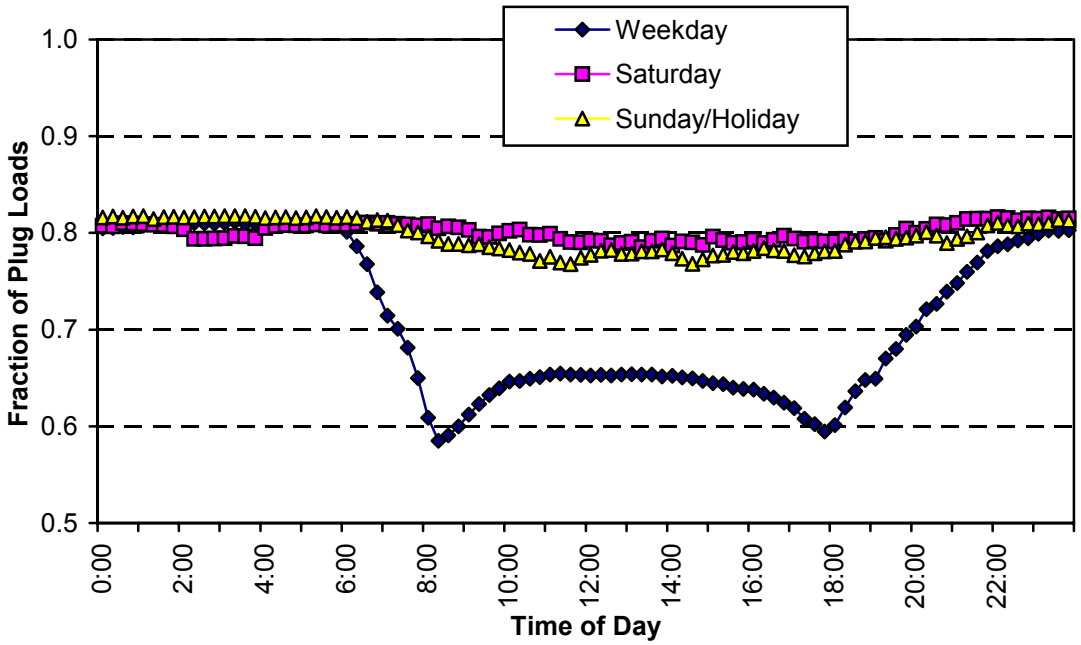


**Figure 5-5 Fraction of first-floor plugs to sum of plugs and lights**

Figure 5-6 shows the entire first-floor lighting data set as a time map with the original problem data on the left and the corrected data on the right. Similarly, Figure 5-7 shows the entire first-floor plug data set with the measured data on the left and the corrected data on the right. Appendix A provides an explanation of the figure art used in Figure 5-6 and Figure 5-7. The image-based data visualizations in the figures have time-of-day across the horizontal (from midnight to midnight) and day along the vertical (from about November 1, 2001 at the top to about April 29, 2003 at the bottom). The colors used in these figures represent actual values (in kilowatt-hours) as shown in the scales depicted as a colorbar.

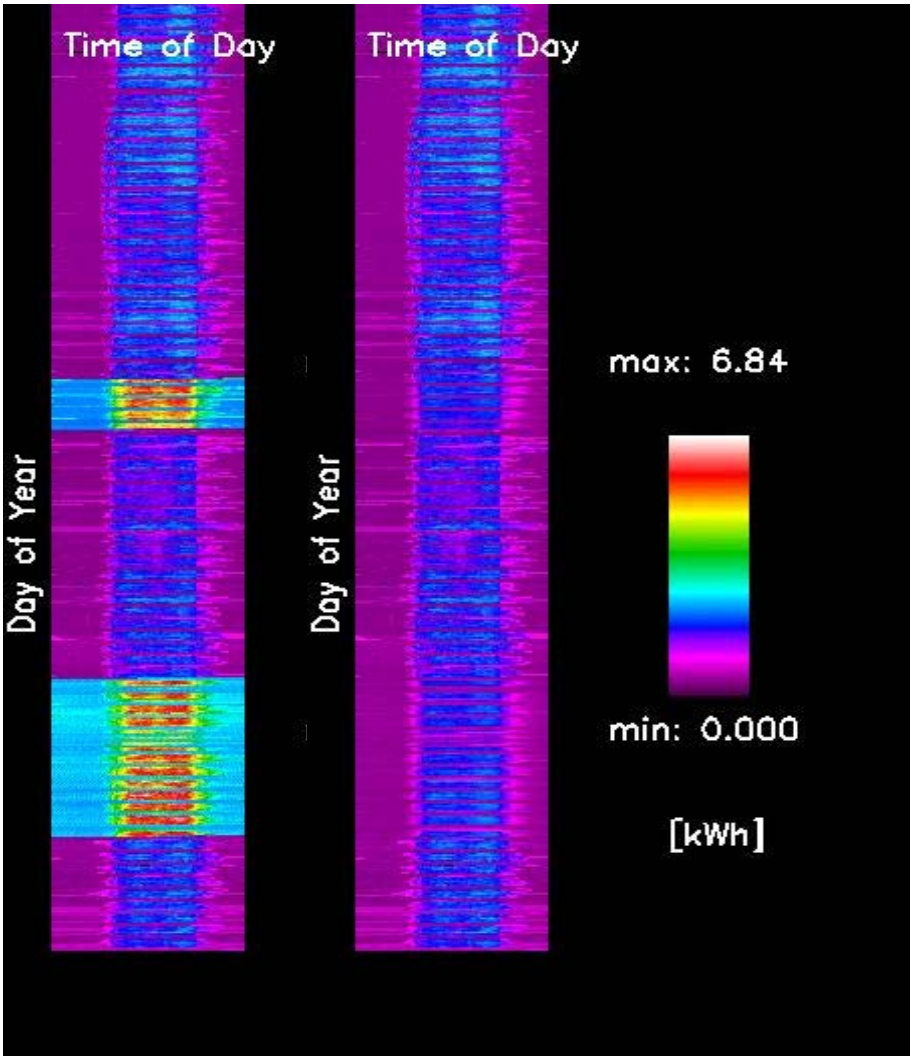


**Figure 5-6** **Lighting load data for main building first floor: left map is the original data, right map is corrected[5]**

[5] Figure is color, inaccurate if reproduced in black and white

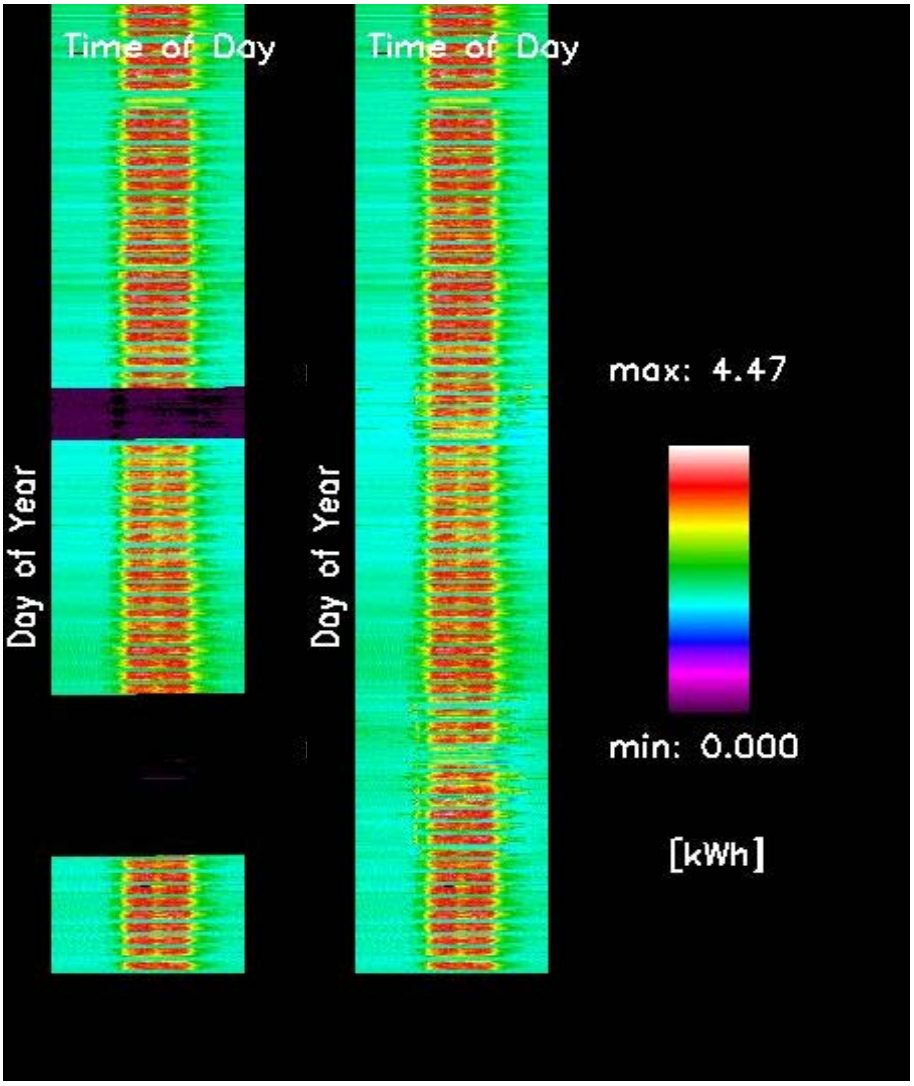


**Figure 5-7 Receptacle/plug load data for main building first floor: left map is original, right map is filled[6]**

*Boiler Operation and Propane Consumption*

The transducer that measures boiler operation was installed on March 7, 2002. To fully characterize the energy used for this type of heating, NREL used data for the boiler operation and associated propane use for the period before transducer installation, which extended from November 7, 2001 to March 7, 2002. The boiler consumes gas at a fixed rate, so a transducer that measures burner start time (when the unit has cycled on) provides the total energy into the system.

The two measured variables available are: (1) the hot-water circulation pump energy use in kilowatt-hours per 15-minute period and (2) the minutes of boiler operation per 15-minute period. The desired quantity is propane consumption with the same 15-minute data frequency as the other measurements. The boiler was assumed to be operating at its full rated capacity (determined from product literature) of 860 kBtu/h (252 kW). Where boiler operation times are available, these running times are converted to energy use by directly multiplying by the appropriate rate.

[6] Figure is shown in color, inaccurate if reproduced in black and white.

The boiler is used to supply hot water to fin-tube heaters located in perimeter zones and unit heaters in various locations as a supplement to and backup for the heat-pump-based air system. The boiler cycles on and off to meet a hot-water fluid set point that is controlled by the central EMS. The data were filled by analyzing the number and duration of boiler operation events. A boiler event is determined by initiating supplementary heating that may extend for varying amounts of time depending on the conditions. Events are characterized by examining electrical data for the circulation pumps, which are usually off. Circulation pumps that are on indicate a boiler event. The duration of the event is shown in the pump data, but these do not directly indicate the boiler cycling. The boiler will cycle during an event. Therefore, a model was developed to determine propane energy used as a function of the duration of a boiler event by assuming a direct relationship between the amount of cycling and the length of a time that heating is required. The model was developed by examining the trends shown in 27 boiler events that occurred after the boiler operation transducer was installed (from March 7, 2002 to November 6, 2002). A pump energy use in excess of 0.09 kWh in a 15-minute period was used as a threshold to determine when a boiler event was occurring. NREL used these data to generate a linear model of energy use as a function of the duration of boiler event. The model was then applied to fill propane energy use for the 67 boiler events that occurred before the boiler operation transducer was installed. Figure 5-8 shows the source data and the line fitted to these data to create the model.

Assuming a propane price of $1.20/gal ($0.32/L), the propane use for heating is about $845 for the model analysis year. Propane was also used for cooking, which was not measured, so the split between cooking and heating was not known. Actual propane expenditures were $827.08, but there was an unknown amount of carryover from the previous year. However, the estimate of $845 is consistent with propane expenditures and provides some confidence in the model for propane use. (Note that the propane use is minor compared to overall electricity; expenditures for propane are just 2.6% of those for electricity, but site energy use for only heating end use is split about evenly between propane and electricity. See Section 6.1.1 and Table 5-6.)

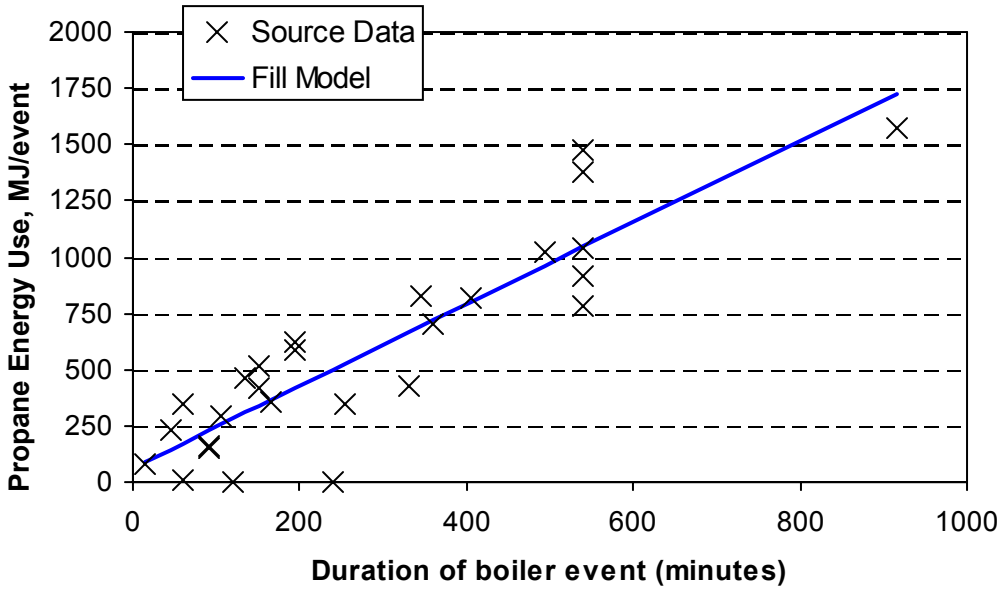


**Figure 5-8 Source data and model used to fill data on boiler propane use**

### 5.2.8 Monitoring System Uncertainty

The accuracy levels for measured data points are listed in Table 5-1 and Table 5-2. These uncertainty estimates are for the sensors and do not always represent how well the actual variable was measured. Most are derived from manufacturer specifications. Thermocouple-based temperature measurement accuracy is a function of the wire's uniformity (±0.5°C, special limits of error), voltage measurement accuracy (±0.009°C), voltage measurement resolution (±0.001°C), and reference junction temperature measurement (±0.2°C). Voltage-to-temperature errors were modeled with a slope of 1.19°C/mV. Combining these uncertainties in quadrature leads to an estimate of measurement accuracy of ±0.54°C for the type-T thermocouple sensors.

Uncertainty arises for monitoring results from transducer inaccuracies and the modeling used to determine boiler propane consumption. The propane consumption is determined indirectly from boiler run time measurement and modeling, and is therefore assigned a relatively high uncertainty of ±10% (by assumption). Individual electricity measurements are 0.5% based on the manufacturer's data. Total values form a summation of as many as seven individual measurements, but the errors are assumed to be independent and to not increase the level of uncertainty.

### 5.2.9 Monitoring Results

This section presents results from the detailed monitoring. First, the electrical measurements are compared to utility bills. Results are then summarized for a one-year period and then broken down into monthly and daily periods. Finally, results for specific systems in the Merrill Center are discussed. Appendices contain a collection of figures showing results in more detail. Appendix A provides an illustration of the time map figure art used to depict a year's worth of 15-minute data. Appendix B contains figures that show selected results from detailed monitoring. Appendix C contains figures that show the resulting weather data used in the weather file for EnergyPlus modeling. Appendix D contains figures that show the calibrated schedules.

#### *Utility Metering*

This section presents results from monthly utility metering of electricity. The CBF provided copies of the utility bills. The electricity costs for the analysis year are listed in Table 5-3. Figure 5-9 plots the data in Table 5-3. The billing data show that demand charges are comparable in size to energy charges, with 47.5 % of the charges billed for energy, 47.3% for demand, and 5.2% for fixed charges and taxes.

**Table 5-3 Electrical Energy Costs from Utility Billing**

| Billing Cycle Month | Costs | | |
|---|---|---|---|
| | Energy ($) | Demand ($) | Fixed, Taxes ($) |
| November 2001 | 1,085.91 | 825.55 | 134.18 |
| December 2001 | 1,119.48 | 990.66 | 134.43 |
| January 2002 | 1,043.78 | 1,147.08 | 132.98 |
| February 2002 | 1,156.89 | 895.07 | 135.36 |
| March 2002 | 1,054.36 | 964.59 | 133.28 |
| April 2002 | 939.28 | 990.66 | 130.97 |
| May 2002 | 1,235.67 | 1,236.26 | 135.13 |
| June 2002 | 1,631.49 | 1,860.30 | 137.67 |
| July 2002 | 1,755.31 | 1,845.99 | 139.60 |
| August 2002 | 1,589.82 | 1,860.30 | 137.36 |
| September 2002 | 1,300.17 | 1,490.12 | 135.51 |
| October 2002 | 1,011.39 | 764.72 | 132.28 |
| **Total** | **14,923.55** | **14,871.30** | **1,618.75** |

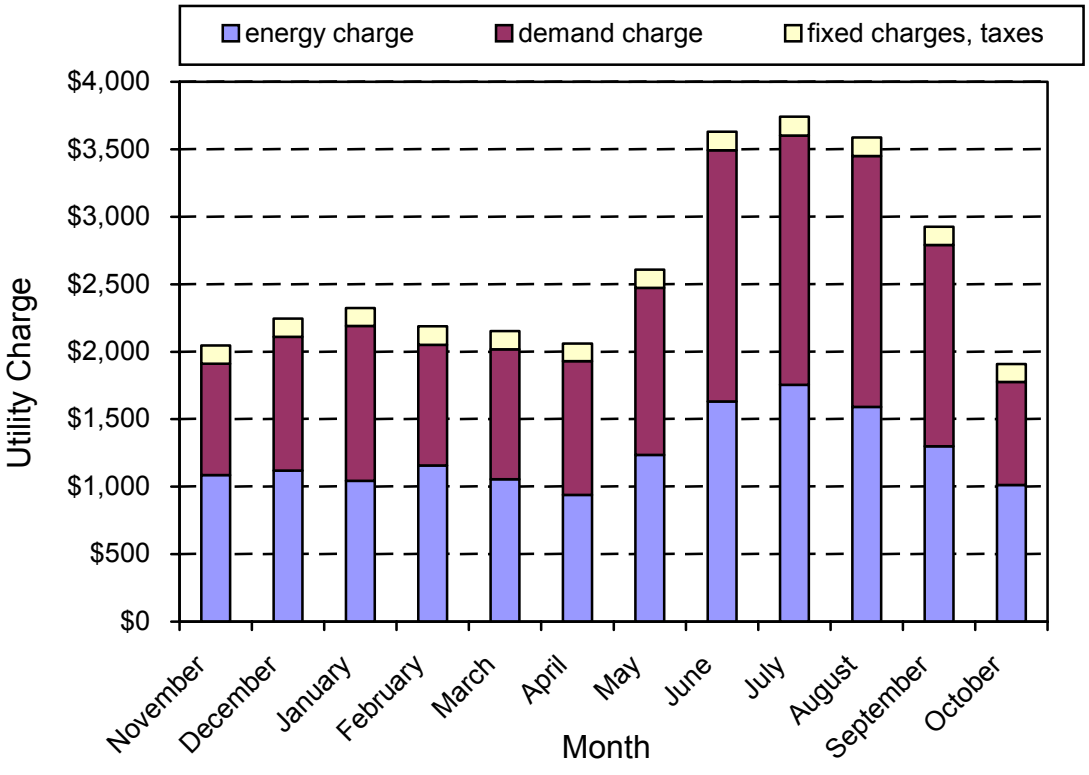


**Figure 5-9 Summary of utility electricity bills**

The billing data also provide a method of checking that the monitored data are valid. Table 5-4 shows a comparison of the utility data to the measured data from the monitoring. The measured data were analyzed in bins that correspond to the billing cycles. Because the exact time the meter was read is not known, we assumed, for convenience, that the transition between billing periods occurred at midnight so that the billing period from November 7, 2001 to December 10, 2001 ends at the beginning of December 10.

**Table 5-4 Comparison of Utility Bills to Measured Data**

| Billing Period | | | | Billing Data | | Measured Data | |
|---|---|---|---|---|---|---|---|
| Month | Days | Start | End | Energy (kWh) | Demand (kW) | Energy (kWh) | Demand (kW) |
| November 2001 | 33 | 11/7/2001 | 12/10/2001 | 27,500 | 95 | 27,389 | 90.8 |
| December 2001 | 31 | 12/10/2001 | 1/10/2002 | 28,200 | 114 | 28,267 | 119.7 |
| January 2002 | 28 | 1/10/2002 | 2/7/2002 | 26,300 | 132 | 26,220 | 136.3 |
| February 2002 | 32 | 2/7/2002 | 3/11/2002 | 29,400 | 103 | 29,487 | 106.6 |
| March 2002 | 29 | 3/11/2002 | 4/9/2002 | 26,700 | 111 | 26,891 | 111.4 |
| April 2002 | 29 | 4/9/2002 | 5/8/2002 | 23,700 | 114 | 23,745 | 117.0 |
| May 2002 | 33 | 5/8/2002 | 6/10/2002 | 29,100 | 126 | 28,625 | 126.0 |
| June 2002 | 30 | 6/10/2002 | 7/10/2002 | 32,400 | 130 | 32,238 | 132.1 |
| July 2002 | 23 | 7/17/2002 | 8/9/2002 | 34,900 | 129 | 34,633 | 128.1 |
| August 2002 | 31 | 8/9/2002 | 9/9/2002 | 32,000 | 130 | 31,619 | 129.4 |
| September 2002 | 29 | 9/9/2002 | 10/8/2002 | 29,600 | 116 | 29,535 | 123.2 |
| October 2002 | 30 | 10/8/2002 | 11/7/2002 | 25,400 | 88 | 25,216 | 88.2 |
| **Total** | | | | **345,200** | | **343,865** | |

Results shown in Table 5-4 provided assurances that monitored electricity data are robust. The total billed electrical energy was 345,200 kWh and the total from monitoring was 343,865 kWh. Although it is difficult to say which method of measuring electricity is more accurate, the fact that they agree to within 0.4% (in aggregate for the year) indicates that the monitored data for electricity appear reliable. The differences in demand are somewhat larger and probably arise because of differing integration times; the utility's demand metering is over 30-minute periods and the monitoring time period is over 15-minute periods. Typically, this would produce a smaller demand on the 30-minute interval compared with the 15-minute interval.

Results shown in Table 5-4 can also be analyzed to determine the electrical utility load factor for the Merrill Center. The load factor is defined as the ratio of the actual electrical energy used (in kWh) to electrical energy that would have been consumed were the peak demand rate used for the entire period. The electrical utility system benefits from load factors closer to unity. For the one-year monitoring period, the load factor was 0.30. The average load factor over the monthly periods was 0.35 with a maximum of 0.49 and a minimum of 0.29.

### *Annual Monitoring Results*

Site energy use was determined from analysis of monitoring results from November 7, 2001 to November 6, 2002. There are two forms of site energy use, net and total, where *net* gives credit for on-site production from solar electric PV panels. Uncertainty in the measured values for site energy use is estimated at just 0.6% because of the high accuracy in the electricity measurements and the low quantity of propane consumed. The purchased electricity was 1,173 MMBtu (1,238 GJ), the estimated propane

consumption was 64.2 MMBtu (67.7 GJ), and the electricity generated on site from PV was 9.1 MMBtu (9.6 GJ = 2,676 kWh). Therefore, the total site energy use was 1,247±7.5 MMBtu (1,315 GJ) for the period from November 7, 2001 to November 6, 2002. The total site EUI was 40.2±0.2 kBtu/ft$^2$ (457±2.7 MJ/m$^2$). The net site energy use was 1,238 MMBtu (1,306 GJ) with intensity of 39.9±0.2 kBtu/ft$^2$ (453±2.7 MJ/m$^2$).

Source energy use is determined from net site energy use with assumed multipliers. Electricity conversion efficiency is assumed at 31%. Propane conversion is assumed at 93%. The level of these assumptions was determined from data in the Energy Information Agency's *Annual Energy Outlook* (EIA 2003). Although such conversions cannot be considered very accurate, their errors were not propagated when uncertainty was estimated. In the present report, source energy consumed for electricity is determined from net (purchased) electricity, which gives credit for the PV generated on site. The net source energy use for electricity was 3,785±15 MMBtu (3,993±16 GJ) and 69±6.9 MMBtu (72.8±7.3 GJ) for propane for a total of 3,854±22 MMBtu (4,066±23 GJ) for the period from November 7, 2001 to November 6, 2002. Therefore, the source energy intensity was 124±0.7 kBtu/ft$^2$ (1.41±0.01 GJ/m$^2$).

Energy costs are determined from utility electricity bills and analysis of propane use. The total electricity expenditures were $31,413.60. The results of analysis for propane use for heating was $875 ±$87 with an assumed price of $1.20/gal ($0.32/L). The result from the monitoring effort for the period from November 7, 2001 to November 6, 2002 is $32,288.60 ±$87. This translates into an energy cost intensity of $1.04/ft$^2$±$0.003/ft$^2$ ($11.31/m$^2$±$0.03/m$^2$).

The annual totals and breakdown for individual end uses are presented in Table 5-5, Table 5-6, and Table 5-7, and graphically in Figure 5-10 and Figure 5-11.

### *Monthly Monitoring Data*

Monthly totals for measured site energy are divided into major end-use categories that are listed in Table 5-5 and shown graphically in Figure 5-10. HVAC energy includes propane. Energy use for HVAC includes equipment such as heat pumps and water pumps. The breakdown of the HVAC components is listed in Table 5-6 and shown graphically in Figure 5-11. Miscellaneous energy use is characterized in Table 5-7; it includes energy use for the elevator, the exterior and garage lighting, and the mechanical room and storage room receptacles.

Plug loads are the largest energy end-use category, followed closely by HVAC. Lighting energy use does not show clear seasonal dependence, which suggests that daylight is not being harvested very well. Miscellaneous loads are significant and show seasonal dependence that indicates there could be heating loads associated with the elevator (oil heating) and the ground-floor receptacles.

HVAC energy use does show seasonal dependence: more energy is used during the cooling season. Site energy use for heating is split evenly between propane and electric heat pumps. In the winter, the heat pumps on the second floor use much less electricity than those on the first floor, but the situation is reversed during the summer. The reversal is likely because the open area between the first and second floors allows warm air to move up to the second floor.

**Table 5-5 Site Energy End-Use Characterization: Monthly**

| Billing Period | HVAC (kWh) | Office Lights (kWh) | Plugs (kWh) | Misc. (kWh) | Conf. Pavilion Lights & Plugs (kWh) | PV Energy Produced (kWh) | Total Site Energy (kWh) |
|---|---|---|---|---|---|---|---|
| November 2001 | 3,291 | 6,433 | 11,770 | 3,406 | 3,361 | 301 | 27,960 |
| December 2001 | 10,791 | 5,927 | 10,246 | 3,622 | 3,011 | 230 | 33,367 |
| January 2002 | 7,718 | 5,811 | 9,669 | 3,570 | 2,799 | 224 | 29,343 |
| February 2002 | 9,842 | 7,739 | 10,623 | 3,328 | 3,005 | 334 | 34,203 |
| March 2002 | 8,327 | 6,243 | 9,817 | 2,907 | 2,907 | 183 | 30,018 |
| April 2002 | 3,012 | 5,958 | 9,899 | 2,331 | 2,745 | 190 | 23,755 |
| May 2002 | 7,081 | 6,125 | 10,373 | 2,197 | 3,060 | 208 | 28,628 |
| June 2002 | 13,136 | 5,416 | 9,202 | 1,776 | 2,896 | 189 | 32,237 |
| July 2002 | 14,356 | 6,645 | 9,244 | 1,807 | 2,800 | 196 | 34,656 |
| August 2002 | 12,483 | 5,429 | 9,303 | 1,767 | 2,850 | 211 | 31,621 |
| September 2002 | 10,706 | 5,430 | 9,210 | 1,607 | 2,828 | 246 | 29,535 |
| October 2002 | 6,452 | 6,066 | 9,978 | 2,426 | 2,592 | 164 | 27,350 |
| **Total** | **107,195** | **73,222** | **119,334** | **30,744** | **34,854** | **2,676** | **362,673** |

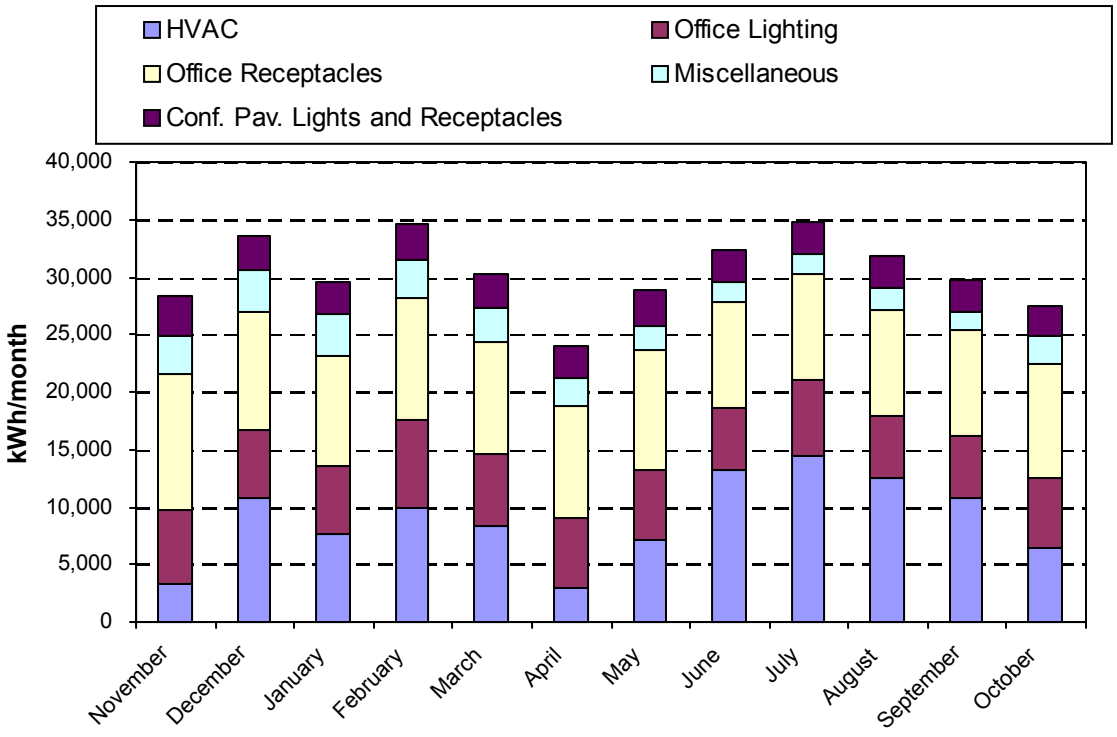


**Figure 5-10 Energy end-use breakdown by billing cycle**

**Table 5-6 HVAC Site Energy Use Characterization: Monthly**

| Billing Period | 1st-Floor Heat Pumps (kWh) | 2nd-Floor Heat Pumps (kWh) | Conf. Pavilion Heat Pumps (kWh) | Ground Loop Pumps (kWh) | Boiler Propane (kWh) | Hot-Water Pumps (kWh) | Total HVAC Electricity (kWh) | Total HVAC Site Energy (kWh) |
|---|---|---|---|---|---|---|---|---|
| November 2001 | 1,163 | 567 | 461 | 514 | 573 | 13 | 2,719 | 3,291 |
| December 2001 | 2,845 | 902 | 1,318 | 511 | 5,100 | 115 | 5,691 | 10,791 |
| January 2002 | 2,174 | 487 | 1,412 | 460 | 3,124 | 61 | 4,594 | 7,718 |
| February 2002 | 3,235 | 471 | 664 | 667 | 4,717 | 88 | 5,125 | 9,842 |
| March 2002 | 3,531 | 471 | 571 | 575 | 3,128 | 50 | 5,199 | 8,327 |
| April 2002 | 1,144 | 632 | 658 | 566 | 11 | 2 | 3,001 | 3,012 |
| May 2002 | 1,700 | 3,164 | 1,440 | 777 | 0 | 0 | 7,081 | 7,081 |
| June 2002 | 3,375 | 5,697 | 2,320 | 1,745 | 0 | 0 | 13,136 | 13,136 |
| July 2002 | 4,129 | 6,822 | 2,537 | 844 | 24 | 0 | 14,332 | 14,356 |
| August 2002 | 3,591 | 5,637 | 2,231 | 1,024 | 0 | 0 | 12,483 | 12,483 |
| September 2002 | 2,993 | 4,978 | 1,752 | 982 | 0 | 0 | 10,706 | 10,706 |
| October 2002 | 2,829 | 429 | 486 | 536 | 2,134 | 38 | 4,318 | 6,452 |
| **Total** | **32,709** | **30,256** | **15,851** | **9,201** | **18,810** | **367** | **88,385** | **107,195** |

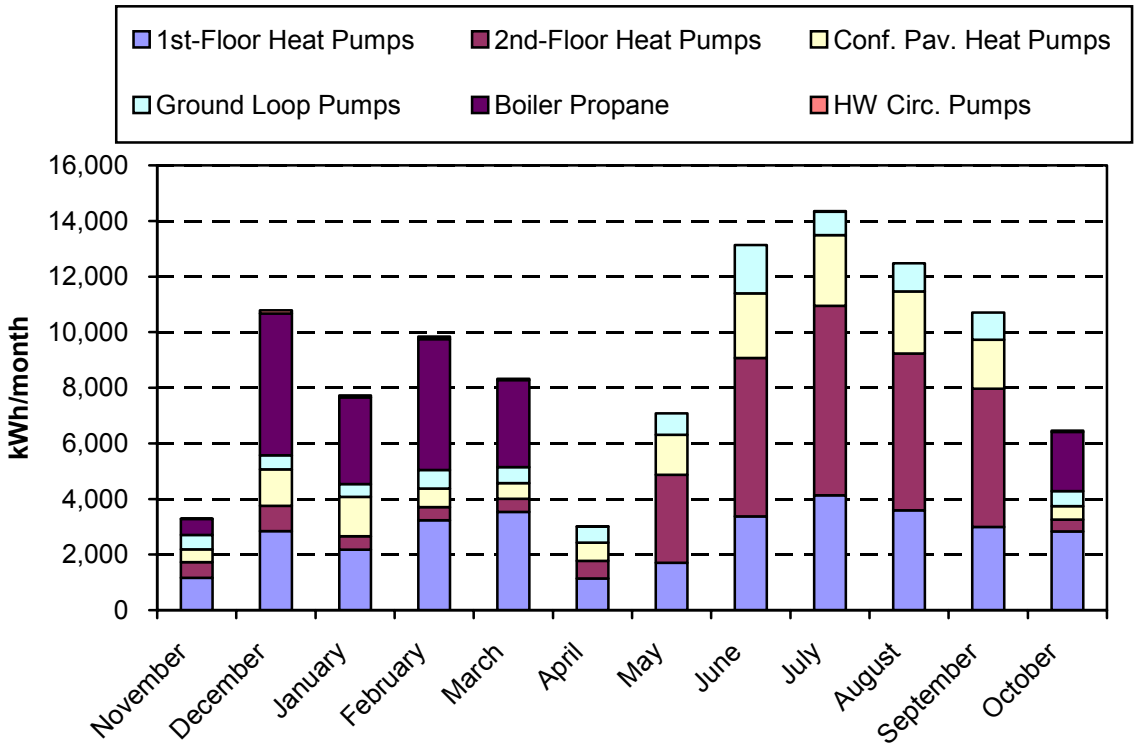


**Figure 5-11 HVAC energy end-use breakdown by billing cycle**

**Table 5-7 Miscellaneous Site Energy Use Characterization: Monthly**

| Billing Period | Elevator (kWh) | Exterior Lighting (kWh) | Mechanical Room Loads (kWh) | Totals (kWh) |
|---|---|---|---|---|
| November 2001 | 421 | 1,564 | 1,421 | 3,406 |
| December 2001 | 424 | 1,210 | 1,988 | 3,622 |
| January 2002 | 405 | 1,171 | 1,994 | 3,570 |
| February 2002 | 444 | 1,105 | 1,779 | 3,328 |
| March 2002 | 407 | 1,033 | 1,467 | 2,907 |
| April 2002 | 375 | 947 | 1,010 | 2,331 |
| May 2002 | 367 | 991 | 839 | 2,197 |
| June 2002 | 316 | 809 | 651 | 1,776 |
| July 2002 | 271 | 880 | 655 | 1,807 |
| August 2002 | 252 | 783 | 732 | 1,767 |
| September 2002 | 267 | 707 | 633 | 1,607 |
| October 2002 | 340 | 931 | 1,155 | 2,426 |
| **Total** | **4,289** | **12,132** | **14,324** | **30,746** |

The better resolution of the monitored data (compared to the utility meter) allows the time that demand charges incur to be characterized and the end uses at the time of demand to be composed. Table 5-8 summarizes the situation at peak demand for the period from November 7, 2001 to November 6, 2002.

**Table 5-8 Electrical Demand Characterization**

| Billing Period | Peak Demand: Date and Time* | HVAC (kW) | Lights (kW) | Plugs (kW) | Ele-vator (kW) | Exter. Lights & Mech. Room (kW) | Conf. Pavilion Lights & Plugs (kW) | PV Power (kW) | Total (kW) |
|---|---|---|---|---|---|---|---|---|---|
| November 2001 | 12/3/01 9:00 a.m. | 27.2 | 18.3 | 18.7 | 12.2 | 10.9 | 4.5 | –0.9 | 90.8 |
| December 2001 | 1/1/02 8:00 a.m. | 79.6 | 15.7 | 14.0 | 0.5 | 5.1 | 4.7 | –0.0 | 119.7 |
| January 2002 | 2/5/02 9:00 a.m. | 83.6 | 18.5 | 19.5 | 2.3 | 6.4 | 6.9 | –0.8 | 136.3 |
| February 2002 | 3/4/02 8:00 a.m. | 61.2 | 19.3 | 13.1 | 2.3 | 6.0 | 4.8 | –0.1 | 106.6 |
| March 2002 | 4/1/02 8:00 a.m. | 66.7 | 19.1 | 12.7 | 3.0 | 4.7 | 5.2 | –0.0 | 111.4 |
| April 2002 | 4/18/02 11:15 a.m. | 66.5 | 17.8 | 22.5 | 2.2 | 2.7 | 6.4 | –1.1 | 117.0 |
| May 2002 | 6/6/02 1:15 p.m. | 80.3 | 17.2 | 20.9 | 1.1 | 2.6 | 4.1 | –0.9 | 125.9 |
| June 2002 | 6/24/02 11:30 a.m. | 85.7 | 17.3 | 19.1 | 2.2 | 2.5 | 5.8 | –0.9 | 132.1 |
| July 2002 | 7/22/02 1:45 p.m. | 85.1 | 16.7 | 18.9 | 0.5 | 2.5 | 5.4 | –1.1 | 128.1 |
| August 2002 | 8/15/02 2:00 p.m. | 85.7 | 17.1 | 20.3 | 0.6 | 3.1 | 3.3 | –0.7 | 129.4 |
| September 2002 | 10/2/02 11:15 a.m. | 77.9 | 17.6 | 20.9 | 0.6 | 1.8 | 6.8 | –2.3 | 123.2 |
| October 2002 | 10/29/02 10:00 a.m. | 34.8 | 20.4 | 23.4 | 0.5 | 4.2 | 5.1 | –0.0 | 88.2 |

* In Eastern Standard Time (add one hour for DST when appropriate)

Figure 5-12 shows the situation at the time of peak demand for each billing cycle. HVAC energy use is consistently the largest contributor to demand charges. HVAC demand can be somewhat managed through controls, which suggests that demand charges might be reduced by changing thermostat set points over the day. Usually, the contributions from plugs and lights are uniform throughout the year. The elevator made a substantial contribution for the November 2001 cycle, but not for other billing cycles. The PV system reduced demand an average of 0.7 kW (the most power reduced was 2.3 kW). The number of kilowatts reduced by the PV system is far below the nominal capacity of 4.2 kW. For 3 of the 12 months, the PV system did not reduce demand at all, which suggests that PV systems do not reduce demand charges as much as might be expected.

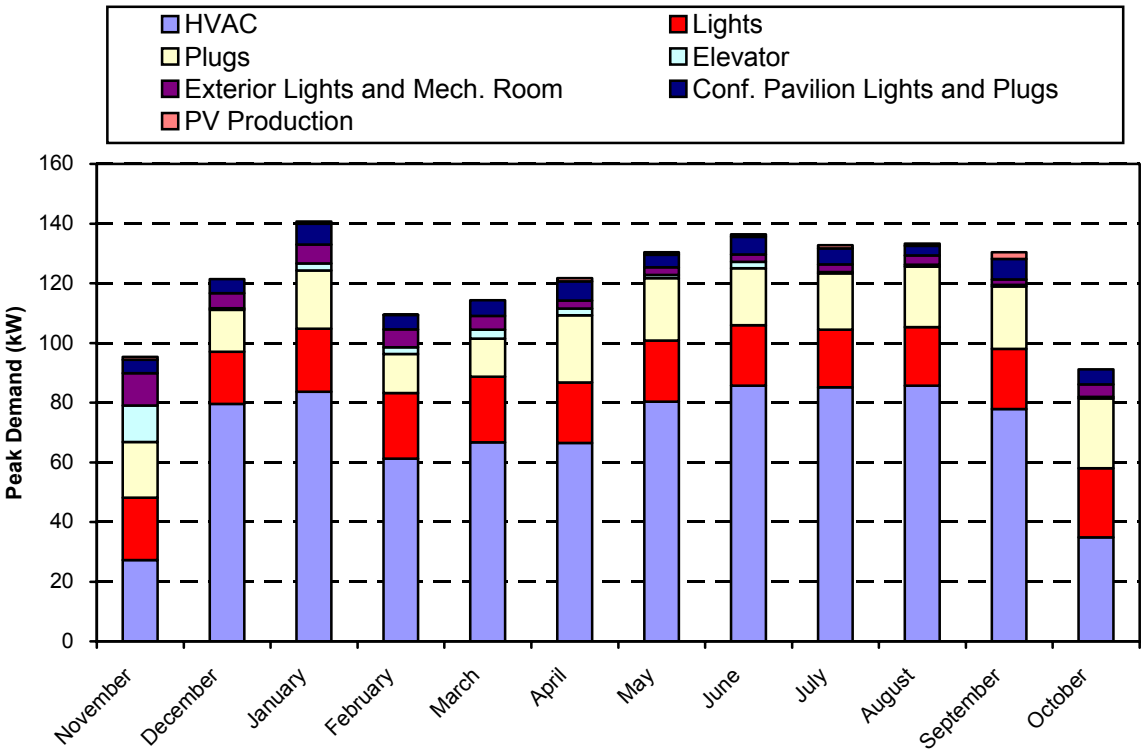


**Figure 5-12 Coincident end uses at time of peak demand by billing cycle**

*Daily Monitoring Data*

NREL reduced the monitoring data presented in this section to daily values and focused on demand issues. Figure 5-13 presents the peak electrical demand for every working weekday for the period from November 7, 2001 to November 6, 2002. The highest of these in a given billing period constitute the basis of demand charges. Figure 5-14 shows similar daily peak demand but for only Saturdays, Sundays, and holidays. Holidays are assumed to be the usual U.S. legal holidays. Figure 5-15 shows the resulting time of day that the peaks occurred for the weekdays and Figure 5-16 shows the time of day for peaks on Saturdays, Sundays, and holidays.

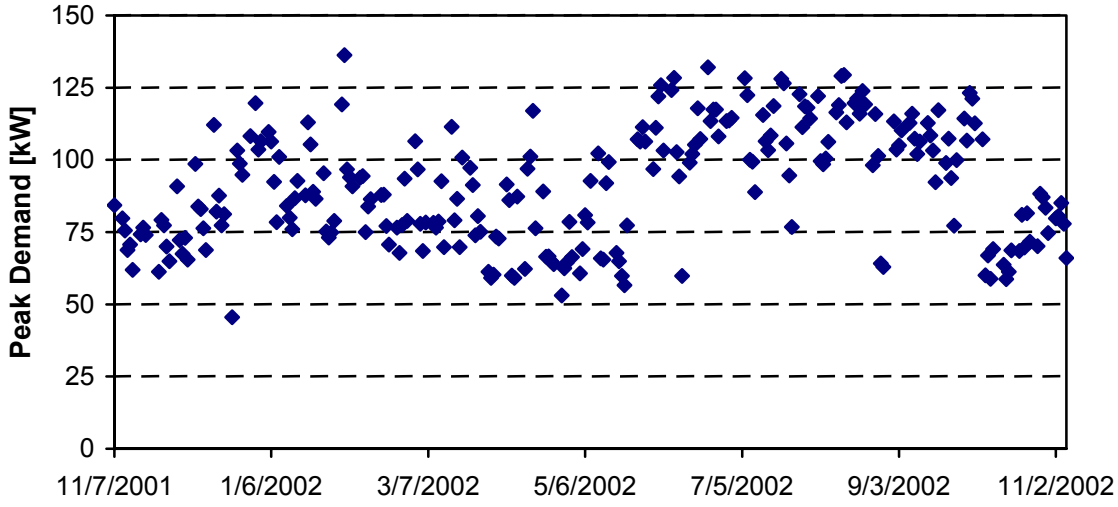


**Figure 5-13 Peak demand: working weekdays**

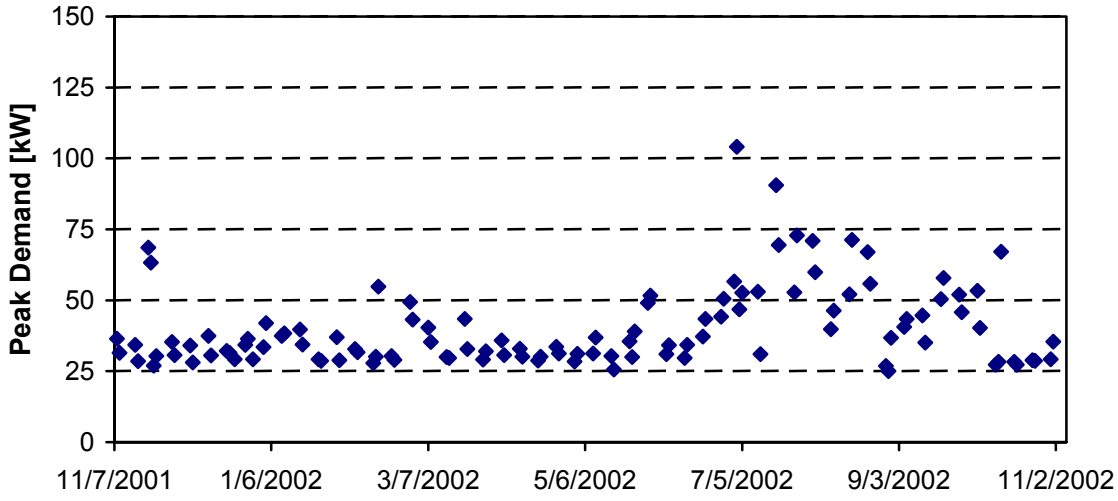


**Figure 5-14 Peak demand: Saturdays, Sundays, and holidays**

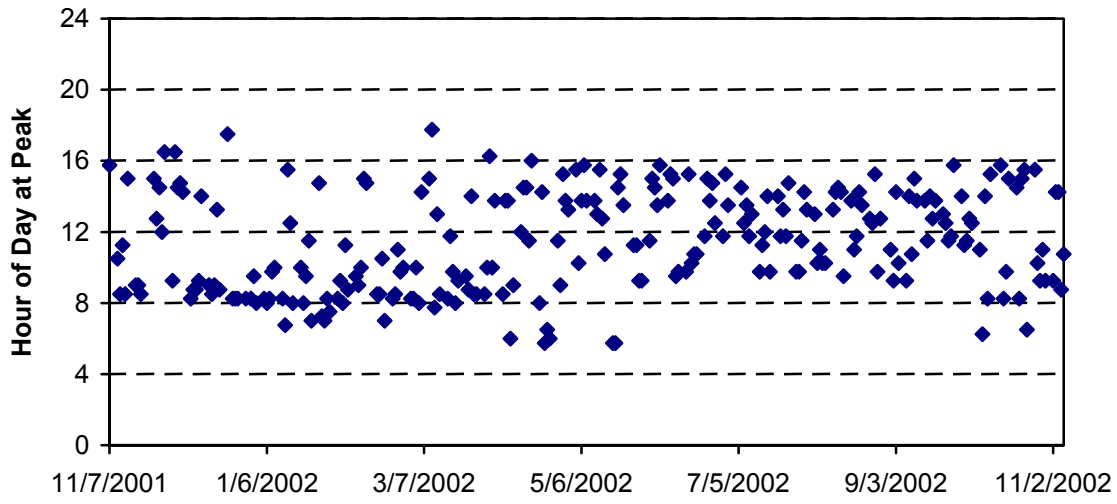


**Figure 5-15 Time of day at peak demand: working weekdays**

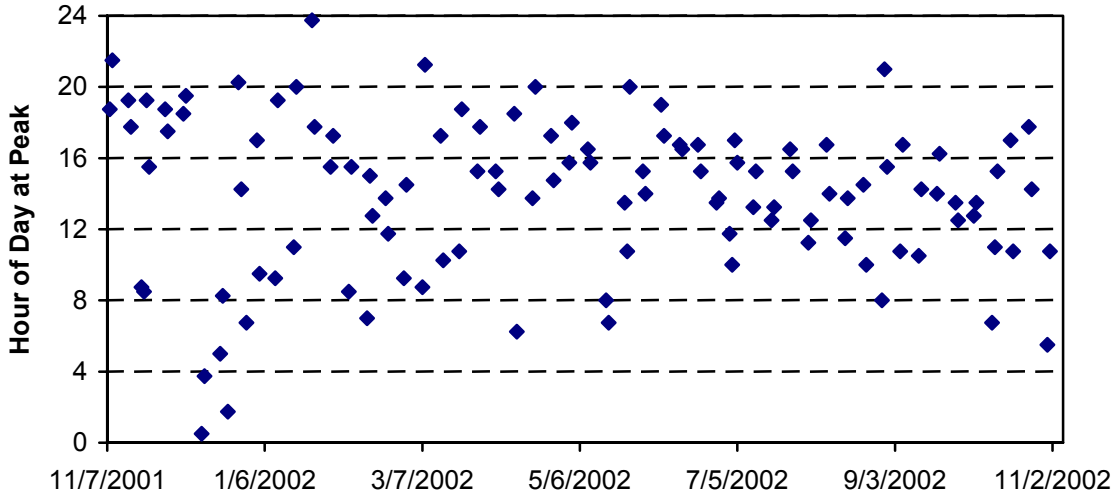


**Figure 5-16 Time of day at peak demand: Saturdays, Sundays, and holidays**

The highest peaks occur during working weekdays. Much of the wintertime peak is caused by morning warmup, as seen with demands clustered around hour 8 (Figure 5-15). Summertime peaks are spread out across the occupied hours between late morning and late afternoon. On weekends and holidays, wintertime peaks can happen any time of the day; summertime peaks tend to occur in the afternoon.

For the year analyzed, we also compared the time of day that the HVAC electrical load peaked to the time of day that the entire facility peaked. Results showed that these two peaks exactly coincided 48% of the days (55% of weekdays). The two peaks differed by two or more hours for 28% of the days (21% of weekdays).

Average daily profiles characterize how energy is used throughout the day. Average profiles were generated by averaging all the data from working weekdays at the corresponding time of day. Figure 5-17 shows the average daily profile for working weekdays in January 2002. Figure 5-18 shows the average daily profile for working weekdays in August 2002.

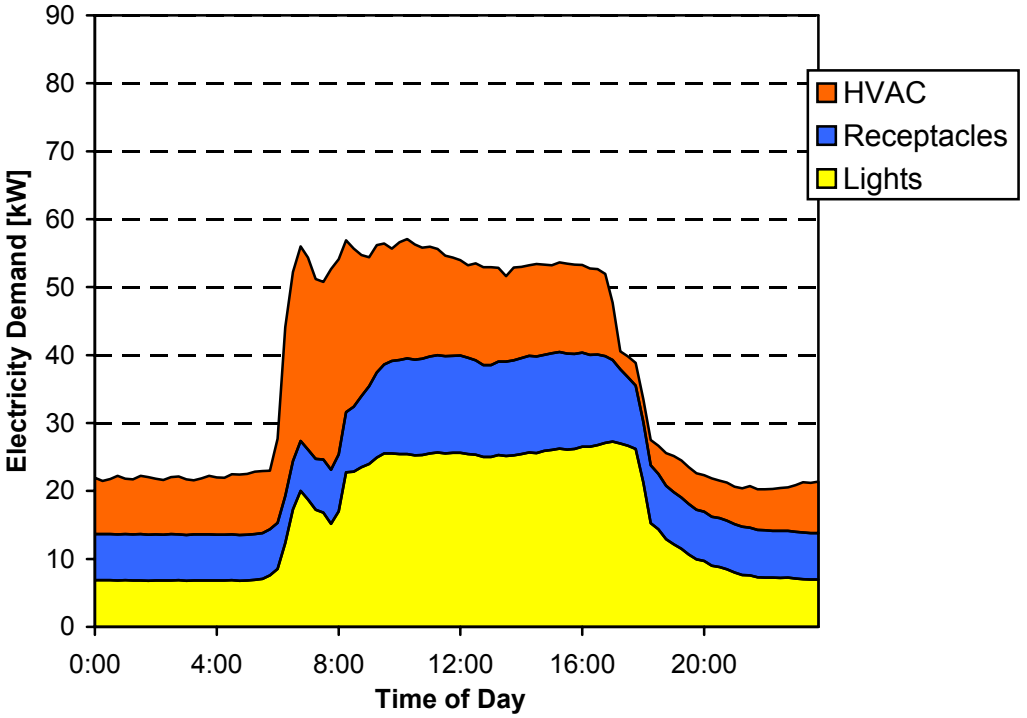


**Figure 5-17 January 2002 average daily profile**

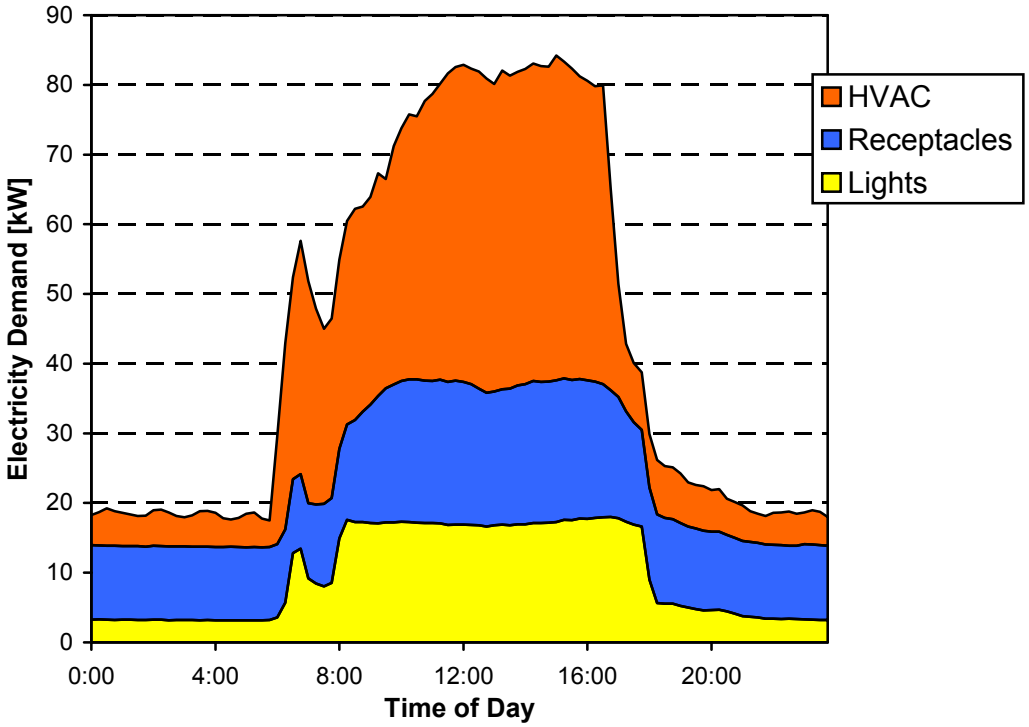


**Figure 5-18 August 2002 average daily profile**

Figure 5-17 and Figure 5-18 reveal energy demand characteristics and opportunities for energy savings at the Merrill Center. After an initial morning spike caused by the cleaning crew, lights come on at the same time the HVAC increases. Figure 5-17 and Figure 5-18 show that lights are on at a relatively constant level. Although daylighting might be used, it does not change the lighting power during the day to match the available solar resource (see Section 6.3). The results show that off-hour receptacle loads are about half of what they are during the day, which indicates that equipment is being left on when not in use. Presumably, this is because a large amount of information technology equipment operates in the offices and server room. The off-hour plug loads in the Merrill Center are probably typical of contemporary offices, but they could be considered an opportunity for improving the energy performance of the building. There are methods that might be used to reduce off-hour plug loads, including communicating with employees about the value of shutting down equipment, deploying new network-based software products that monitor and reduce computer power, and replacing equipment with energy-saving sleep modes.

## 5.3 Development of Building Energy Models

Building energy modeling is an important complement to detailed measurements when assessing the performance of a specific building. As with most commercial buildings, this building is unique. There is no actual side-by-side comparison, and as a result, the building must be compared with a simulation of a baseline building. Several parameters, including operating schedules, plug and miscellaneous loads, and weather, are the same between the buildings.

This section presents baseline energy models used to provide a reference performance level to better understand the performance of the Merrill Center. The goal is to determine how the building in question would perform if it were built differently, which usually means a building that meets minimum energy code, but otherwise meets the same programmatic requirements of the building being evaluated. Although it would be fairer to use the energy code in place at the time the Merrill Center was designed and built issued by the American Society of Heating, Refrigerating, and Air-Conditioning Engineers (ASHRAE) e.g., ASHRAE 90.1-1989, this report is based on the current version of the consensus Standard 90.1-2001 for nonresidential buildings (ASHRAE 2001b). This code was selected to be consistent with other baseline activities of NREL's building research program.

ASHRAE 90.1 was developed to provide a threshold for energy performance as opposed to a tool for assessing the energy performance of a building. To assist in using the code for comparative purposes, Appendix G of ASHRAE 90.1 was developed as a method of applying the Energy Cost Budget to rate buildings (ASHRAE 2002, ASHRAE 2003a). Appendix G will be included in the 2004 version of ASHRAE 90.1 (and currently published as Addendum e to ASHRAE 90.1-2001). NREL applied useful definitions from Appendix G in the analysis of the energy performance of the Merrill Center.

The intended application for Appendix G is to compare results of two models: one for a proposed building and another for a comparable baseline building. The methodology that is evolving for comparing *two* models often deals with modeling difficulties by declaring that difficult-to-determine input be the same in both models. However, this study compares baseline modeling to measurements of a real building, so ascertaining the variability in the predictions of baseline models of energy performance is natural. Therefore, this study includes considerable additional analysis of baseline modeling to estimate the uncertainty in model predictions (see Appendix F).

Section 5.3.2 summarizes the input data used to generate the baseline model results. Results of the baseline modeling are presented in Section 5.3.3. Many more details on the geometry and error analysis for baseline modeling are provided in Appendix F.

### 5.3.1 EnergyPlus Building Simulation Tool

NREL selected EnergyPlus (Crawley et al. 2001) to model baseline energy performance. EnergyPlus is a relatively new building energy simulation program that was first released in April 2001. The program builds on the capabilities and features of BLAST and DOE-2. It collects many capabilities into a single program that models building performance. Some key capabilities include variable time steps, configurable modular HVAC systems integrated with heat balance-based zone simulation, multiple comfort models, daylighting and advanced fenestration, multizone airflow, displacement ventilation, flexible system modeling, and PV and solar thermal simulation. Since EnergyPlus was released in April 2001, more than 24,000 copies have been downloaded. EnergyPlus can accept 15-minute weather files and complex schedules (with 8,760 values) for internal gains. This ability is very important for a measurement-to-simulation comparison, as weather and internal gains must be calibrated as accurately as possible.

### 5.3.2 Modeling Inputs

NREL processed some monitored data to provide inputs for modeling exercises. Appendix C presents plots of the weather data and Appendix D presents plots of schedules for internal gains that were developed from on-site measurements. The rest of this section documents details involved in developing modeling inputs from monitoring data.

This section describes the envelope materials, floor areas, internal gains, HVAC, and energy pricing used in all the baseline models. Wherever possible, this study attempted to adhere to the forthcoming Appendix G of ASHRAE 90.1 by substituting *proposed* design with *actual* monitoring results from the Merrill Center, as appropriate.

#### *Modeling Analysis Year*

NREL selected a year's worth of data for annual energy analysis. More were available from monitoring, but the energy simulations are typically for a single year. Therefore, we selected a subset of the complete measured data set to constitute a modeling analysis year. This year was selected based on the criteria that the measured data are as complete as possible and that times coincide with the electric utility's billing cycles. The period selected was November 7, 2001 to November 6, 2002.

The measured data were rearranged so that data from November 7, 2001 to December 31, 2001 follow data from November 6, 2002 (see Figure 5-19). This was done to have a calendar year for the data. All data used to generate modeling inputs (schedules for internal gains and weather) were rearranged in this manner. This rearrangement distinguishes the modeling analysis year from the actual monitoring period.

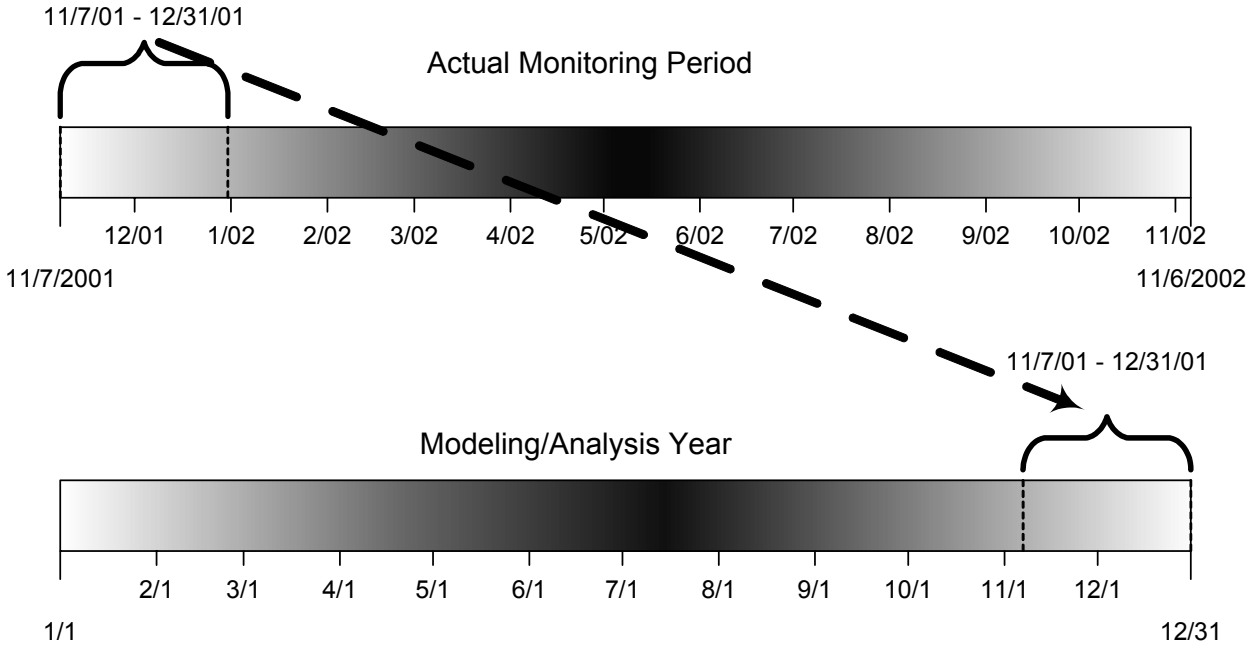


**Figure 5-19 Data rearrangement for modeling analysis year**

*Weather Data*

Building energy models use weather data. Because measured data were obtained on-site for weather-related parameters, it was desirable to use these data for the energy models. Routines were developed to create annual weather files for use with EnergyPlus.

Some measured data were fixed to avoid problems. Relative humidity sensors are notoriously poor at high humidity. Readings in excess of 100% were screened and set to 100% to avoid problems in psychrometric calculations. Radiation measurements less than 0.1 $W/m^2$ were set to 0.0.

Dew-point temperatures were calculated with a direct relation from Chapter 6 of the *ASHRAE Handbook of Fundamentals* (ASHRAE 2001a), Equations 37 and 38.

The on-site pyranometer measures global horizontal solar radiation. The Perez All-Weather Sky Model (Perez 1992) was used to calculate the direct component of this radiation. NREL adapted computer routines provided by Perez for use in the data analysis application HPBAnalyzer. In addition, solar position routines were adapted from EnergyPlus (Crawley et al. 2001) source code and from the *TARP Manual* (Walton 1983).

Cloud cover is used to compute sky temperatures or horizontal infrared radiation intensity. EnergyPlus uses horizontal infrared radiation intensity to compute outside surface temperatures of surfaces exposed to the outside. Cloud cover was not observed directly and so was inferred from solar radiation measurements with a method developed by Auer (see Appendix E).

The processed weather data were then written to a text file with the format for EnergyPlus weather files. Because EnergyPlus allows subhourly weather data, the weather file was formulated with 15-minute time steps to preserve the resolution of the measurements. The data included in the weather file are listed in Table 5-9. The estimated level of uncertainty in the weather data are also listed in Table 5-9 along with notes on the sources of error that contribute to the uncertainty.

**Table 5-9 Weather Data for Energy Simulations Derived from Measurements**

| Parameter | Units | Source | Uncertainty | Source of Error |
|---|---|---|---|---|
| Month | Integer | Datalogger | ±0 | |
| Day | Integer | Datalogger | ±0 | |
| Hour | Integer | Datalogger | ±0 | |
| Minute | Integer | Datalogger | ±1 | Possible mismatch |
| Dry-Bulb Temperature | °C | Directly measured | ±0.5°C | Transducer error |
| Dew-Point Temperature | °C | ASHRAE equations | ±1.5°C | Estimated error propagation |
| Relative Humidity | % | Directly measured | ±6% | Transducer error |
| Atmospheric Pressure | Pa | Not measured, sea level | ±200 Pa | Estimated error |
| Horizontal IR | $W/m^2$ | TRNSYS Type 69 model | ±20% | Model; latitude concerns |
| Global horizontal Radiation | $W/m^2$ | Directly measured | ±3% | Transducer error |
| Direct Normal Radiation | $W/m^2$ | Perez model | ±65 $W/m^2$ | Model validation RMS (Perez 1992) |
| Diffuse Horizontal Radiation | $W/m^2$ | Perez model | ±65 $W/m^2$ | Complement of direct radiation |
| Wind Direction | degrees | Directly measured | ±5° | Transducer error |
| Wind Speed | m/s | Directly measured | ±0.5 m/s | Transducer error |
| Total Sky Cover | tenths | TRNSYS Type 69 model | ±1.0 tenth | Estimated error propagation |
| Opaque Sky Cover | tenths | TRNSYS Type 69 model | ±1.0 tenth | Estimated error propagation |

NREL created two additional versions of the weather file to understand the errors associated with inaccurate weather data in EnergyPlus modeling results (see Section F.5). One file (CBF_minus.epw) was created by altering all the variables down (to a lower energy state) and reducing all the parameters by their respective uncertainty. Similarly, a second file (CBF_plus.epw) was created by shifting all the variables up. The solar radiation data were not shifted at night and relative humidity was not shifted outside physical limits.

### *Schedules*

In this study, NREL developed two types of schedules from the monitoring data. The first, referred to as a *smoothed schedule*, is a simplified schedule that is meant to represent average conditions, which is usual practice for building energy modeling. The second is for detailed calibration of internal gains from receptacles and process loads.

The smoothed schedules are used in all simulations to describe a variety of time-dependent input parameters for an energy model. Building operation parameters were determined by observing measured data. These include settings such as thermostat set points, setup and setback schedules, equipment

availability, lighting design levels and schedules, and occupancy schedules. Thermostat set points were developed from studying the measured zone air temperatures. Lighting schedules were determined from analyzing lighting patterns. A cleaning crew, which arrives at 6:00 a.m., is included in the lighting schedule. Some lights are turned off or down after cleaning and turned on again at 8:30 a.m. The cleaning crew switched from evening schedule to morning schedule during the analysis year, apparently at the beginning of January 2002.

Detailed calibration schedules that have 8,760 values were generated. Bronson et al. (1992) developed methods of calibrating nonweather-dependent loads that produce more compact schedules. However, their method was more complicated to implement than the method of using an entire year of measured data. The approach taken here was to develop calibration schedules that directly followed from monitoring data. The 15-minute measured data were totaled or averaged to produce hourly data. Routines were implemented in HPBAnalyzer, which writes EnergyPlus input objects for the schedules.

Table 5-10 lists the calibration schedules that were developed from monitored data. The data are plotted in Appendix D. Baseline modeling requires schedules for certain uses of electricity. One type of baseline building geometry combines the separate conference pavilion with the main office building. Special blended schedules were developed for the first and second floors of such baseline buildings. One blended schedule includes the measured first-floor receptacles and 18.4% of the conference pavilion plugs and lights. A second blended schedule includes the measured second-floor receptacles and 81.6% of the conference pavilion plugs and lights. The 18.4%/81.6% split was selected based on floor area distributions.

**Table 5-10 Calibration Schedules for Modeling from Measured Data**

| Calibration Schedule | Notes |
|---|---|
| First-floor plugs | Main building receptacle loads |
| First-floor lights | Main building lighting loads |
| Second-floor plugs | Main building receptacle loads |
| Second-floor lights | Main building lighting loads |
| Conference plugs and lights | Conference pavilion receptacle and lighting loads |
| Miscellaneous ancillary loads | Elevator, mechanical room, storage, exterior lights |
| Blended first-floor plugs | For baseline models, combines main and conference |
| Blended second-floor plugs | For baseline models, combines main and conference |

### *Internal Gains*

NREL calibrated receptacle and miscellaneous loads so that the baseline models would have the same level and timing of internal gains as the real building did for the model analysis year. The calibration process required two steps:

1. Determine schedule (as described in Table 5-10) of factors (0.0–1.0) that are applied to the design levels.
2. Iteratively determine design levels that, when used with the schedules, result in annual energy consumption that matches monitoring results.

Different schedules were used depending on the geometry of the baseline model and how conference pavilion loads and floor areas were handled. The details of the schedules are shown in Appendix D and are documented in the EnergyPlus input files. Because the real building includes daylight harvesting, lighting schedules for baseline models used schedules typical for day shift operation.

### *Envelope*

ASHRAE 90.1-2001 has different requirements based on climatic differences. The envelope requirements are listed in Table B-13 in ASHRAE Standard 90.1-2001. Baltimore was selected as the climate area closest to Annapolis. Table 5-11 lists the building envelope minimum performance specifications and shows resulting performance levels computed by the EnergyPlus model because these are calculated from complete constructions (and cannot be modeled explicitly). The EnergyPlus results for assembly R- and U-factors do not include the added resistance of surface film coefficients.

**Table 5-11 Envelope Performance Specifications for Baseline Models**

| Envelope Component | 90.1 Minimum Requirements | EnergyPlus As-Modeled |
|---|---|---|
| Exterior Walls $ft^2 \cdot h \cdot °F/Btu$ *($m^2 \cdot K/W$)* | R = 13 *(2.3)* | R = 15.5 *(2.73)* |
| Built-Up Roof $ft^2 \cdot h \cdot °F/Btu$ *($m^2 \cdot K/W$)* | R = 15 *(2.6)* | R = 15.3 *(2.70)* |
| Windows $Btu/ft^2 \cdot h \cdot °F$ *($W/m^2 \cdot K$)* | U = 0.6 *(3.24)*<br>SHGC = 0.39 | U = 0.6 *(3.14)*<br>SHGC = 0.397 |

### *Floor Area*

The total floor area of the Merrill Center is taken as 31,000 $ft^2$ (2,880 $m^2$). Of this, 5,000 $ft^2$ (466 $m^2$) are mechanical and storage rooms on the ground floor; the rest of the building is elevated. These ground-floor spaces are not occupied and are not completely conditioned. To simplify the modeling, these spaces were not included in models. Instead, a smaller floor area of 26,000 $ft^2$ (2,414 $m^2$) was modeled and the energy associated with the mechanical and storage rooms is taken as a given and counted as a miscellaneous load. However, the entire 31,000-$ft^2$ (2,880-$m^2$) floor area was used to calculate EUIs (where overall energy performance values are normalized by the floor area of the building). The miscellaneous ground-floor loads also include the elevator and exterior lights and are input into the models with an 8760-value hourly schedule to include their contribution to demand charges.

### *HVAC Systems*

For the climate and size of the Merrill Center, informational Appendix G specifies that the baseline HVAC system should be based on single-zone rooftop packaged unit with gas-fired heating and no economizer. The air-to-air package unit was modeled in EnergyPlus as diagrammed in Figure 5-20. There is one package for each thermal zone. The air-to-air cooling was governed by performance curves fit to catalog data for a nominal 4-ton unit; however, the capacity of the units was autosized by EnergyPlus. The cooling coefficient of performance is 3.1, which includes compressor and condenser fan. The heating efficiency is 0.8. The fan static pressure is assumed to be 2 in. (500 Pa) of water. Each unit is configured to automatically size using design day calculations that precede the annual simulations. Outside air ventilation rates for the baseline are determined during autosizing based on a requirement 20 cfm (10 L/s) of air per person. Infiltration was set at 0.4 ACH and scheduled for off hours when the HVAC system is not operating.

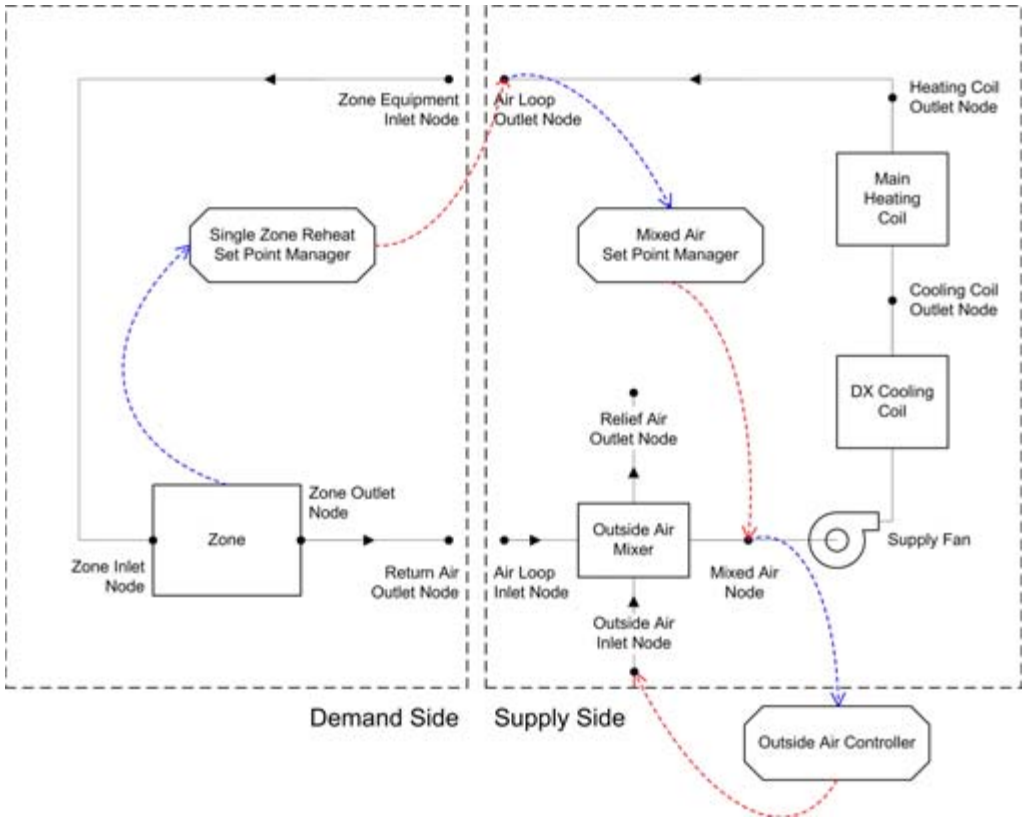


**Figure 5-20 System diagram of EnergyPlus model for rooftop packaged unit**

### *Energy Prices*

The baseline building was assumed to use propane rather than natural gas. Although 90.1 Appendix G specifies natural gas heat, only electricity and propane are available at this building site. Therefore, the modeling proceeds assuming the building is using natural gas-fired coils for heating, but with pricing typical of propane. The price for propane was assumed to be $1.20/gal ($0.32/L) based on local utility bills. The heating value of propane is 0.91 therm/gal (25.4 GJ/m$^3$) or $1.317/therm ($12.48/GJ). This rate was used to calculate heating energy costs and is considerably higher than natural gas at roughly $0.75/therm ($7.11/GJ) (ASHRAE 2001a).

Table 5-12 shows the utility pricing structure used to compute electricity costs. Post-processing routines were developed that compute energy costs from hourly results for energy use. The price per kilowatt-hour includes distribution and tax surcharges of $0.01932/kWh. Demand metering in the calculations is for the highest rate of use over a 15-minute period. Saturdays, Sundays, and national holidays are considered off-peak by the utility, but the routines only account for weekends and not the holidays.

**Table 5-12 Electricity Pricing Structure**

| Season | Charge Category | On-Peak 10:00 a.m. – 8:00 p.m. | Intermediate 7:00 a.m. – 10:00 a.m. 8:00 p.m. – 11:00 p.m. | Off-Peak 11:00 p.m. – 7:00 a.m. |
|---|---|---|---|---|
| Summer (Jun–Sep) | Energy Charge (¢/kWh) | 6.194 | 5.003 | 3.552 |
| | Demand Charge ($/kW) | 14.310 | 14.310 | 14.310 |
| Winter (Oct–May) | Energy Charge (¢/kWh) | 4.515 | 4.172 | 3.578 |
| | Demand Charge ($/kW) | 8.690 | 8.690 | 8.690 |

### *5.3.3 Summary of Baseline Results*

A thorough evaluation of baseline energy performance was performed with EnergyPlus. This study looked at a variety of baseline building descriptions to determine a best estimate for performance along with an estimate of the uncertainty in the results. The modeling used 15-minute weather data based on one year of actual on-site measurements. Receptacle and miscellaneous electrical loads were calibrated with hourly data based on actual measurements. Figure 5-21 shows the breakdown by end uses for site energy consumption. Figure 5-22 shows the breakdown by end use for source energy consumption. Figure 5-23 shows the breakdown by end use for energy costs. Demand costs include contributions from all end uses.

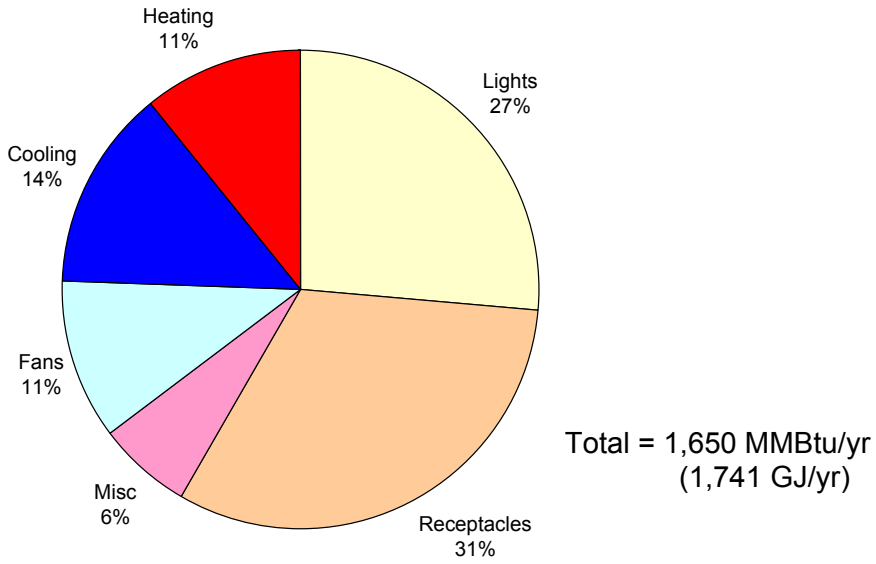


**Figure 5-21 Mean baseline result for site energy consumption by end use**

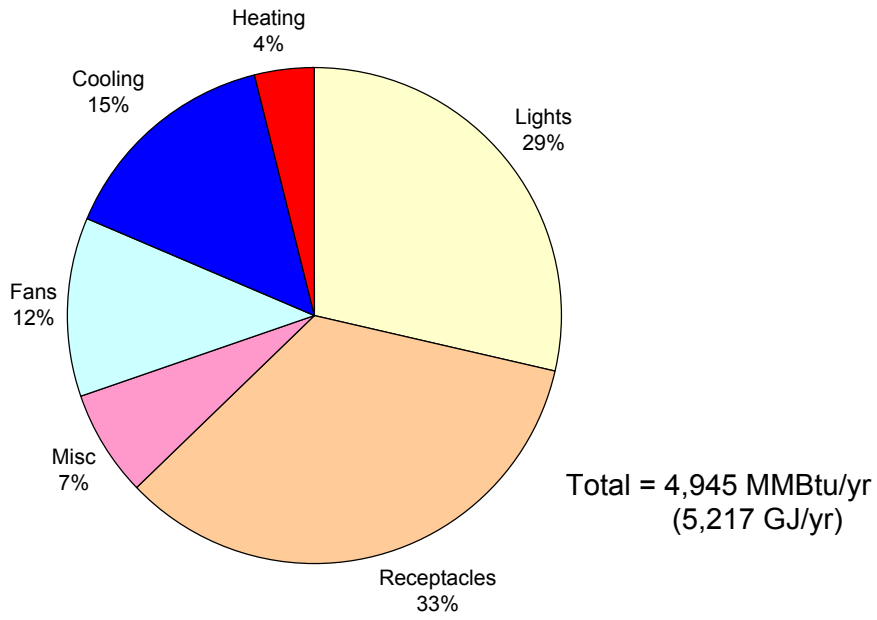


**Figure 5-22 Mean baseline result for source energy consumption by end use**

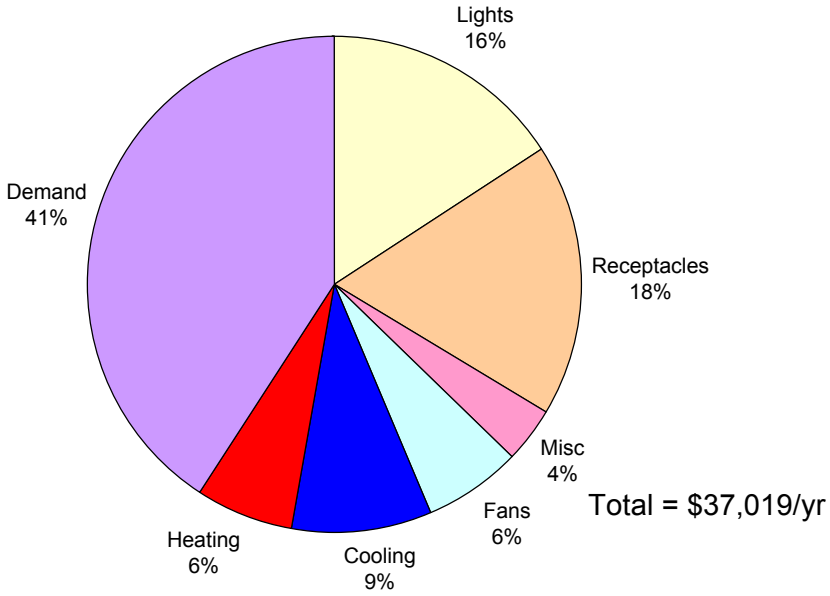


**Figure 5-23 Mean baseline result for energy cost by end use**

Table 5-13 summarizes the overall energy intensity performance of the baseline model and estimated uncertainty. Input perturbation methods (Lomas and Eppel 1992) were used to develop uncertainty estimates and are described in detail in Appendix F.

**Table 5-13 Summary of Results for Overall Energy Intensity - Baseline Building**

| | **Site EUI** kBtu/ft$^2$·yr *(MJ/m$^2$·yr)* | **Source EUI** kBtu/ft$^2$·yr *(MJ/m$^2$·yr)* | **Energy Cost Intensity** $/ft$^2$·yr *($/m$^2$·yr)* |
|---|---|---|---|
| Baseline Model | 53.3 ±7.3 *(604.8 ±82.8)* | 159.6 ±20.0 *(1,812 ±227)* | 1.20 ±0.17 *(12.87 ±1.8)* |
| Uncertainty | ±14% | ±13% | ±14% |

## 5.4 Whole-Building Energy Performance Results

### *5.4.1 Site versus Source Energy and Energy Cost Savings*

This section compares the results of measurements presented in Section 5.2 to the results of baseline building models presented in Section 5.3. When discussing low-energy buildings, it has become common to characterize performance with the term *percent savings*. Baseline modeling provides data to use as a reference when calculating the level of savings as a percentage. This section presents percent savings calculated from various performance metrics (such as site energy use, source energy use, and energy cost) that were calculated with

$$\text{percent savings} = \frac{(x_{base} - x_{meas})}{x_{base}} * 100 \quad (1)$$

Where

$x_{base}$ = a performance metric from the baseline modeling and

$x_{meas}$ = a performance metric from monitoring results.

Table 5-14 summarizes the results and shows percent energy savings. The mean values represent a best estimate of the results. Error propagation assumed independent random errors and added fractional uncertainties in quadrature (see Appendix F). The estimated uncertainty levels represent a confidence interval of 98%.

**Table 5-14 Overall Energy Savings Levels**

| | **Total Site EUI** kBtu/ft$^2$·yr *(MJ/m$^2$·yr)* | **Net Site EUI** kBtu/ft$^2$·yr *(MJ/m$^2$·yr)* | **Net Source EUI** kBtu/ft$^2$·yr *(MJ/m$^2$·yr)* | **Energy Cost Intensity** $/ft$^2$·yr *($/m$^2$·yr)* |
|---|---|---|---|---|
| Baseline Model | 53.3 ±7.3 *(604.8 ±82.8)* | 53.3 ±7.3 *(604.8 ±82.8)* | 159.6 ±20.0 *(1,812 ±227)* | 1.20 ±0.17 *(12.87 ±1.8)* |
| Monitoring | 40.2 ±0.3 *(456.8 ±2.9)* | 39.9 ±0.3 *(453.2 ±2.9)* | 124.3 ±0.7 *(1,412 ±8)* | 1.05 ±0.003 *(11.31 ±0.03)* |
| Savings | (24.5 ±14.1)% | (25.0 ±14.1)% | (22.1 ±12.8)% | (12.1 ±14.1)% |

On-site energy production from the PV system makes it important to distinguish between net and total energy use. Net energy use is the difference between the total energy use and the energy produced by PV. The small difference between net and total site energy use savings occurs because there is only a small amount of PV production. Cost saving levels are not as high as energy saving levels because the Merrill Center is predominantly electric and incurs substantial demand charges; propane is a secondary heat source. The baseline model uses propane-fired heating.

Table 5-14 also includes results for uncertainty estimates for both the baseline energy model and monitoring. The accuracy of whole-building energy performance results for the baseline model results is about 13%; the accuracy of the monitoring results is better than 1%. When developing values for percent savings, the contribution of uncertainty in the baseline modeling is significant.

Another method of characterizing energy savings levels is to consider only the energy used for HVAC&L by removing that energy used by the activities of the occupants inside the building. This method of comparing energy use is used in the Energy Cost Budget of ASHRAE Standard 90.1-2001. The USGBC has also used this method in its LEED rating system. However, some researchers and professionals in the building industry disapprove of this method because it tends to overstate the level of savings. Others approve because it focuses on the energy impacts directly attributable to building design. Results from the current study were reanalyzed to provide such data and provide context to such discussions and an assessment of earlier predictions. A significant difficulty arises in trying to remove plug loads from the energy costs because of their contribution to demand charges. Therefore, energy costs without plug loads were modeled by subtracting the contribution from plug loads from the overall costs using a virtual electricity rate of $0.091/kWh that was determined from a year of billing data. This represents a cost difference of $14,014/yr for the baseline model and $14,030/yr for the monitored results. Table 5-15 shows the results of this analysis.

**Table 5-15 HVAC&L Energy Savings Levels**

| | **Net Site EUI without Plug Loads** kBtu/ft$^2$·yr *(MJ/m$^2$·yr)* | **Energy Cost Intensity without Plug Loads** $/ft$^2$·yr *($/m$^2$·yr)* |
|---|---|---|
| Baseline Model | 36.3 *(412.2)* | 0.74 *(7.99)* |
| Monitoring | 23.0 *(260.6)* | 0.59 *(6.34)* |
| Savings | 36.8% | 20.6% |

### *5.4.2 Measured Versus Predictions*

The design team predicted the energy performance of the Merrill Center to prepare application materials for LEED 1.0 documentation. The design team used a combination of simulations (TRACE 600) and off-line analyses for natural ventilation and active solar systems to predicted performance values before the building was constructed. Table 5-16 summarizes the predicted results. This represents the original energy goals for the building.

The building was monitored as documented in this report. Monitoring provides an opportunity to assess the accuracy of predictions made before the building was built. Table 5-16 also compares predicted to monitored energy performance. The comparison here does not take into account the differences between the actual weather and the typical weather year used in the modeling. (The actual weather was generally

warmer and sunnier than the weather file for Baltimore. See Table C-1.) Nor does it taken into account changes in the building's architectural program that may have increased plug loads (such as adding computer servers).

**Table 5-16 Predicted versus Monitored EUIs**

| Category | Predicted kBtu/ft$^2$·yr *(MJ/m$^2$·yr)* | Monitored kBtu/ft$^2$·yr *(MJ/m$^2$·yr)* |
|---|---|---|
| Heating EUI | 0.7 *(8.4)* | 3.9 *(46)* |
| Cooling EUI | 7.2 *(82)* | 7.8 *(89)* |
| Lighting EUI | 6.8 *(77)* | 10.0 *(113)* |
| Plug load EUI | 8.8 *(100)* | 15.0 *(171)* |
| Miscellaneous | 0.0 *(0.0)* | 3.4 *(38)* |
| PV Power Production | 0.5 *(5.4)* | 0.3 *(3.3)* |
| Net Site EUI | 23.0 *(262)* | 39.9 *(453)* |

The measured data indicate that the whole-building energy performance realized was lower than predicted. Heating energy use was predicted to be very low, but the measurements showed about five times more energy use for heating than was predicted. Lighting energy use turned out to be 47% higher than predicted. Plug and miscellaneous loads were twice those assumed for the predictions. Predictions for cooling were within 10%, which is very good considering the additional lighting and plug loads. PV power production was 40% lower than predicted. Overall, the net site EUI was 73% higher than predicted.

These results indicate that the performance predictions made during design development were optimistic. The largest deviation in terms of magnitude was from underestimating the amount of electricity drawn by plug loads in the occupied spaces and miscellaneous loads such as exterior lighting, mechanical room accessories, and the elevator, which were not accounted for in the original prediction. Efforts to improve the accuracy of predictions of whole-building energy performance during the design phase should focus on better methods of developing assumptions for receptacle and miscellaneous electrical loads.

# 6 Subsystem Evaluations

Although NREL's monitoring effort focused on an overall assessment of the energy performance of the Merrill Center, the data did allow more detailed evaluation of some specific systems. The Merrill Center has at least four systems that warrant further analysis. This section presents monitoring results related to the ground-source heat pumps, natural ventilation, PV power generation, and daylighting.

## 6.1 HVAC Performance Evaluation

Figure 6-1 compares the HVAC energy use with outdoor air temperatures for the analysis year. The results show that the building is cooling dominated. The relatively low energy use in the middle suggests that natural ventilation helps to reduce HVAC energy use.

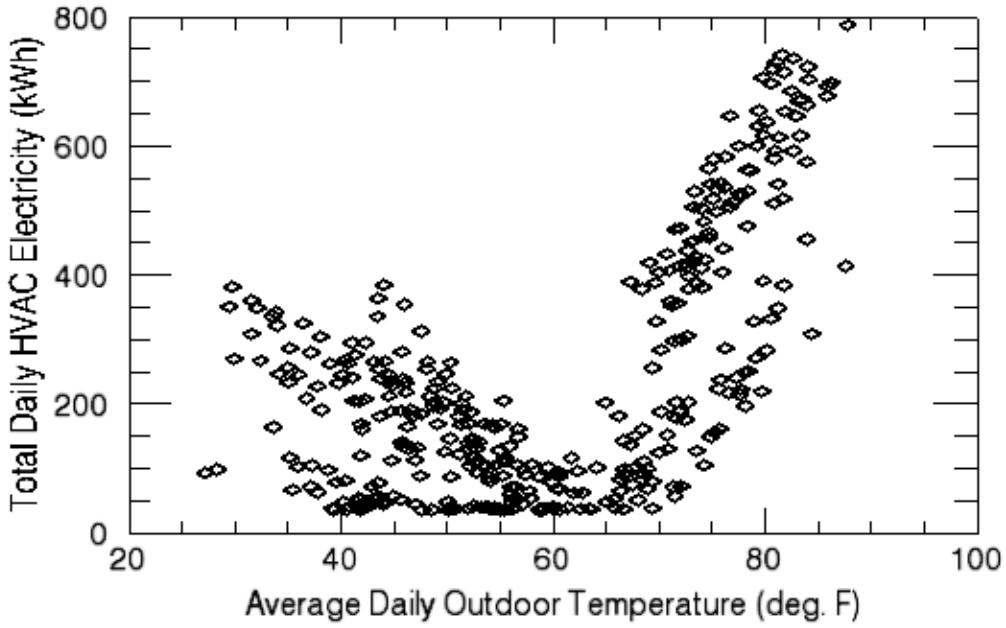


**Figure 6-1 Daily HVAC electricity consumption versus average outdoor air temperature**

The HVAC systems installed in the Merrill Center include desiccant wheel dehumidification systems for both the main building and the conference pavilion. The systems remain installed, but they are used only to provide outside air via the integral supply fans. The desiccant wheels are not operated because the building operator has determined that (1) the heat pumps provide effective dehumidification during cooling and (2) it is not desirable to continuously run the boiler solely to regenerate the desiccant. Because the desiccant systems are not being used, they complicate the air system; therefore, they should not have been specified. The potential benefit of using the desiccant systems should be evaluated with an integrated analysis. If the wheels are never to be used, they should be removed because they only contribute to increased static pressure and fan energy. One suggestion is that the wheels could be used for energy recovery but not regenerated for dehumidification. Care must be used to control heat recovery such that the cost of operating the systems is less than the recovered heat (Pless and Torcellini 2004).

The Merrill Center's HVAC systems do not include an economizer, which is a noticeable shortcoming for a low-energy building; it is probably related to the inclusion of natural ventilation, space conflicts, and overall airflow rates between the desiccant wheel systems and what would be needed for an economizer. Distributed heat pump packages also lead to an outside air system with smaller ducts that feed the individual air units with fresh air.

Our results indicate that HVAC heat pumps are large contributors to demand charges because they often all come on at once. Therefore, energy costs could be reduced by reconfiguring the EMS to reduce the number of heat pumps that can run at the same time. We suggest that more time be allowed for warmup and that controls be organized so that half the pumps run for 15 minutes and then the other half for 15 minutes. This change would not necessarily save energy, but it could reduce the peak electricity demands, which would reduce costs.

### 6.1.1 Ground-Source Heat Pumps

The Merrill Center's main source of cooling and heating consists of small packaged water-to-air heat pumps that are connected in parallel to a vertical ground heat exchanger via a closed-loop. Heat pumps provide both cooling and heating in the same unit, but the electrical data do not indicate the heat pumps' operating mode. In addition to the electrical measurements, water temperatures were measured for the ground loop's supply and return. Here, *supply* indicates that water arrives from the ground heat exchanger and supplies the heat pumps, and *return* refers to the water that returns to the ground heat exchanger. The temperature sensor for supply is located after the main pump(s), so it also includes the heat added by pumping. This effect was neglected because it would be difficult to formulate an accurate correction and the high heat capacity of water suggests the temperature rise from pump work would be slight.

The temperature difference between the ground-loop supply and return was used to formulate an estimate of the split between energy used for cooling and for heating. Although several heat pump air system temperature sensors were added on March 7, 2002, the data for air temperatures were not comprehensive enough to be used to separate heating and cooling. The sign of the temperature difference between supply and return in the water loop shows whether the heat pumps were, in aggregate, adding or removing heat from the ground loop. We assumed that the HVAC energy use could be split between heating and cooling end uses by examining the sign of the ground-loop temperature difference. When the return temperature is higher than the supply, we assign HVAC energy use to cooling; when the return temperature is lower than the supply, we assign HVAC energy use to heating. Table 6-1 shows the results of this analysis for billing cycles. The method of sorting HVAC electricity use between heating and cooling is aggregated, which introduces errors when different parts of the building are being heated and cooled at the same time. The results show that the building is cooling dominated in its energy use, but heating affects the peak electrical demand almost as much as cooling (although demand charges are lower in the winter).

**Table 6-1 Heat Pump Cooling and Heating Characterization**

| Billing Period | Cooling Site Energy (kWh) | Heating Site Energy (kWh) | Cooling Demand (kW) | Heating Demand (kW) |
|---|---|---|---|---|
| November 2001 | 1,950 | 769 | 0 | 27 |
| December 2001 | 1,635 | 4,056 | 0 | 80 |
| January 2002 | 966 | 3,628 | 0 | 84 |
| February 2002 | 1,853 | 3,272 | 0 | 61 |
| March 2002 | 2,468 | 2,730 | 0 | 67 |
| April 2002 | 2,460 | 541 | 66 | 0 |
| May 2002 | 6,906 | 174 | 80 | 0 |
| June 2002 | 13,136 | 0 | 86 | 0 |
| July 2002 | 14,332 | 0 | 85 | 0 |
| August 2002 | 12,483 | 0 | 86 | 0 |
| September 2002 | 10,691 | 15 | 78 | 0 |
| October 2002 | 2,573 | 1,745 | 0 | 35 |
| **Total** | **71,454** | **16,931** | | |

Because the building was built before the monitoring effort was conceived, flow meters could not be installed on the ground loop. The initial measurement plan called for ultrasonic flow meters to monitor the flow rates, but the pipe configuration was not suitable. One lesson learned is that future monitoring efforts on buildings with ground-source loops should attempt to change or otherwise influence mechanical plumbing designs so that relatively long, straight, horizontal sections of pipe are available to form suitable locations for ultrasonic flow meters. An alternative is to install flow meters as part of the system engineering.

The flow rate through the loop is controlled in response to pressure through variable speed drives on the pumps. (The central EMS controls the pressure set point.) The resistance of the loop can vary based on the number of heat pumps requesting water. Each heat pump opens a valve when it is operating.

Although the flow rates were not measured directly, loop pump energy use was measured and we used this to model water loop flow rates. The model assumed that:

- There was a simplistic linear relationship between power and flow.
- The maximum flow rate equals the rated capacity of the pumps.
- Both pumps have the same performance.
- The peak measured pumping power corresponds to the maximum flow rate (full operation occurred at least once).

With a model for ground-loop flow and measured supply and return fluid temperatures, heat transfer can be analyzed to and from the Earth through the vertical ground heat exchanger. Because it is important to consider ground-source performance over a long period, all the available 15-minute data were included in an analysis that extended for 640 days from November 3, 2001 through August 4, 2003. The results of this estimate are provided in Figure 6-2 as daily totals for heat rejected to the ground. The data in Figure 6-2 form a best estimate, but they are very sensitive to the estimated flow rates. Figure 6-3 shows the daily average supply temperature over the same period. Results indicate an imbalance in that more heat is rejected into the ground for cooling than is extracted for heating. The relative finding is that 3.9

times more heat is being rejected than extracted over 640 days. However, the supply temperature data shown in Figure 6-3 do not show evidence of long-term drifting over the period, which indicates that the ground appears capable of transferring the heat away from the heat exchangers.

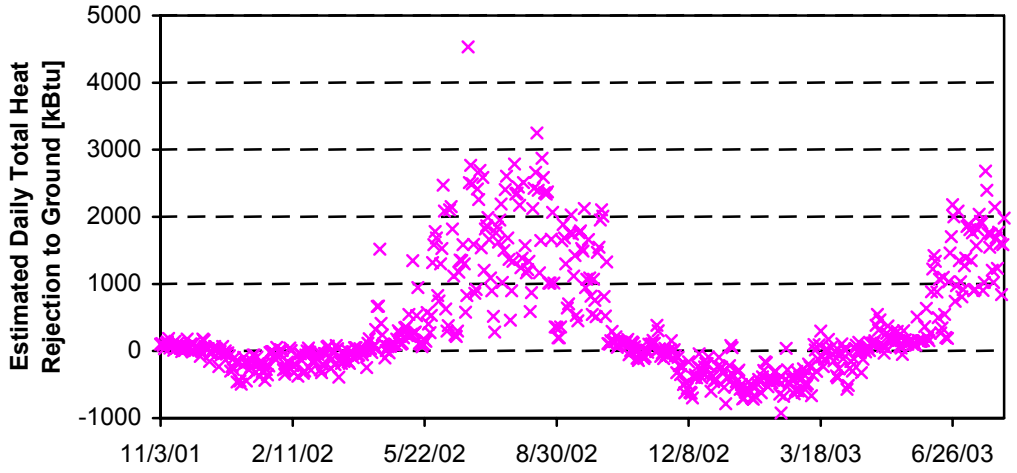


**Figure 6-2 Daily total estimate for heat rejection to ground**

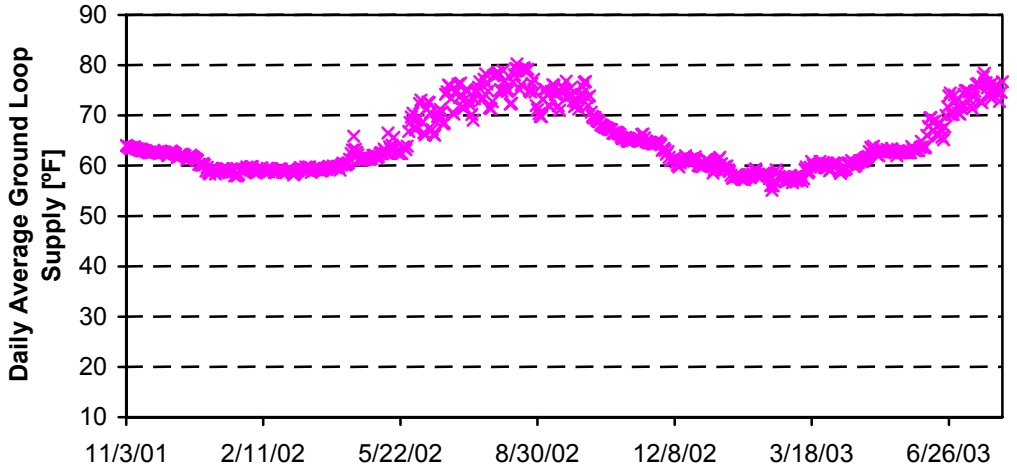


**Figure 6-3 Daily average ground-loop supply temperature**

The monitored data also show interesting short-term responses in the ground loop. Figure 6-4 shows the supply and return temperatures for a selected winter day and Figure 6-5 shows them for a selected summer day. On the winter day, the system appears to change from heating to cooling during the morning. On these particular days, supply temperatures varied by 3.9°F (2.2°C) over the course of single winter day and by 14.8°F (8.2°C) over a summer day. These results show the importance of short-term modeling, although sizing of ground-source heat pump systems is usually based on models with a time resolution of one month.

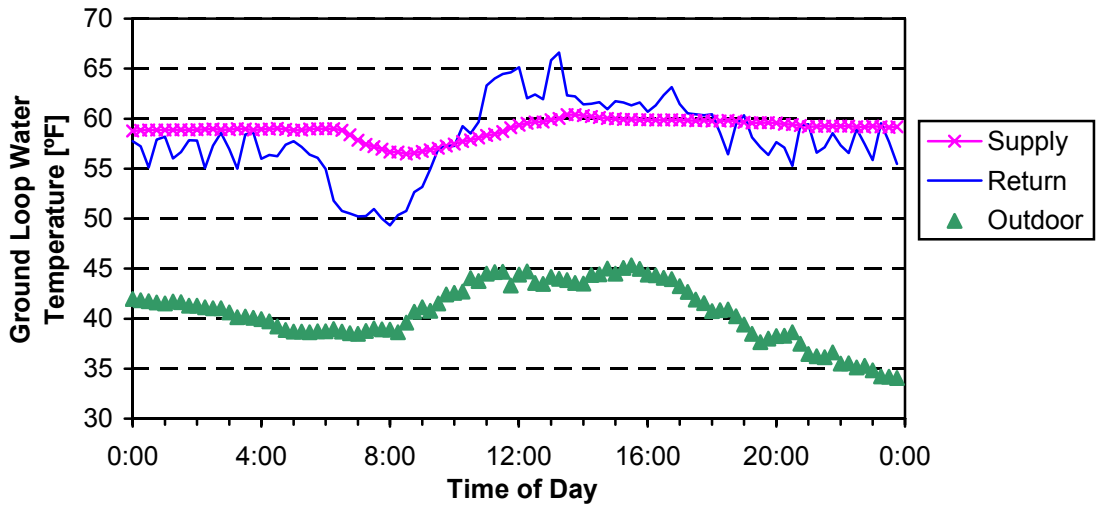


**Figure 6-4 Short-term response of ground loop: January 18, 2002**

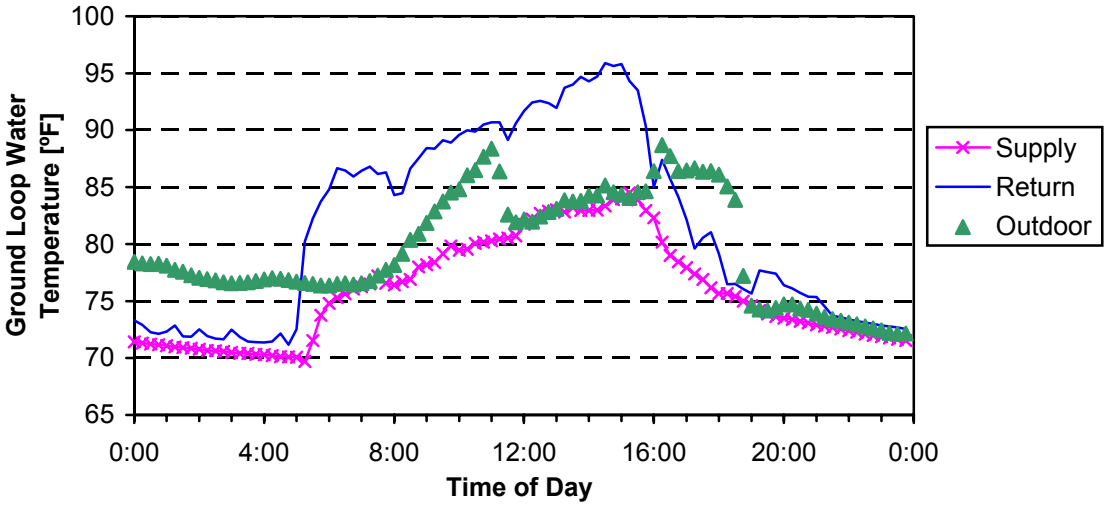


**Figure 6-5 Short-term response of ground loop: June 27, 2002**

The monitored data also provide a way to compare the ground-loop supply temperatures to the outside air temperature. The temperatures of heat sinks largely determine the thermodynamic efficiency of heat pump cooling. The purported advantage of a ground-loop arrangement that uses water-to-air heat pumps over rooftop packages with air-to-air direct expansion mechanical cooling is that ground-loop temperatures are expected to be lower than air temperatures and lead to more efficient cooling. NREL analyzed this assumption for the Merrill Center by comparing the ground loop and outdoor air temperature data for the model analysis year (November 7, 2001 to November 6, 2002). We first sorted the data every 15 minutes during this time to determine when cooling occurred—83% of the time, loop return fluid temperature was warmer than supply. We then analyzed the data to determine how outdoor air dry-bulb temperatures compared to the ground-loop temperature. The data show that for 61% of the time, cooling occurred and the outdoor air was actually cooler than the ground loop that supplies the heat pumps. Analysis of energy use shows that of the 71.4 MWh of electricity used for cooling, 42% was used when the outdoor temperature was cooler than the ground-loop supply. Figure 6-6 shows a time map of this and shows the magnitude of the temperature difference (calculated by subtracting the outdoor air dry

bulb temperature from the ground-loop supply) when the situation occurs. The problem is minimal during the summer but significant during fall, winter, and spring.

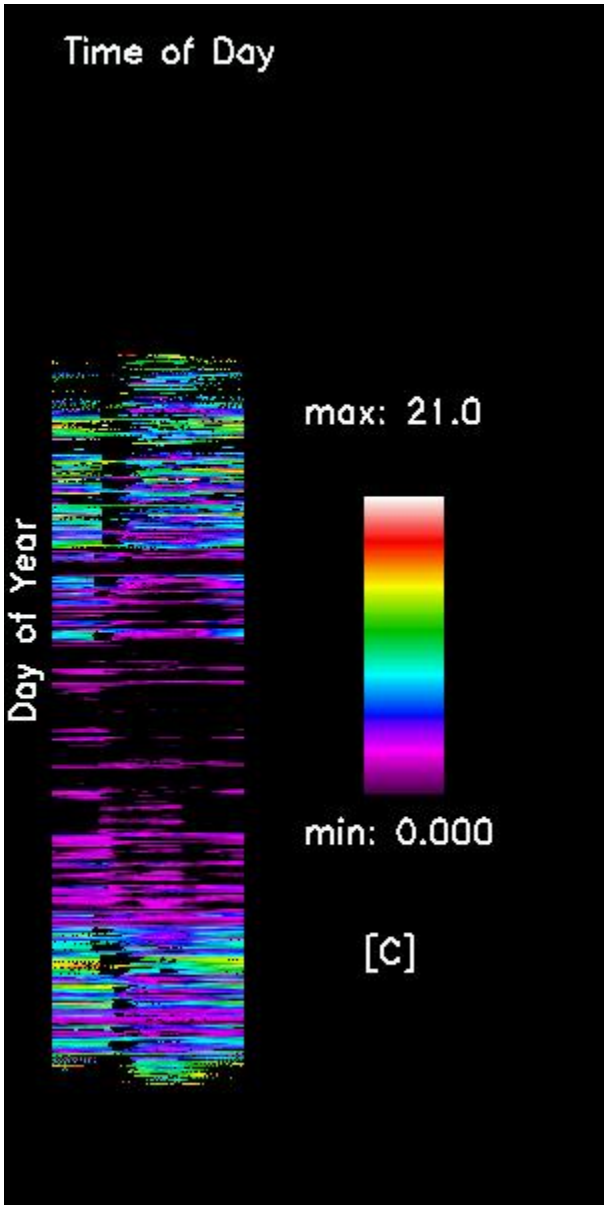


**Figure 6-6 Temperature difference between water loop supply and outdoor air when greater than 0.0 and not heating**

The results show that temperatures in the ground loop fluctuate widely and are sometimes higher than air temperatures. The fluctuating temperatures could result because the ground wells are undersized for this application, a plumbing problem artificially short-circuits the loop, or some other phenomenon restricts the performance of the system. An alternative method of solving the problem would be to add a conventional cooling tower to cool the water when ambient conditions are more favorable than ground conditions.

The data also allowed NREL to examine how much of the cooling energy is consumed when outdoor air conditions would be favorable for economizer operation (were the building to have this feature). For this examination, we sorted and summed HVAC cooling energy use for times when the outdoor air temperatures are below 58°F (14.3°C). The analysis revealed that of the 71.4 MWh of electricity used for cooling, 15% was used when the outdoor temperatures were favorable for so-called free cooling.

### *6.1.2 Natural Ventilation Evaluation*

Although the monitoring effort did not specifically focus on evaluating natural or mixed-mode ventilation in the Merrill Center, some data that were collected are useful for evaluating the system.

Earlier research by Chang noted that the designer's intent was to take advantage of winds that flow from south to north, but that winds in the area tend to flow from the northwest when outdoor conditions are good for natural ventilation. The current study measured wind direction and velocity, and enabled researchers to further quantify this assessment. The monitored data were analyzed to determine the distribution of wind directions for times when the following conditions were met:

- Outdoor dry-bulb temperatures were between 39.4°F (4°C) and 71.8°F (22°C).
- Relative humidity was between 20% and 65%.
- Daytime hours were between 8:00 a.m. and 6:00 p.m.
- Wind velocity was stronger than 2.2 mph (1.0 m/s).

Figure 6-7 shows the results of a histogram analysis of the wind direction when these conditions were all met between November 7, 2001 and November 6, 2002. The data confirm that winds often come from the northwest. They also come from the east as often as from the south. The monitoring data show that designers should not have assumed that the winds from the south (off the bay) would be the most important winds for natural ventilation cooling.

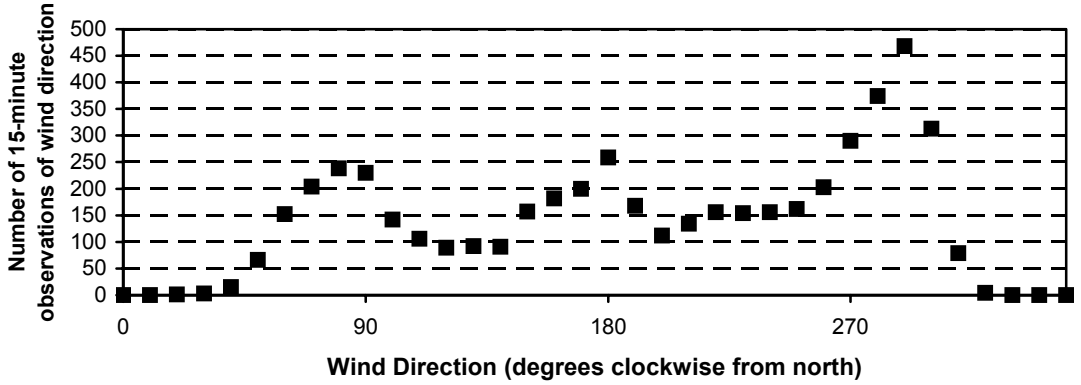


**Figure 6-7 Distribution of wind direction during periods amenable to natural ventilation over the model analysis year**

Although winds do not come from the north, designing for cross ventilation in the east to west and west to east directions would have been an improvement. The discrepancy between expected and measured wind directions also suggests that engineered natural ventilation systems should be designed to operate by stack forces rather than by wind.

In practice, the so-called natural ventilation in the Merrill Center is often operated as a hybrid system with the aid of exhaust fans. The system essentially fits the role of an economizer, but without the controlled

air distribution provided by ductwork and registers or the control afforded by controlling to a mixed-air set point. This mode of hybrid operation could be more efficient because of lower static losses.

The exhaust fans are used in the winter when the windows are closed and makeup air comes from infiltration. This type of system operation makes up for the lack of economizer operation. However, an economizer would be better because it is controlled to a mixed air set point and could be expected to provide more uniform comfort. Infiltration does little to ensure that cooling effects are evenly distributed; it also increases static pressure, which causes the exhaust fan to work harder.

## 6.2 Photovoltaic System Evaluation

### *6.2.1 Photovoltaic System Evaluation Methods*

The Merrill Center includes a 4.2-kW, thin-film PV power system that generates electricity. The electricity produced by the inverters is metered where it enters an electrical panel on the second floor. The solar resources are measured with two photometers, one situated horizontally and the other vertically facing south. The system was evaluated by examining the measured electricity generation and by comparison to simulations of the PV system (Mermond 1996).

### *6.2.2 Photovoltaic System Evaluation Results*

Table 6-2 provides a summary of the monthly consumption, production, net purchased, maximum production, and percent load met by PV power. The net purchased electricity is the difference between the total electricity consumed in the building for a month and the total electricity produced for the month. The maximum recorded power over a 15-minute period was 3.4 kW compared to the nominal rated power capacity of 4.2 kW. Higher power was delivered during winter than during summer; Table 5-8 showed that the largest reduction to demand charges was 2.3 kW. The PV system contributes about 0.8% of the electricity used in the Merrill Center.

**Table 6-2 PV Power Performance Summary: November 7, 2001 – November 6, 2002**

| Month/Year | Total Electrical Consumption (kWh) | PV Production (kWh) | Net Electrical Purchased (kWh) | Max PV Power (kW) | % Electrical Load Met by PV |
|---|---|---|---|---|---|
| November 2001 | 27,690 | 301 | 27,389 | 3.00 | 1.1% |
| December 2001 | 28,497 | 230 | 28,267 | 2.92 | 0.8% |
| January 2002 | 26,444 | 224 | 26,220 | 3.10 | 0.8% |
| February 2002 | 29,821 | 334 | 29,487 | 3.38 | 1.1% |
| March 2002 | 27,074 | 183 | 26,891 | 3.21 | 0.7% |
| April 2002 | 23,935 | 190 | 23,745 | 1.88 | 0.8% |
| May 2002 | 28,833 | 208 | 28,625 | 1.72 | 0.7% |
| June 2002 | 32,427 | 189 | 32,238 | 1.45 | 0.6% |
| July 2002 | 34,829 | 196 | 34,633 | 1.83 | 0.6% |
| August 2002 | 31,830 | 211 | 31,619 | 1.96 | 0.7% |
| September 2002 | 29,781 | 246 | 29,535 | 3.26 | 0.8% |
| October 2002 | 25,380 | 164 | 25,216 | 3.31 | 0.6% |
| **Totals (Sum or Average)** | **346,541** | **2,676** | **343,865** | **3.31** | **0.8%** |

Figure 6-8 shows measured results for daily electricity production and compares them to the solar resources for the model analysis year. The solar electric production closely tracks the solar resource on a south-facing vertical surface and produces more energy in the winter months. This is atypical of PV systems as most produce more electricity in the summer. The PV panels are tilted at 30° from horizontal, and it is unusual that the performance tracks vertical insolation more closely than horizontal.

Figure B-3 (in Appendix B) shows a time map of all the 15-minute measurements. Shading of the panels is evident in the unusual patterns of production compared to the solar radiation shown in Figure C-5.

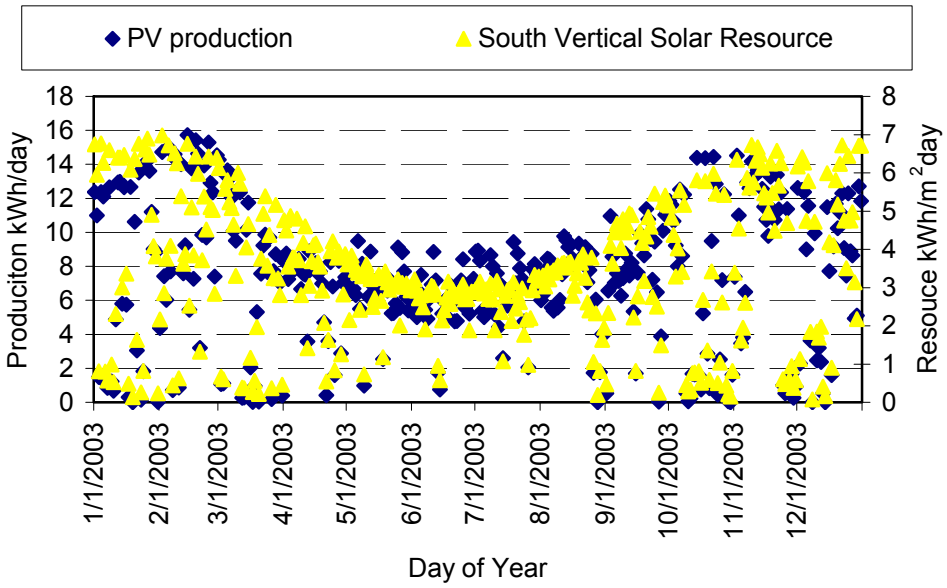


**Figure 6-8 Daily PV power production and solar resource**

Figure 6-9 shows the average hourly power profile for AC PV production for each billing period from November 7, 2001 through November 6, 2002. The monthly comparison of PV production profiles demonstrates the unexpected increase in PV production from summer to winter months. The maximum 15-minute average AC PV power production varies from 1.8 kW in September to 0.4 kW in April (Eastern Standard Time).

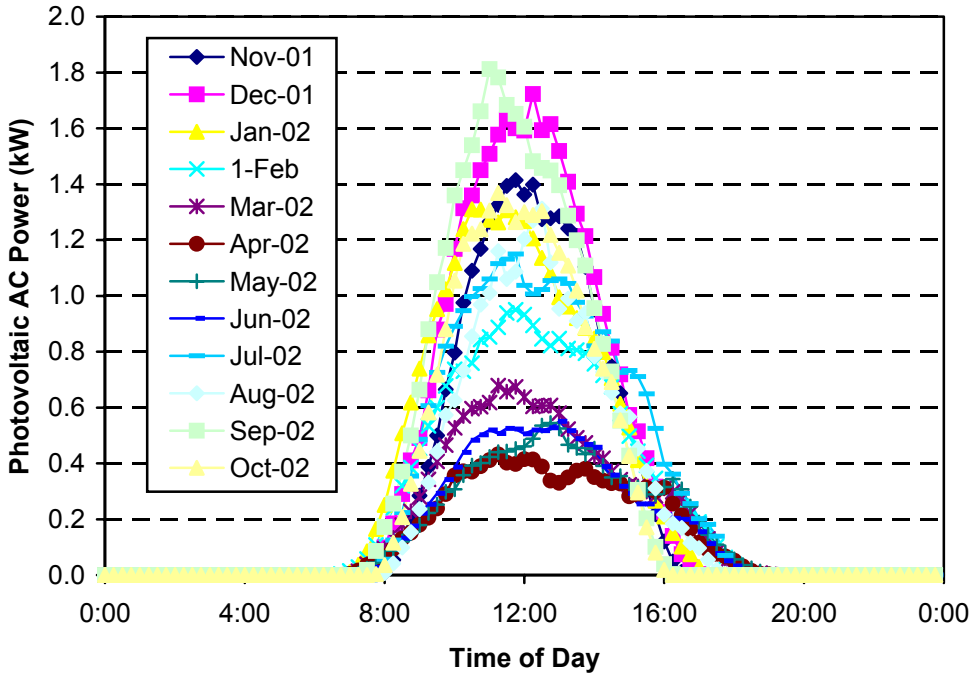


**Figure 6-9 Average hourly AC power profile by month for PV power production by billing period**

Figure 6-10 shows the results from simulation compared to the measurements. Simulations (Mermond 1996) were run with weather data for the measurements and the typical meteorological year data for Baltimore. To determine the potential of the PV array, the simulations account for tilt, but not for shading by overhangs or the conference pavilion.

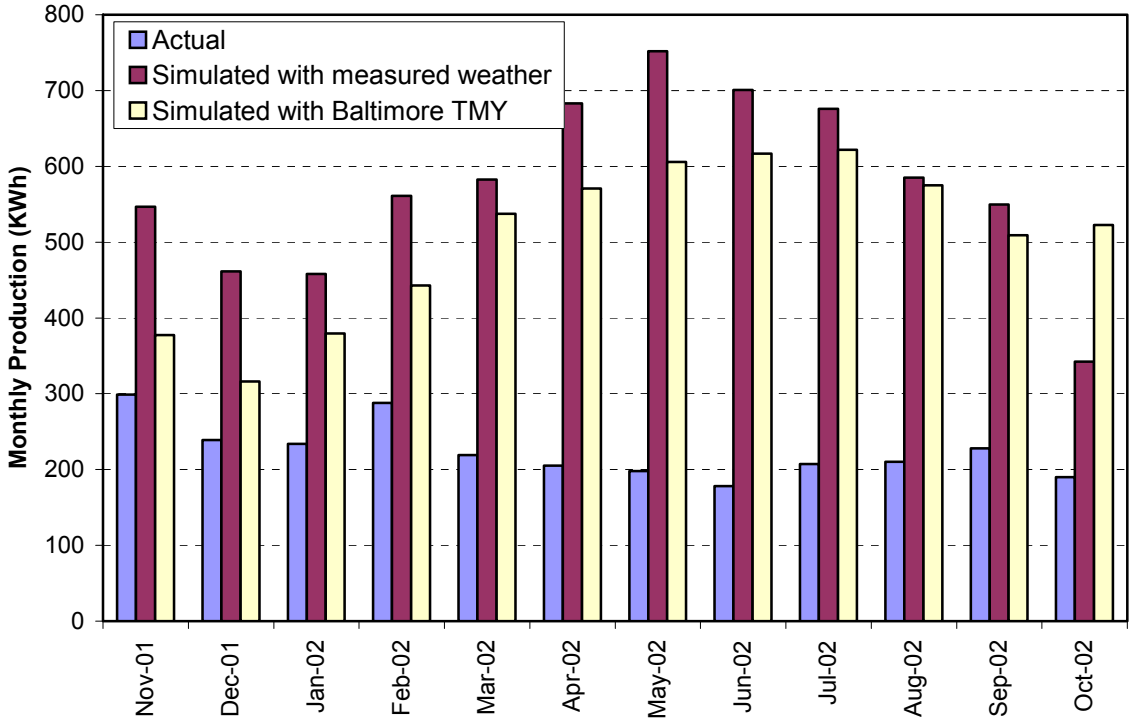


**Figure 6-10 Monthly PV power production compared to simulated results**

This section presented results for performance of the PV system that clearly show the system is producing less energy than it should because of the shading from the overhead trellis and the conference pavilion. PV systems should be located where the panels will not be shaded.

## 6.3 Ancillary Daylighting Evaluation

### *6.3.1 Daylighting Evaluation Methods*

Additional measurements were made with photometers to evaluate how well the building is lit by daylight that enters the building through the windows. In contrast to continuous monitoring over a year, we obtained these ancillary measurements over short time periods and used a mixture of handheld and continuous measurements, which were closely supervised by researchers. The daylighting evaluation protocol was derived from the work of Atif et al. (1997). The intent of this analysis is to understand how well this resource is being used by determining the extent to which daylight might meet the lighting needs. Recommended lighting levels are 30–50 f.c. (300– 500 lux), and where daylight can provide the recommended lighting levels, the analysis shows where electric lighting can be reduced.

Daylighting was measured over the course of three site visits at different times of the year. The first measurements were taken near the summer solstice from June 28 to July 1, 2001. The second period was near the autumn equinox from September 21 to September 22, 2001. The third visit was during winter from January 17 to January 22, 2002. During each visit, dataloggers were set up to continuously collect data from photometers at 5-minute intervals. Additional measurements taken with handheld photometers to collect supplementary data that cover a wider distribution of locations in the building.

For daylighting to save energy, the use of electric lighting must be reduced in response to natural light. An aggressively daylit building should show significant reductions in lighting electricity during daytime

hours. Therefore, to quantify the amount that daylighting reduces electric lighting in the Merrill Center, we compared the daily average lighting profiles for working weekdays between the summer and the winter. The early darkness in January that overlaps with working hours shows the lighting levels without daylight harvesting.

### *6.3.2 Daylighting and Lighting Evaluation Results*

The measured data, which indicate there is good daylight availability on the second floor and less on the first floor, support qualitative assessments of the Merrill Center. Although research protocols for gathering photometric data are adequate, and the data collected are considered robust, more research needs to be done to improve methods of processing the data to make them more useful. Therefore, this study does not present results in detail, but provides samples of the measurements.

Figure 6-11 shows a sample of the 5-minute interval photometer results from a sunny day on the second floor. Figure 6-12 shows the locations for the results shown in Figure 6-11. A typical target for lighting is 30–50 f.c. (300–500 lux). Results show higher values everywhere except location 2, which indicates that enough natural light is available. Samples of the handheld measurements are provided in Figure 6-13, Figure 6-14, and Figure 6-15 for locations spread around the entire second floor at a height of 3 ft. (1 m).

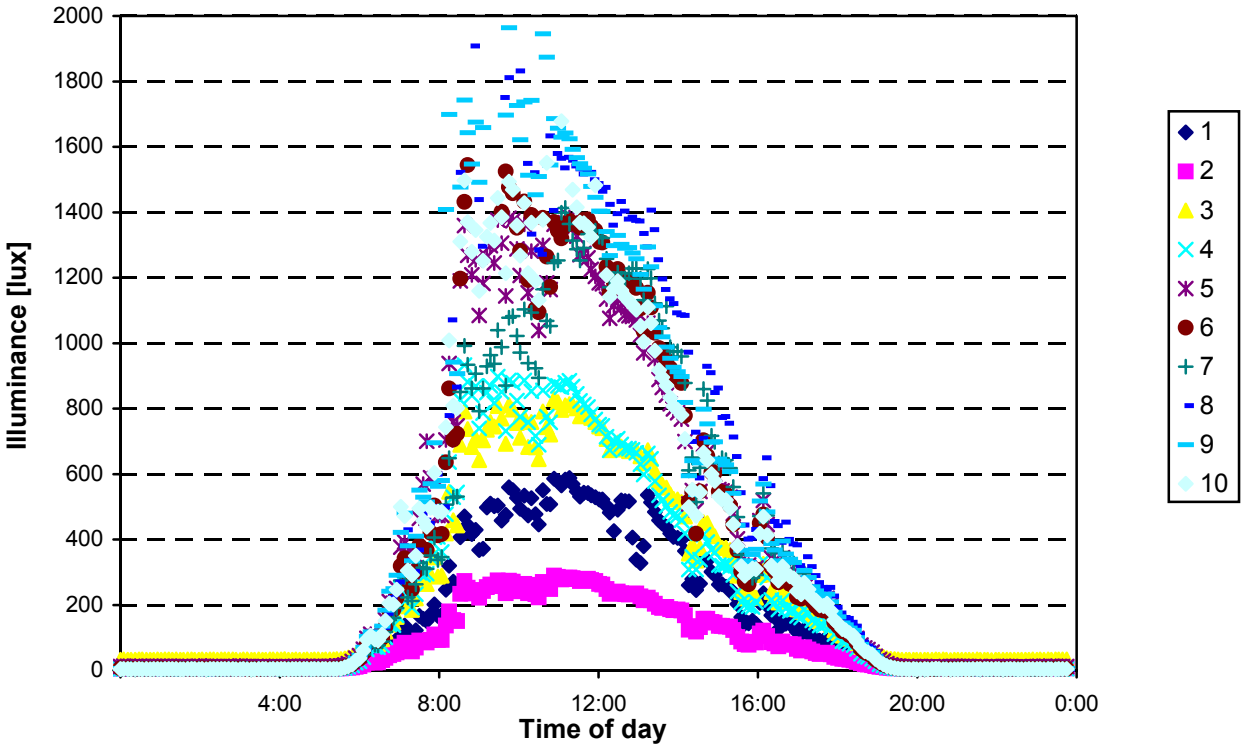


**Figure 6-11 Sample of automated photometric measurements on the second floor (September 22, 2001)**

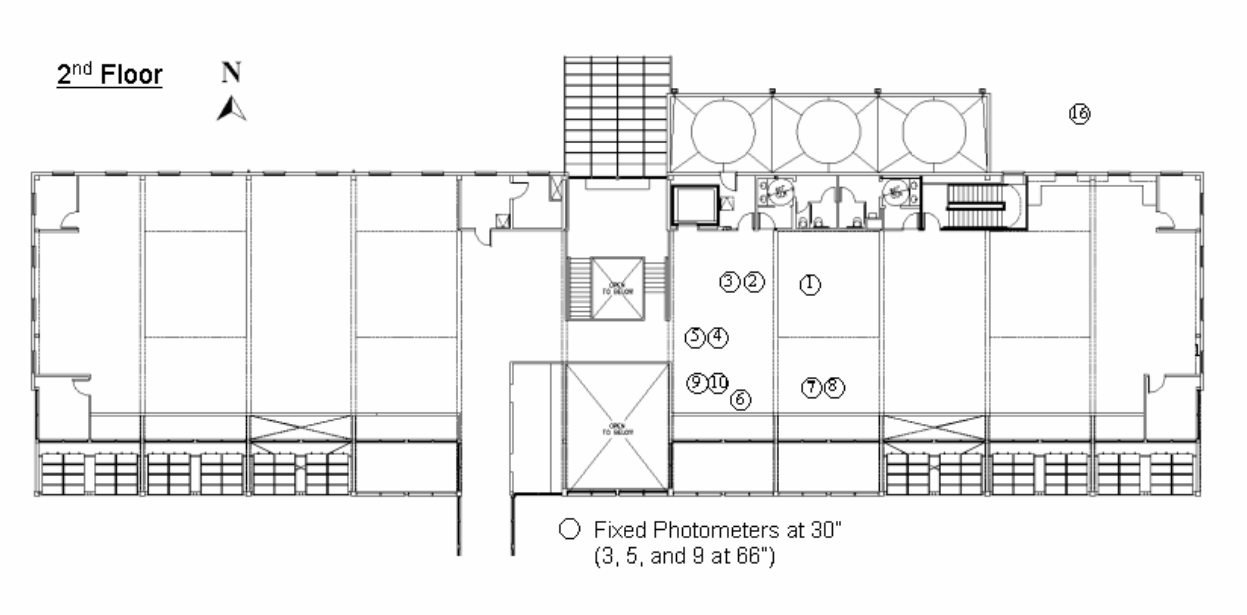


**Figure 6-12 Locations for automated photometric measurements on the second floor (September 22, 2001)**

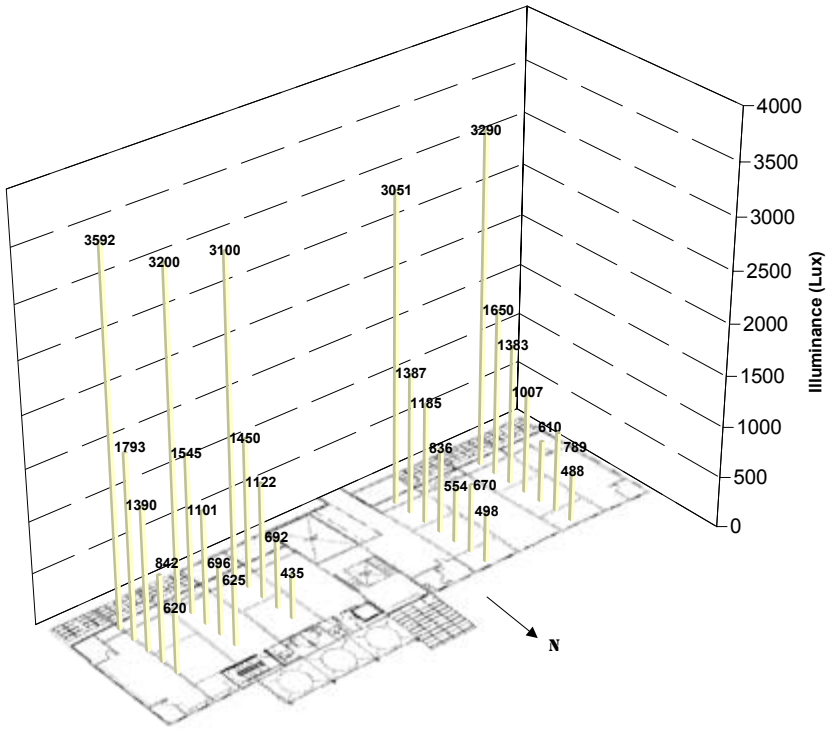


**Figure 6-13 Handheld photometric measurements on second floor: June 30, 2001: 1:00 p.m. (bright diffuse sky with electric lights off)**

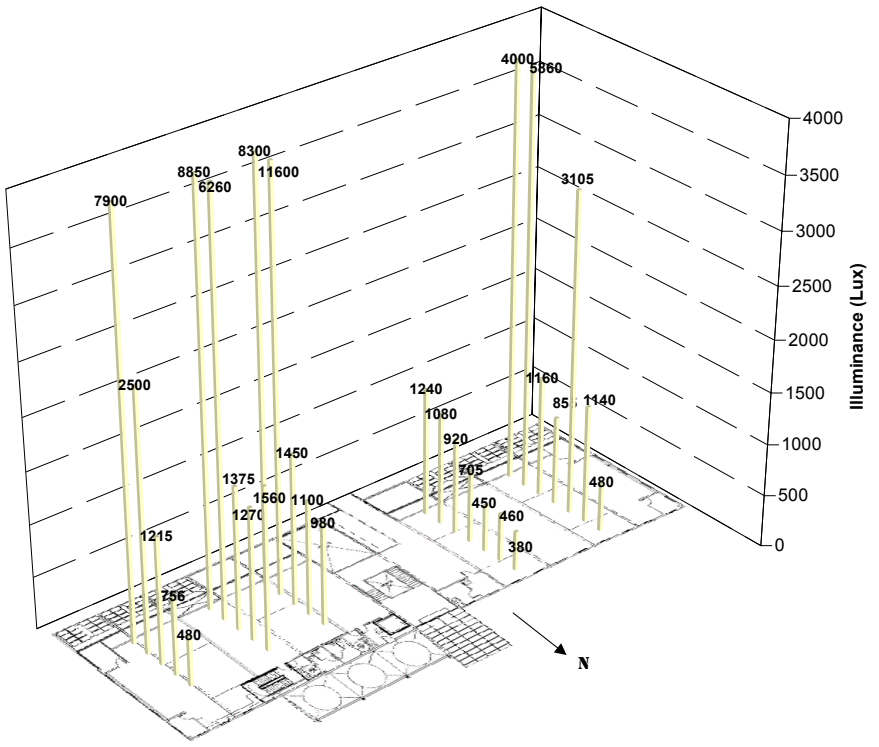


**Figure 6-14 Handheld photometric measurements on second floor: January 2, 2002: 9:00 a.m. (clear sky with electric lights off)**

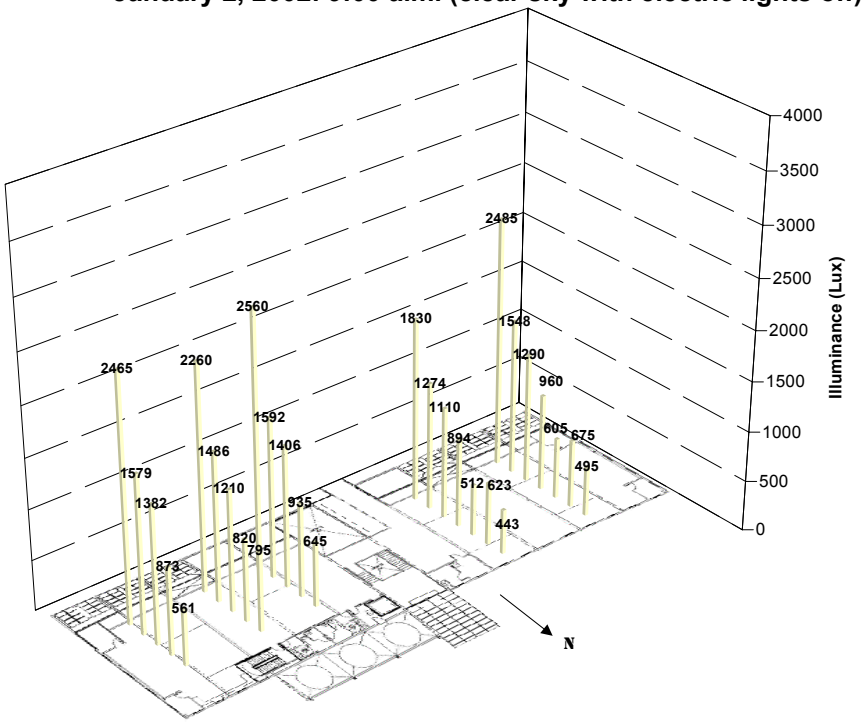


**Figure 6-15 Handheld photometric measurements on second floor: September 22, 2001: 12:00 p.m. (mostly clear sky with electric lights off)**

**Figure 6-16 Glare problems caused by daylighting**

The results indicate that daylight penetrates across the second floor, but that glare problems can be expected, as shown by the high readings (greater than 186 f.c. [2000 lux]) and observations of occupants setting up makeshift shading devices (shown in Figure 6-16). The problem suggests that a more robust solution for reducing glare should be explored. The broad expanse of windows along the south façade has more area than would be needed for daylighting purposes alone. (In addition, this wall probably creates additional cooling and heating loads.) There are several solutions to this problem, and a detailed design solution should be engineered. Placing diffusing films on the glass is the easiest solution; however, this solution would reduce the view to the bay. The diffusing films, as well as light-deflecting devices, would help light the ceiling. Hanging translucent shades would also minimize the glare.

Figure 6-17 shows the average weekday lighting energy use for the lights (except task lighting) on the second floor of the main building for January and June 2002. The shorter days in January mean that in the evening, less light is available and more electric lights are in use. The data indicate that because of daylighting, the average reductions in electric lighting on the second floor of the main building are roughly 20%. The difference is seen from January through June between 5:00 p.m. and 6:00 p.m. The early morning peak is related to the cleaning crew. A lighting power reduction of 20% is considered low for an aggressively daylit building, which leads to the conclusion that daylight is not harvested well or the daylighting design is not adequate.

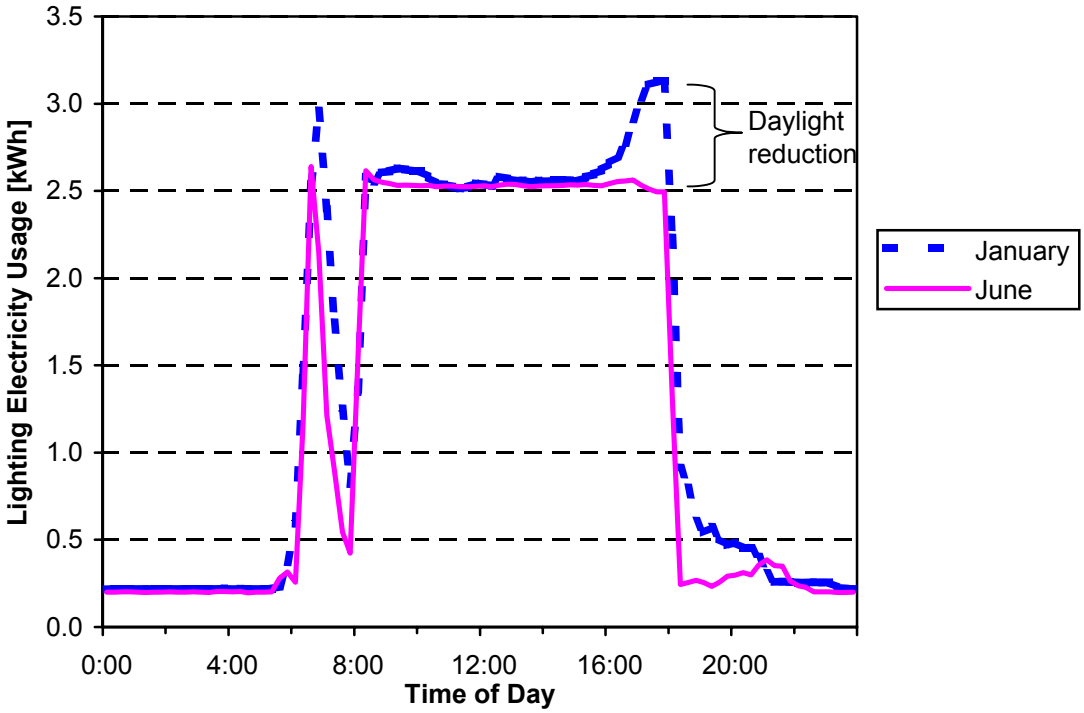


**Figure 6-17 Average weekday profile of energy use for second-floor lighting for January and June**

Daylighting and indirect lighting fixtures benefit from lightly colored interior surfaces that reflect light. Figure 6-18 shows the relatively dark colors in the Merrill Center's interior because of unfinished wood products, the rough surface of OSB and laminated beams, and exposed ductwork. Dark colors are counter to design for daylighting. Finishing the interior, especially the ceiling, would provide surfaces with higher reflectivity and brighten the space, which would allow for increased use of daylighting and less waste from the indirect fluorescents. Although results indicate that daylight is sufficient, this is because of the large amount of glazed area and despite the dark interior colors. The *distribution* of natural daylight and indirect electric lighting would be improved by using lighter colored interior finishes. Daylighting design analysis should take into account obstructions from structural beams and ductwork.

**Figure 6-18 Second-floor ceiling, beams, and ducts**

The lighting controls in the open second-floor office are manual on/off (except for the first two rows, which are dimmable and connected to photocells). More of the lighting on the second floor could be controlled to harvest daylight. The operator currently switches banks of lights off (sometimes by removing bulbs), but automatic controls would represent a better long-term solution. Furthermore, the overhead fixtures are wired so that both the indirect and direct sections must be switched on or off together. The fixtures should be replaced or rewired so that the indirect up lights can be turned off separately from the down lights. Replacing the fixtures or rewiring would allow the indirect lights to be turned off when daylighting is present. User satisfaction is usually higher for dimming systems—the data indicate that nearly all areas of the second floor receive some daylighting and can therefore achieve some level of electric lighting saving. It may be possible to switch some fixtures off, especially up lights when daylighting is present.

Experience with another building project (Torcellini et al. 2003) showed that a single photometer could be used to measure natural light and then used to control separate lighting zones (where each has its own setting relative to the single photometer). A photometer would work well on the second floor of the Merrill Center because light from the south windows dominates the daylighting. In addition, each lighting zone should have occupancy sensors and individual overrides so lights can be turned off when no one is present. Lights on the second floor used 37,980 kWh of electricity, which at a virtual rate of $0.091/kWh represents expenditures of $3,470/yr. Although detailed as-built analyses would produce a more refined estimate, improving the lighting controls and fixtures could probably reduce second-floor lighting energy use by 50%, which would save $1,700/yr. Some lighting fixtures in closets do not have on/off switches and do not need to run continuously; switches should be installed to allow lights to be turned off.

# 7 Recommendations

This section discusses recommendations developed from lessons learned from our analysis of the Merrill Center. The term *lessons learned* is used in this paper to refer to either positive or negative aspects of a project that have a clear educational message that can help subsequent building projects or research efforts. Recommendations are intended to help those interested in low-energy design avoid repetition of mistakes and to improve the process of constructing low-energy buildings. The Merrill Center can be considered an excellent example of a green building. However, its energy performance is not what it could have been, so this section discusses aspects that could have been done better. This section is organized to correspond to the phases of the Merrill Center project: design process, operation, postoccupancy alterations, and performance analysis.

## 7.1 Design Process

Listed here are some general recommendations to improve the process of designing low-energy buildings. Although the design process was not explicitly studied, examining the energy performance of the Merrill Center illustrated several factors that could improve this process.

### *Recommendation # 1–Design passive cross ventilation for multiple airflow paths and natural stack effect.*

Winds are important resources for daytime, natural cross ventilation. Section 6.1.2 showed that when designing for cross ventilation in the Merrill Center, seemingly safe assumptions about the direction of winds may be false. For this project, cooling breezes off the bay appeared to be ample for daytime cooling. The design of the building's operable fenestration and intended natural ventilation airflow pathways were based on a single wind direction. Chang (2002) first observed, and monitoring data support the finding, that often the winds are not off the bay from the south. For the Merrill Center, it would have been better to design for more east-west cross ventilation. The Merrill Center should serve as an example of the importance of designing naturally ventilated buildings for a variety of airflow pathways and wind directions. Natural ventilation should be designed to rely primarily on stack effect unless winds are reliable. Designers should use appropriate computer models that predict airflow to help design such systems. Finally, although occupant operation of manual windows has not been a problem for the Merrill Center, designers should be aware that interest in operating them has waned somewhat and that automated operation of windows may be preferable.

### *Recommendation # 2–Install PV panels where they will not be shaded.*

PV panels should always be located where they will not be shaded to maximize their energy production. In the case of CBF, the panels are shaded, especially in the summer, which reduces their efficiency. Figure 4-7 shows the panels shaded by structures above them and by the conference pavilion. One benefit to the panels in the current location is that they are highly visible from both inside and outside the building, which is useful for educating visitors.

### *Recommendation # 3–Use models with short-term response when designing ground-source heat exchangers.*

Ground-source heat exchangers and heat pumps have been promoted for low-energy buildings. Experience with the Merrill Center indicates that although the system can deliver good space comfort, temperature fluctuations in the ground loop are greater than expected. Monitored data for fluid temperatures that return from the ground heat exchanger clearly show that loop temperatures can be high and show considerable seasonal (see Figure 6-3) and daily (see Figure 6-4 and Figure 6-5) fluctuations. When modeling is used to design such systems, the models typically use constant fluid temperatures for each month. Although such analysis attempts to ensure that the field can perform over a long period

(years), they do not capture the fluctuation of temperatures over the short term, as shown in Figure 6-4 and Figure 6-5. The next-generation design tools for ground-source heat pumps, such as those now available in EnergyPlus, should be developed and applied when evaluating and designing such systems.

## 7.2 Operation

This section discusses issues related to how the building is operated.

*Recommendation # 4–Reprogram the EMS to run heat pumps based on current utility demand to better manage demand charges.*

As discussed in Section 6.1, the HVAC heat pumps often contribute significantly to demand charges. The EMS could be programmed to reduce the number of heat pumps that can run at the same time to reduce demand charges. During the winter, the heat pumps lead to demand peaks during morning warmup. More time for warmup should be allowed and the warmup should be staged to minimize the demand. This change would not necessarily save energy, but it could reduce the peak electricity demands and reduce costs.

*Recommendation # 5–Reduce receptacle loads during off hours.*

As discussed in Section 5.2.9, off-hour receptacle loads are about half what they are during the day, which indicates that equipment is left on when not in use. Presumably, this is because a large amount of information technology equipment operates in the offices and server room. CBF could deploy new network-based software products that monitor and reduce computer power. Because the receptacle loads are already submetered, the Merrill Center would be a good candidate for future efforts to research the effectiveness of such software-based solutions to control off-hours plug loads.

## 7.3 Alterations

This section suggests postoccupancy alterations. Predictive capabilities during the design phase are not perfect, and once the building is up and running, there should be an opportunity to revisit the design and make changes. The usual commissioning activities do little to improve the operation of a building beyond its designed capabilities. Experience with other low-energy buildings shows that after a building is constructed (and has been commissioned to verify its system components are as designed) there remains a significant need to adjust lighting and HVAC controls to further reduce energy use and improve occupant satisfaction. In addition, capital equipment changes can be made to improve performance.

### *7.3.1 Lighting*

*Recommendation # 6–Provide second-floor interior with high-reflectivity finish.*

Daylighting and indirect lighting fixtures benefit from lightly colored interior surfaces that reflect light. The Merrill Center's unfinished engineered wood products are good from the point of view of resource use, but the relatively dark colors and rough surfaces of OSB and laminated beams reduce the effectiveness of the daylighting and the indirect lighting system. Finishing the interior, especially the ceiling, to provide surfaces with higher reflectivity would brighten the space and make the daylighting more effective. In addition, the high ceilings reduce the effectiveness of indirect lighting. Indirect lighting should be used only when the ceiling is close to the lighting source.

*Recommendation # 7–Install new lighting controls in open office.*

Automatic lighting controls should dim and energize lighting circuits according to available daylight. Manual controls limit the amount of daylighting that can be harvested. A single photocell could be installed on the second floor, and second-floor lighting zones could be calibrated against this sensor for

on/off control. Dimming fixtures should be controlled with local photocells to maintain a lighting level of 40 f.c. (431 lux).

*Recommendation # 8–Monitor and design a system to minimize glare issues.*

The south wall has more glazing than necessary for daylighting and causes glare problems on the second floor. There are several potential solutions to this problem, and a detailed design solution should be engineered in follow-on efforts. Diffusing films on the glass are the easiest solution; however, this will reduce the view to the bay. These films, as well as light deflecting devices, would help light the ceiling of the building. Hanging translucent shades would also minimize the glare. Flat screen computer monitors would help with glare problems and reduce plug loads.

*Recommendation # 9–Install light switches in closets*

Some closets in the Merrill Center have linear fluorescent fixtures that cannot be turned off. Simple light switches or motion sensors should be installed to allow these to be turned on and off as needed.

### *7.3.2 Ground-Source Heat Pumps*

*Recommendation # 10–Evaluate and inspect the ground-loop system and consider increasing heat exchanger capacity and control improvements.*

This recommendation stems from the findings, discussed in Section 6.1.1, that temperatures in the ground loop fluctuate widely and are often higher than expected. Additional detailed analysis of the ground loop, including a detailed review of the construction drawings, should be performed to understand how the system was designed. Based on the measured energy performance, the field may be undersized for the actual loads. The sizing calculations should be redone to include the unused desiccant dehumidification system. However, a simple mistake could be to blame: some of the 48 wells may be inactive or there may be a poor balance of flow between the four circuits. Follow-on efforts should verify that the field has been installed as designed and that all wells have the appropriate flow rates. Future projects should include field tests to verify that ground heat exchangers are installed as designed.

As part of a follow-up evaluation, the addition of a cooling tower should be considered. Currently, temperatures are cooler than the ground-loop temperatures 61% of the time (mostly during the winter and shoulder seasons) and about four times more heat is added to the ground for cooling than is extracted for heating. With such a California-style heat pump arrangement, the ground-source heat pumps would be used only when ground temperatures are more favorable than ambient conditions. Further analyses should be done to study the rainwater collection system to see if a wet cooling tower would be feasible; otherwise, a dry cooling tower would need no water.

As part of this recommendation, the control algorithms for variable-speed ground-loop pumps should be examined. It may be better to control loop pumps based on supply temperatures (or temperature differences) with limits set by pressure. Such research should seek to balance pump energy, ground heat exchanger effectiveness, and heat pump efficiencies.

The server room contains a small water-to-air cooling system that requires continual operation of the main ground loop regardless of the heating or cooling needs of the rest of the building. The water flow needed by this small system should be compared to the minimum flow rates that the large variable speed pumps can deliver. If a mismatch is found, alternative methods of cooling the server room should be explored so that the main ground loop pumps do not need to run continuously.

### 7.3.3 Outside Air System

*Recommendation # 11–Refit the air system to allow economizer operation.*

The outside air system in the Merrill Center includes natural ventilation features as well as air handlers. One way to think about passive natural ventilation is that it essentially economizes without fans, and, if it is fan assisted, it is much like running an economizer. However, from a thermal comfort point of view, it is limited to moderate temperatures. An economizer-based system can control supply air temperature to provide thermal comfort for a wider range of outdoor temperatures.

This study found that considerable energy is being expended for heat pump cooling during the winter (see Table 6-1), which indicates that natural ventilation systems do not always deliver cooling during the heating season. This recommendation is put forth with the caveat that additional analysis should be conducted to better understand the implications for fan energy use (exhaust fans versus air handler supply fans), and the costs and benefits of refitting the air handlers for economizer operation. Because the conference pavilion does not have the fan-assisted natural ventilation, it may be more important to install an economizer there.

*Recommendation # 12–Refit the Merrill Center's air system to either remove or use the desiccant wheel system.*

The desiccant wheel dehumidification system in the Merrill Center is not used as designed and its potential benefits should be evaluated. If the wheels are not going to be used, they should be removed because they increase the pressure drop and fan energy used to provide fresh air. One option is to use the wheels in a heat recovery mode without regeneration. If the wheels are retained for use and an economizer system is added, the revised air handler should be configured to allow the wheels to be bypassed during economizer operation to minimize fan energy.

### 7.3.4 Exterior Shading

*Recommendation # 13–Examine exterior shading options and add shading where beneficial.*

Cooling requirements may be further reduced by adding exterior shades. Some exterior shading on the conference pavilion was removed and should be reinstalled. The structure outside the south-facing glass on the main building might be refitted with additional shading. Before adding shading, a detailed analysis of the benefits that takes into account increasing heating loads, reducing PV output, decreasing daylighting, and mitigating glare problems should be made.

## 7.4 Energy Performance Monitoring and Analysis

Conducting this study of the Merrill Center led to the identification of additional topics that warrant research.

### 7.4.1 Monitoring Equipment

Future research and analysis of the Merrill Center should consider various changes and additions to the detailed monitoring. The dedicated monitoring system was very successful and provided robust data for the analysis. Many channels on the data acquisition system are still available.

*Recommendation # 14–Add temperature sensors to record the temperature of fluid in the four pipes that return from the ground wells.*

There are two advantages to installing sensors on the pipes that return from the ground wells. First, the data may show how well balanced fluid flow and heat transfer is between the four circuits. Individual

readings may show a plumbing or design problem. Second, it would be good to have readings before and after the loop pump to quantify any temperature rise from the pump.

### *Recommendation # 15–Add flow sensors to record the flow rate of fluid in the ground-loop wells.*

With the current plumbing configuration, it was not possible to install a single flow transducer. Follow-up research activities that focus on ground-source heat pumps should attempt to directly measure the total flow in the loop. For the Merrill Center, this may require installing four meters on each circuit. For future projects, it is advantageous for maintenance and monitoring to install flow meters in the ground loops at time of construction. This should be considered an integral part of a ground-loop system.

### *Recommendation # 16–Reinstall outdoor weather station.*

Contractors removed the weather station instrumentation in November 2002. These sensors should be reinstalled as part of any ongoing research efforts.

### *Recommendation # 17–Record data from the energy management system.*

Several sensors in the building are connected to the EMS and are not recorded with the monitoring data. For example, the current monitored data do not indicate when the building is in natural ventilation mode, but the EMS has these data. The attentive building operator often uses the EMS to adjust the building, so modeling the ever-changing building controls is difficult. A preliminary list of data that should be recorded from the EMS includes thermostat set points, states of all systems related to natural ventilation (exhaust fans, window operators, and the *Windows Open* signage), $CO_2$ sensor, air-handler stage, and propane flow. The robust recording of EMS data for long periods and successful merging of these data with the stand-alone dataloggers are challenges. One option is to add analog and relay outputs to the EMS and monitor them with the dataloggers.

### *Recommendation # 18–Instrument domestic hot-water system.*

The Merrill Center meets all its DHW needs with solar thermal collectors. This study did not account for the energy performance and savings from this system. Thermal instrumentation should be checked for accuracy and any additional instrumentation needed added to allow proper analysis of the DHW system.

### *Recommendation # 19–Instrument natural ventilation system.*

This study did not focus on natural ventilation. However, such systems are of interest because of their potential application in office buildings. Follow-up research on natural ventilation should consider adding instrumentation to submeter electricity used for assist fans, count opening and closing events of selected windows, and additional metrics related to occupant thermal comfort. Chang's attempt to use low-cost cameras to monitor window operations merits further study.

### *Recommendation # 20–Develop monitoring capability to directly measure horizontal infrared radiation weather data.*

This project generated weather data from monitoring results for use with EnergyPlus. However, we discovered a lack of appropriate methods (see Appendix E) for determining values for either cloud cover or horizontal infrared radiation from the weather data that were collected. It is not practical to have an observer manually record cloud cover. Furthermore, such data are being dropped from standard weather station observations. For future monitoring projects, techniques should be developed to directly measure horizontal infrared sky radiation. Silicon-based photometers can be used to apply thermopile-type detectors that directly measure infrared radiation (or effective sky temperature) in a manner analogous to solar measurements.

### 7.4.2 As-Built Modeling

*Recommendation # 21–Complete an as-built EnergyPlus model.*

The original plan for this study was to use the EnergyPlus whole-building energy analysis program to develop a detailed as-built model of the Merrill Center. Unfortunately, the model was not completed because the model for water-to-air heat pumps was not available in EnergyPlus until late in the project. Usually, it is difficult for most energy modeling programs to accurately simulate two separate types of HVAC systems that serve the same zone, such as the heat pumps and hot-water baseboards used at the Merrill Center. However, EnergyPlus can model various types of equipment that serve the same zone and a large number of measured data are available for comparison to model results; therefore, we recommend that the as-built model be revisited if future research is done on the building.

*Recommendation # 22–Model natural ventilation systems.*

Additional modeling of the Merrill Center is warranted because of the current level of interest in natural ventilation for commercial buildings. Although current monitoring data are insufficient to provide high-quality validation of natural ventilation modeling, the availability of well-calibrated internal gains and measured weather data, along with the possibility of follow-up monitoring, make the Merrill Center an attractive test case for such efforts.

### 7.4.3 Real-Time Modeling

*Recommendation # 23–Develop a near real-time energy savings meter.*

The original measurement and verification plan called for implementing a near real-time energy savings meter. The concept for such a meter is to continuously take measured data and automatically run baseline or as-built models to determine how well the building performs. Such a meter could not be implemented because the weather station was dismantled. The Merrill Center is a good candidate for this type of research because the building has already been instrumented and it has a motivated operator who is likely to use the information to improve the operation of the building.

# 8 Conclusions

The Merrill Center is a 31,000-ft$^2$ (2,880-m$^2$) building that successfully demonstrates a variety of sustainable building practices. This report assessed the energy performance of the Merrill Center through a combination of physical monitoring and computer simulation. (Results are summarized in Table 8-1.) The assessment leads to the following conclusions about the Merrill Center:

- The level of total site energy use savings, including receptacle and miscellaneous loads, is 24.5% compared to a minimally code-compliant building.
- The level of source energy savings, including receptacle and miscellaneous loads, is 22.1% compared to a minimally code-compliant building.
- The level of energy cost savings, including receptacle and miscellaneous loads, is 12.1% compared to a minimally code-compliant building.
- The use of building monitoring and calibrated simulations can quantify differences between design expectations and actual building energy performance.
- During the cooling season, the temperature of water that returns from the ground heat exchanger, which supplies the water-to-air heat pumps, is often warmer than might be expected. This indicates a need for additional research on the performance of the ground-source heat pumps.
- Daylight is not harvested as well as it could be on the second floor.
- The Merrill Center is a good candidate for follow-up research.

This study led to the following general conclusions:

- A long-term monitoring effort can collect detailed, annual data sets for energy use and weather that are suitable for evaluating energy performance.
- The new Appendix G for standard ASHRAE/IESNA 90.1 2001 is helpful for defining baseline energy models.
- An analysis of error in the baseline building energy models shows that such models have considerably more uncertainty than actual measurements that establish a true energy balance.
- Significant differences were found between the actual energy performance and predictions made for rating purposes. This indicates a need to improve protocols for rating and to continue efforts to study actual buildings.

**Table 8-1 Energy Savings Summary: November 2001–November 2002**

| | **Total Site Energy Use Intensity** kBtu/ft$^2$·yr *(MJ/m$^2$·yr)* | **Net Site Energy Use Intensity** kBtu/ft$^2$·yr *(MJ/m$^2$·yr)* | **Net Source Energy Use Intensity** kBtu/ft$^2$·yr *(MJ/m$^2$·yr)* | **Energy Cost Intensity** $/ft$^2$·yr *($/m$^2$·yr)* |
|---|---|---|---|---|
| Baseline Model | 53.3 *(604.8)* | 53.3 *(604.8)* | 159.6 *(1,812)* | 1.20 *(12.87)* |
| Monitoring | 40.2 *(456.8)* | 39.9 *(453.2)* | 124.3 *(1,412)* | 1.05 *(11.31)* |
| Savings | 24.5% | 25.0% | 22.1% | 12.1% |

# 9 References


ASHRAE. (2001a). *Handbook of Fundamentals – 2001*. Atlanta, GA: American Society of Heating, Refrigerating and Air-Conditioning Engineers, Inc.

ASHRAE. (2001b). *ANSI/ASHRAE/IESNA Standard 90.1-2001–Energy Standard for Buildings Except Low-Rise Residential Buildings*. Atlanta, GA: American Society of Heating, Refrigerating and Air-Conditioning Engineers, Inc.

ASHRAE. (2002). *BSR/ASHRAE/IESNA Addendum e to ANSI/ASHRAE/IESNA Standard 90.1-2001*. First Public Review. July 2002. Atlanta, GA: American Society of Heating, Refrigerating and Air-Conditioning Engineers, Inc.

ASHRAE. (2003a). *BSR/ASHRAE/IESNA Addendum e to ANSI/ASHRAE/IESNA Standard 90.1-2001*. Second Public Review. April 2003. Atlanta, GA: American Society of Heating, Refrigerating and Air-Conditioning Engineers, Inc.

ASHRAE. (2003b). *HVAC Applications Handbook*. Atlanta GA: American Society of Heating Refrigerating and Air-Conditioning Engineers, Inc.

Atif, M.; Love, J.; and Littlefair, P. (1997). *Daylighting Monitoring Protocols & Procedures for Buildings*. Report #T21/D2.1/97-01. IEA Solar and Heating Program Task 21 Subtask D. Canada: Institute for Research in Construction.

Bronson, D.J.; Hinchey, S.B.; Haberl, J.S.; and O'Neal, D.L. (1992). A Procedure for Calibrating the Doe-2 Simulation Program to Nonweather-Dependent Measured Loads. *ASHRAE Transactions. Vol.* 98 (1): pp. 636-652. Atlanta GA: American Society of Heating, Refrigerating and Air-Conditioning Engineers, Inc.

Chang, J.-C. (2002). *Case Studies of Naturally Ventilated Commercial Buildings in the United States*. MSc Thesis. Cambridge, MA: Department of Mechanical Engineering. Massachusetts Institute of Technology.

Crawley, D.B.; Lawrie, L.K.; Winkelmann, F.C.; Buhl, W.F.; Huang, Y.J.; Pedersen, C.O.; Strand, R.K.; Liesen, R.J.; Fisher, D.E.; Witte, M.J.; and Glazer, J. (2001). EnergyPlus: Creating a New-Generation Building Energy Simulation Program. *Energy and Buildings.* Vol. 33 [4], pp. 319-331. Amsterdam: Elsevier Science. Available at www.elsevier.com or www.energyplus.gov.

DOE. (2004). *2004 Buildings Energy Databook*. Washington, D.C.: U.S. Department of Energy. http://buildingsdatabook.eren.doe.gov/. Accessed September 2004. EIA *Annual Energy Outlook 2003*. Washington, D.C.: Energy Information Administration. U.S. Department of Energy.

Klein, S.A.; Duffie, J.A.; et al. (1976). TRNSYS – A Transient Simulation Program. *ASHRAE Transactions.* Vol. 82, p. 653. Atlanta GA: American Society of Heating, Refrigerating and Air-Conditioning Engineers, Inc. See also http://sel.me.wisc.edu/trnsys/.

Lomas, K.J. and Eppel, H. (1992). Sensitivity Analysis Techniques for Building Thermal Simulation Programs. *Energy and Buildings.* Vol. 19, pp 21-44. Amsterdam: Elsevier Science. Available at www.elsevier.com.

MacDonald, I.A. (2002). *Quantifying the Effects of Uncertainty in Building Simulation*. Ph.D Thesis. Glasgow, UK: Univ. of Strathclyde.

Maxwell, E.L.; Marion, W.F.; Myers, D.R.; Rymes, M.D.; and Wilcox, S.M. (1995). *National Solar Radiation Data Base: Final Technical Report*. NREL/TP-463-5784. Golden, CO: National Renewable Energy Laboratory.

Mermond, A. (1996). PVSYST Version 3.2. User's Manual. Geneva: University of Geneva, University Center for the Study of Energy Problems. Available online at www.pvsyst.com/. Last accessed December 2002.

Perez, R., Ineichen, P.; Maxwell, E.; Seals, R.; and Zelenka, A. (1992). Dynamic Global-to-Direct Irradiance Conversion Models. *ASHRAE Transactions.* Research Series, pp. 354-369. Atlanta, GA: American Society of Heating, Refrigerating and Air-Conditioning Engineers, Inc.

Perez, R.; Ineichen, P.; Moore, K.; Kmiecik, M.; Chain, C.; George, R.; and Vignola, F. (2002). A New Operational Model for Satellite-Derived Irradiances: Description and Validation. *Solar Energy.* Vol. 73, (5), pp. 307-317. Amsterdam: Elsevier Science.

Pless, S.; Torcellini, P. (2004). *Energy Performance Evaluation of a Low Energy Academic Building* NREL/TP 550-33180. Golden, CO: National Renewable Energy Laboratory

Taylor, J.R. (1982). *An Introduction to Error Analysis*. Mill Valley, CA: University Science Books.

Torcellini, P.A.; Griffith, B.; Ketcham, M.; and Hayter, S. (2003). *Thermal Test Facility: Evaluation of the Energy Performance and Design Process*. NREL/TP-550-34832. Golden, CO: National Renewable Energy Laboratory.

USGBC. (2003). U.S. Green Building Council. Web site last accessed July 15, 2003: www.usgbc.org/LEED/Project/project_list.asp.

Walton, G.N. (1983). *Thermal Analysis Research Program Reference Manual*. Gaithersburg, MD: National Bureau of Standards. (now National Institute of Standards and Technology). NBSIR 83-2655.

## Appendix A Explanation of Time Map Figure Art

This appendix describes the map figures in this report. Figure A-1 shows a sample time map and explains some of its features. Because color is used quantitatively, if color figure art is reproduced in black and white, the data become inaccurate. For this reason, many figures contain both color and gray scale maps so that if the report is printed in black and white, the figures are still accurate.

Time maps are image-based plots where individual pixels represent quantities. They provide powerful data visualization without the geometric interpretation problems of three-dimensional plots. The color or gray-scale maps provide a third dimension. Time is represented in two dimensions with time-of-day across the width and day-of-year along the height. The upper left corner represents 0:00 on the first day. The upper right corner represents 23:45 (or 23:00 if hourly) on the first day. The lower edge is the last day of the data set. In the figures in this report, color scales are divided into 256 levels and gray-scales are divided into 16 levels. For 15-minute data, there is a one-to-one correspondence between pixels and measured data. For hourly data, four pixels in the width direction represent a single hourly data point. Each pixel in the vertical direction represents a single day. Most figures in this report represent 365 days so that images are derived from plots that have 96 x 365 pixels. (Pixel sizes in the original plotting routines are sized for a computer screen and are not the same as pixel sizes in the final document artwork.)

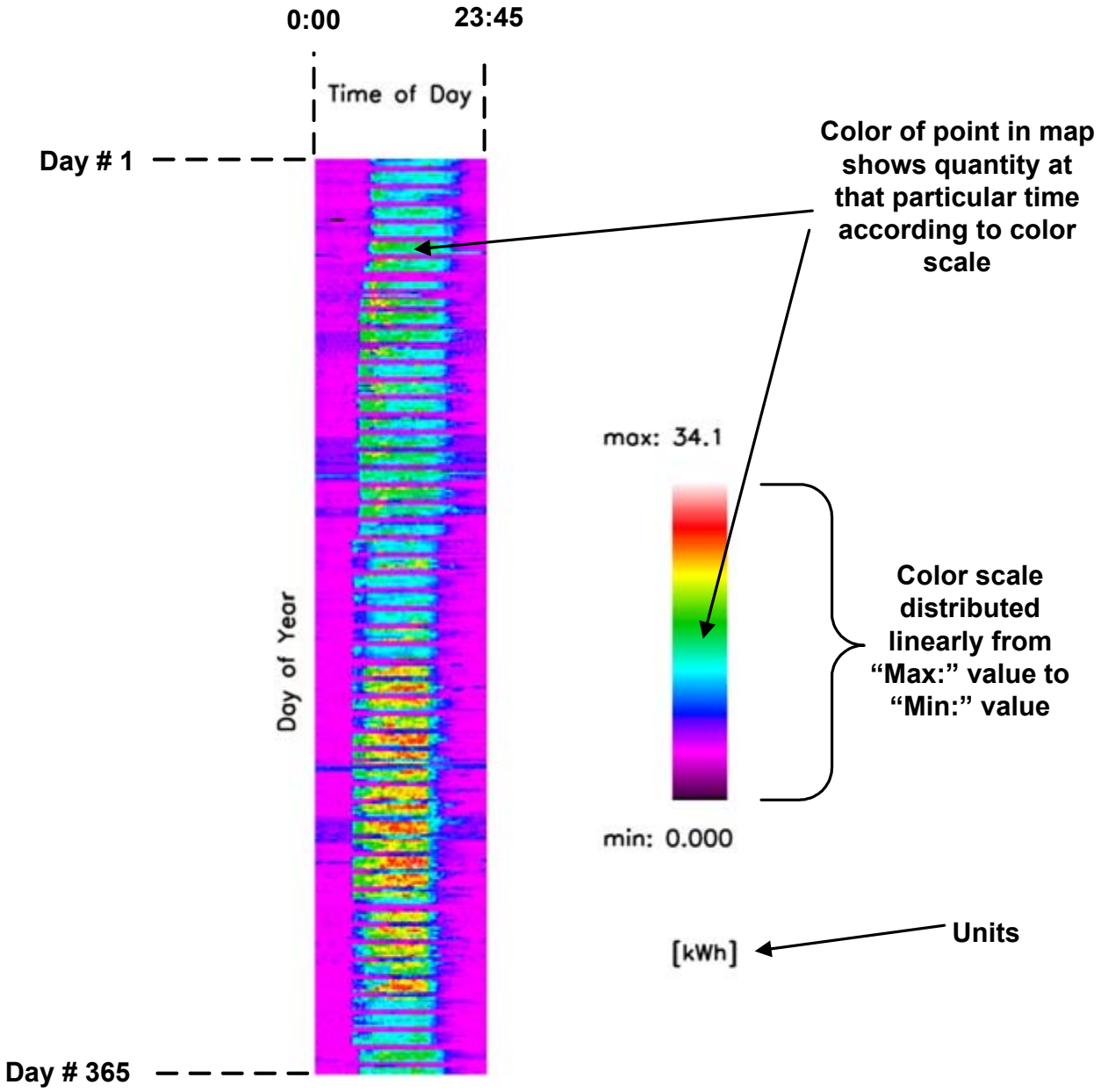


**Figure A-1 Explanation of time map figure art**

## Appendix B Selected Results from Detailed Monitoring

This appendix presents a selection of detailed data from the monitoring effort. All data sets in this appendix are from the period November 7, 2001 through November 6, 2002. In contrast to the data sets used in modeling, these have not been rearranged so the top of the time map contains data for November 7, 2001. Appendix A describes the time map figure art.

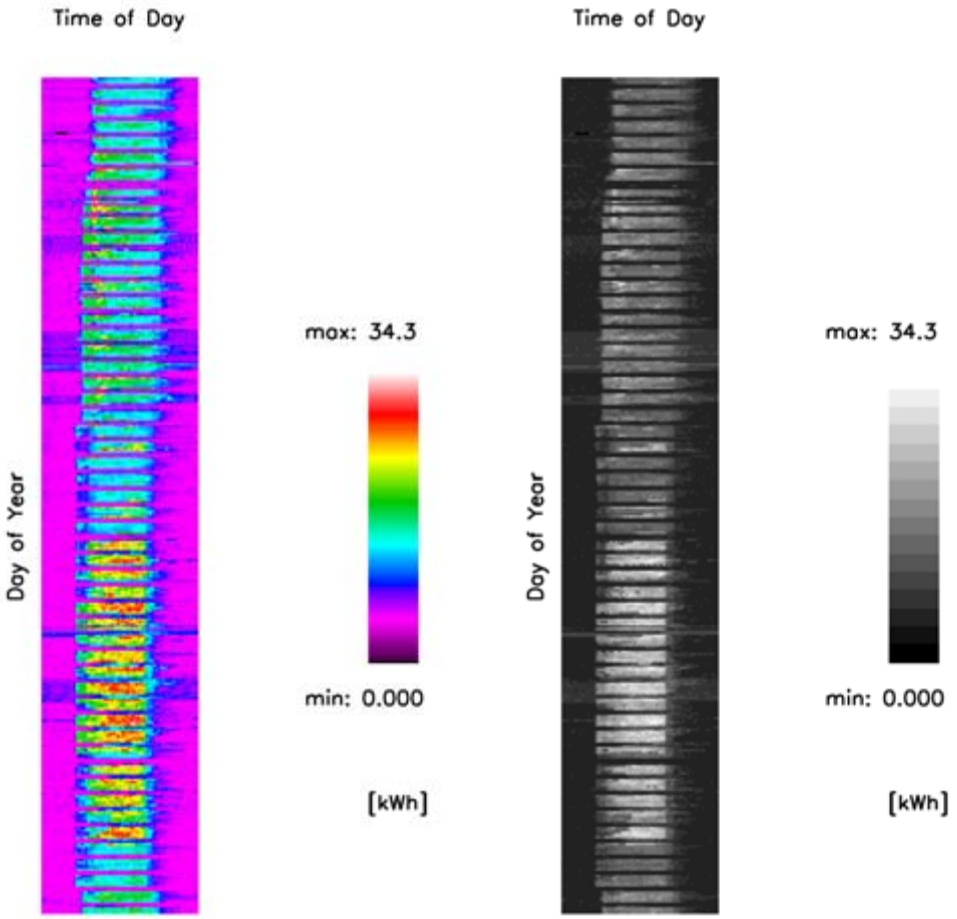


(a) (b)

**Figure B-1 Time map of total site electricity use (kWh/15-min) in Eastern Standard Time in (a) color and (b) gray-scale**

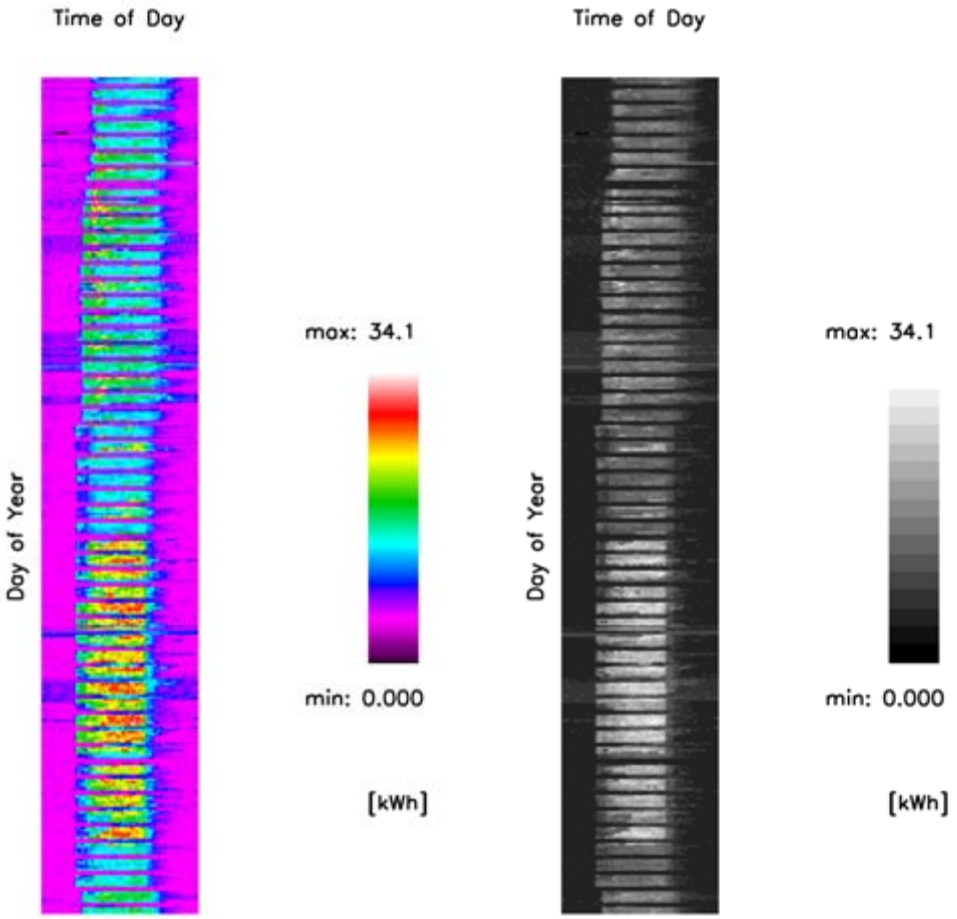


(a) (b)

**Figure B-2 Time map of net site electricity use (kWh/15-min) in Eastern Standard Time in (a) color and (b) gray-scale**

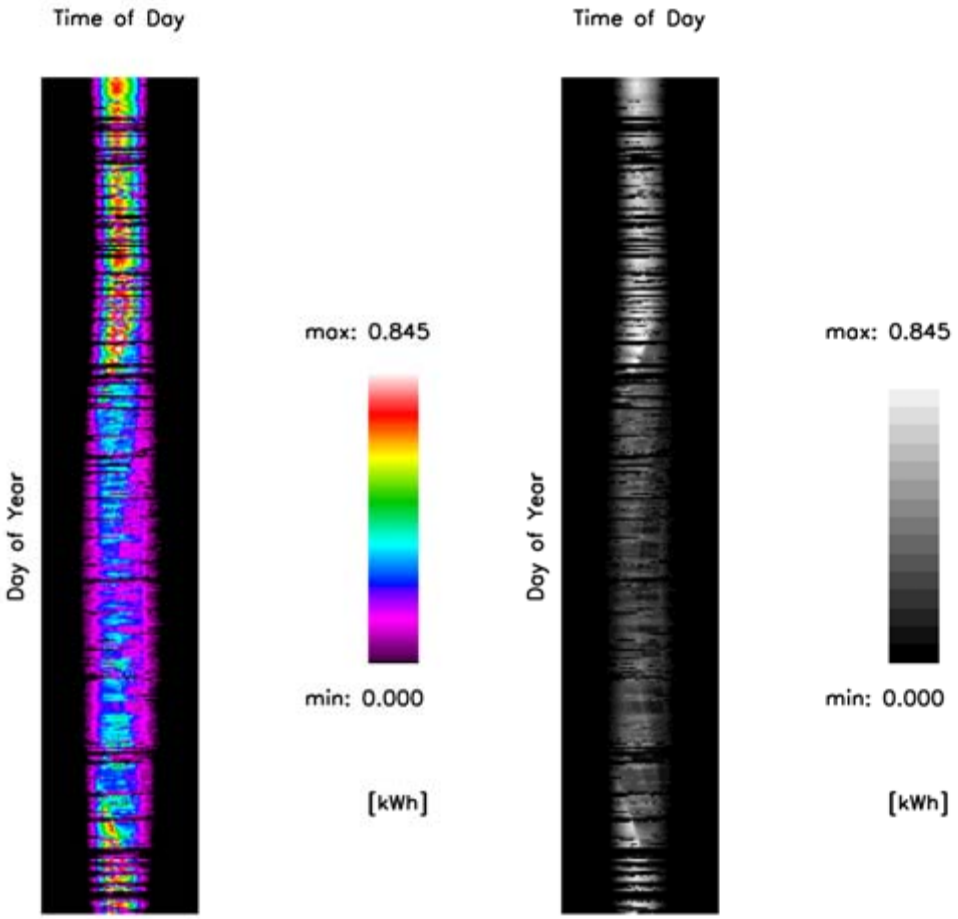


(a) (b)

**Figure B-3 Time map of PV electricity generation (kWh/15-min) in Eastern Standard Time in (a) color and (b) gray-scale**

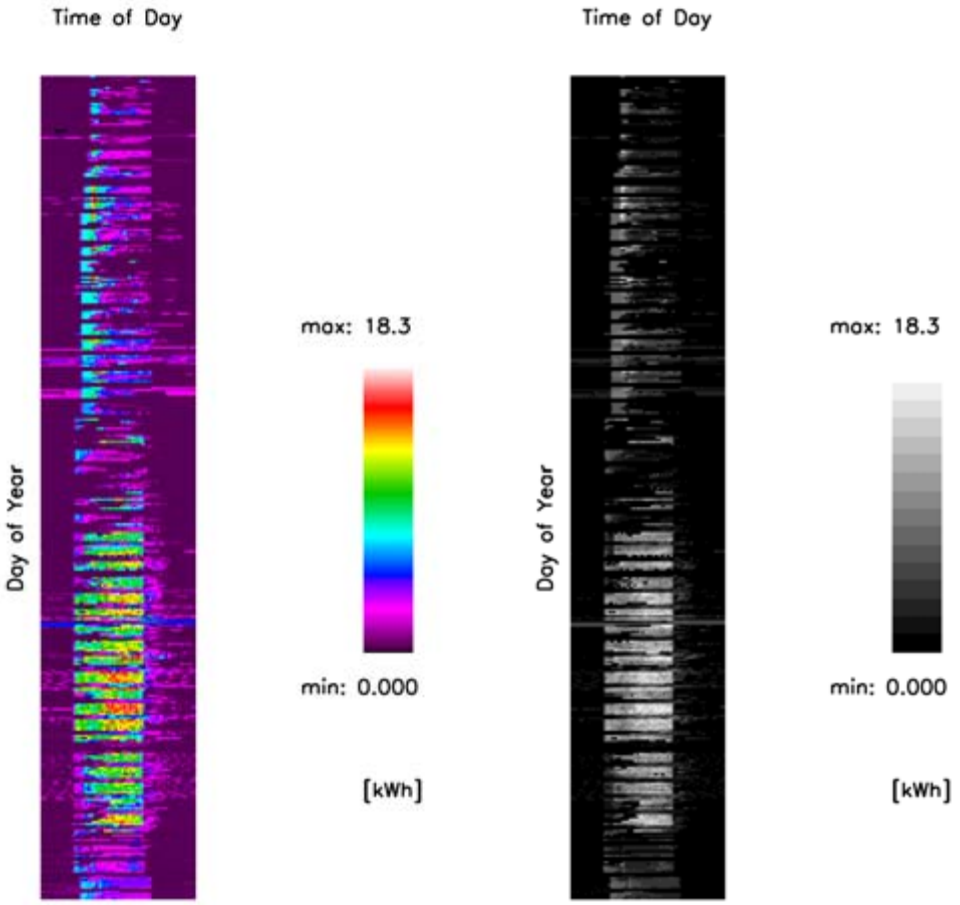


(a) (b)

**Figure B-4** **Time map of HVAC energy use for main building (kWh/15-min) in Eastern Standard Time in (a) color and (b) gray-scale**

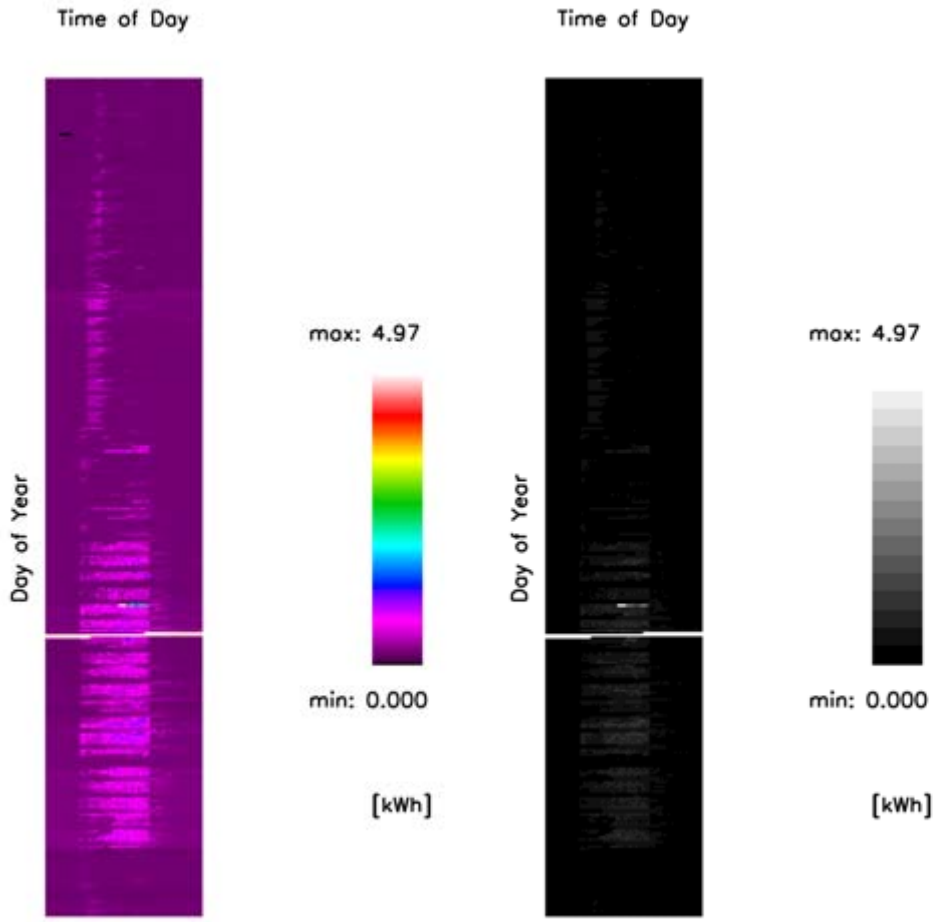


(a) (b)

**Figure B-5 Time map of ground-loop pump energy use (kWh/15-min) in Eastern Standard Time in (a) color and (b) gray-scale**

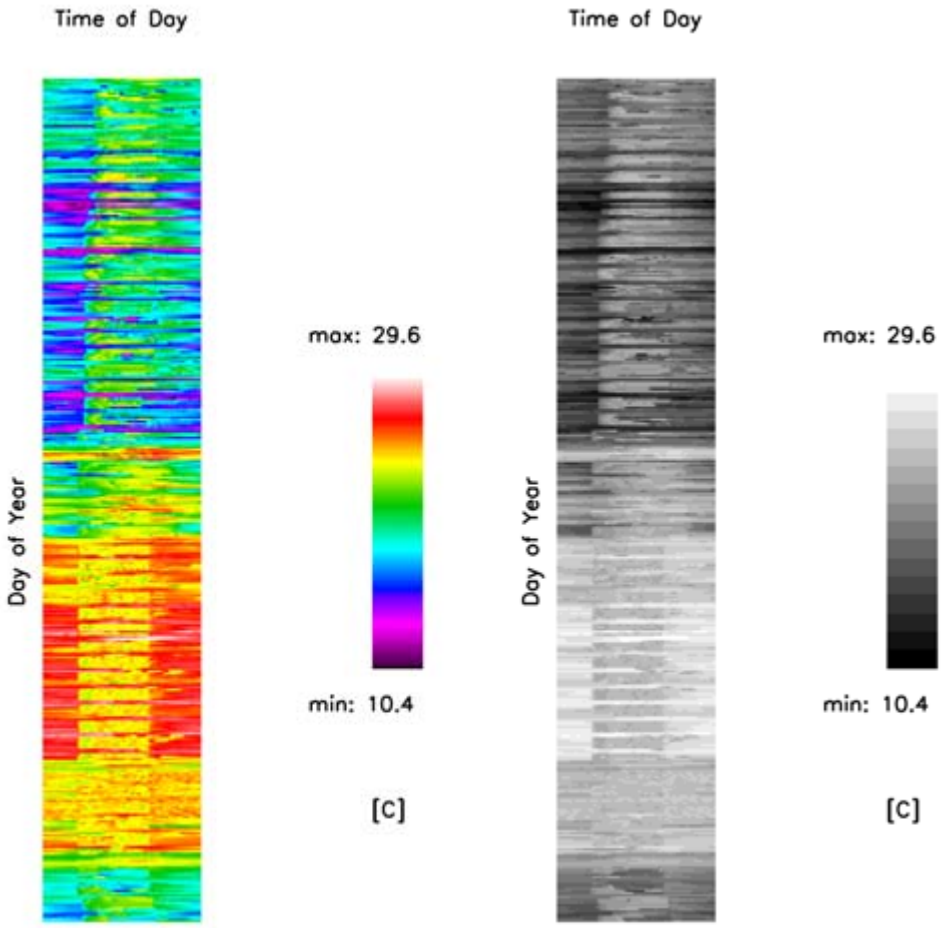


(a) (b)

**Figure B-6 Time map of first-floor air dry-bulb temperature (°C) in Eastern Standard Time in (a) color and (b) gray-scale**

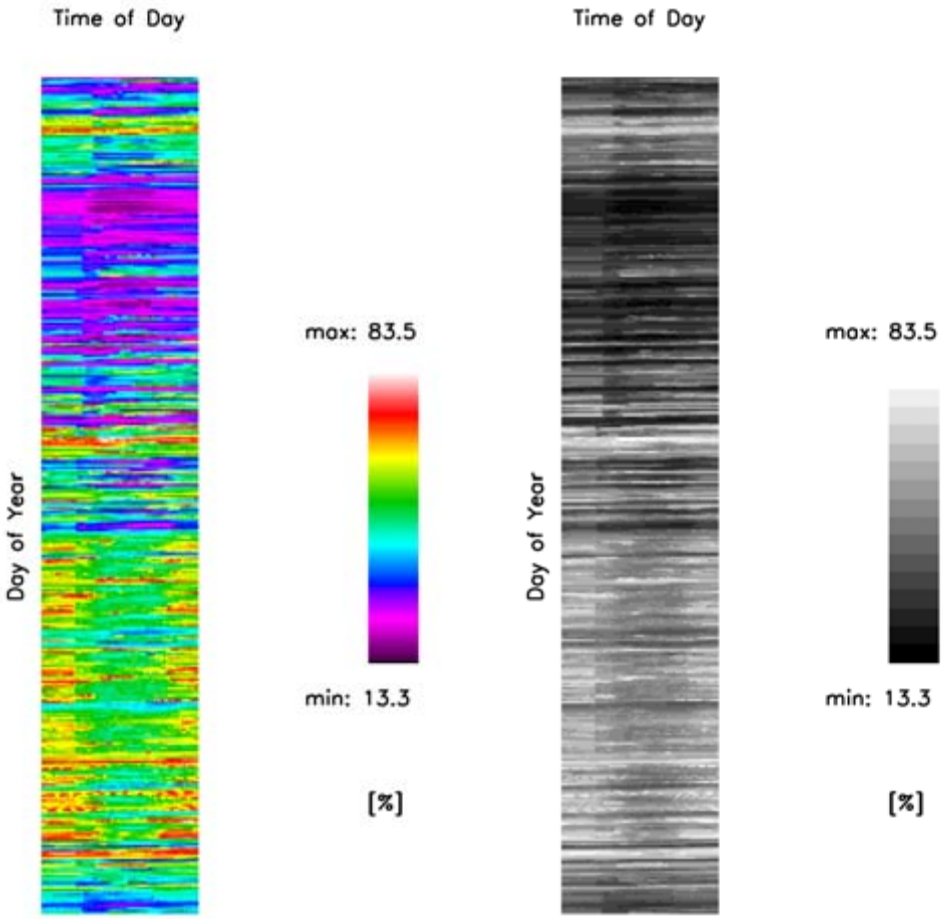


(a) (b)

**Figure B-7** **Time map of first-floor air relative humidity (%) in Eastern Standard Time in (a) color and (b) gray-scale**

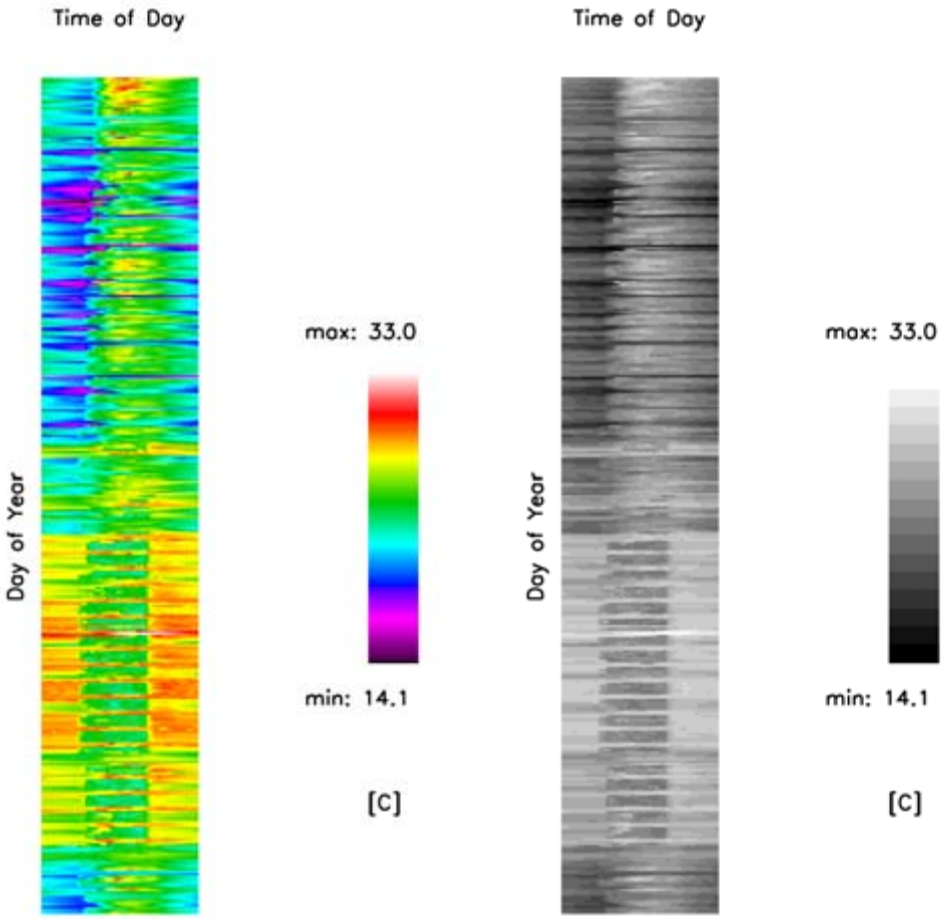


(a) (b)

**Figure B-8** **Time map of second-floor air dry-bulb temperature (°C) in Eastern Standard Time in (a) color and (b) gray-scale**

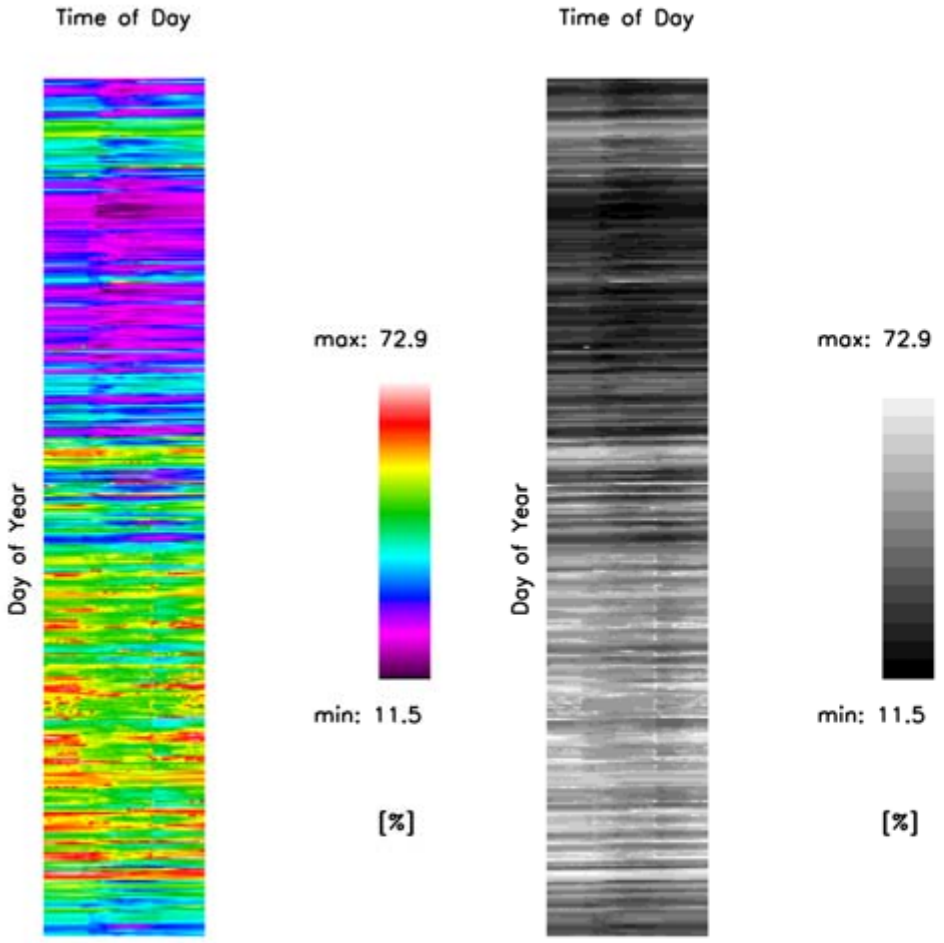


**(a)** **(b)**

**Figure B-9** **Time map of second-floor air relative humidity (%) in Eastern Standard Time in (a) color and (b) gray-scale**

## Appendix C Weather Data for EnergyPlus Modeling

Table C-1 lists summary statistics for the weather data and compares them to the nearest typical meteorological year (TMY2) weather file for Baltimore, Maryland. The figures in this appendix depict the 15-minute data contained in the weather file created for use with EnergyPlus, called CBF.epw. These data were obtained from measurements from November 7, 2001 to November 6, 2002. Data were rearranged to start on January 1 and end on December 31. Appendix A describes the time map figure art.

**Table C-1 Weather Summary Statistic: Measurement versus Baltimore TMY2**

| | | Units | Mean | Minimum | Maximum | Standard Deviation |
|---|---|---|---|---|---|---|
| Outdoor Air Dry-Bulb Temperature | Measurement | °F *(°C)* | 59.7 *(15.3)* | 20.2 *(-6.7)* | 98.2 *(36.6)* | 15.9 *(8.8)* |
| | Baltimore TMY2 | °F *(°C)* | 54.9 *(12.6)* | 2.1 *(-16.7)* | 96.3 *(35.6)* | 18.6 *(10.3)* |
| Outdoor Dew-Point Temperature | Measurement | °F *(°C)* | 48.9 *(9.3)* | 2.4 *(-16.6)* | 79.0 *(26.0)* | 17.3 *(9.6)* |
| | Baltimore TMY2 | °F *(°C)* | 43.1 *(6.1)* | -11.7 *(-24.4)* | 80.3 *(26.7)* | 19.2 *(10.7)* |
| Outdoor Relative Humidity | Measurement | % | 68.7 | 14.0 | 100.0 | 18.6 |
| | Baltimore TMY2 | % | 67.1 | 18.0 | 100.0 | 19.3 |
| Wind Speed | Measurement | mph *(m/s)* | 6.2 *(2.8)* | 0.0 *(0.0)* | 26.5 *(11.8)* | 3.7 *(1.7)* |
| | Baltimore TMY2 | mph *(m/s)* | 9.2 *(4.1)* | 0.0 *(0.0)* | 40.3 *(18.0)* | 4.8 *(2.2)* |
| Wind Direction | Measurement | degree | 203 | 1 | 352 | 80 |
| | Baltimore TMY2 | degree | 207 | 0 | 360 | 96 |
| Diffuse Solar | Measurement | $Btu/h \cdot ft^2$ *($W/m^2$)* | 23.2 *(73.3)* | 0.0 *(0.0)* | 213.6 *(673.9)* | 32.8 *(103.4)* |
| | Baltimore TMY2 | $Btu/h \cdot ft^2$ *($W/m^2$)* | 23.2 *(73.3)* | 0.0 *(0.0)* | 152.1 *(480.0)* | 31.5 *(99.5)* |
| Direct Solar | Measurement | $Btu/h \cdot ft^2$ *($W/m^2$)* | 57.6 *(181.8)* | 0.0 *(0.0)* | 321.1 *(1013.0)* | 92.8 *(292.8)* |
| | Baltimore TMY2 | $Btu/h \cdot ft^2$ *($W/m^2$)* | 51.4 *(162.2)* | 0.0 *(0.0)* | 310.0 *(978.0)* | 84.7 *(267.2)* |

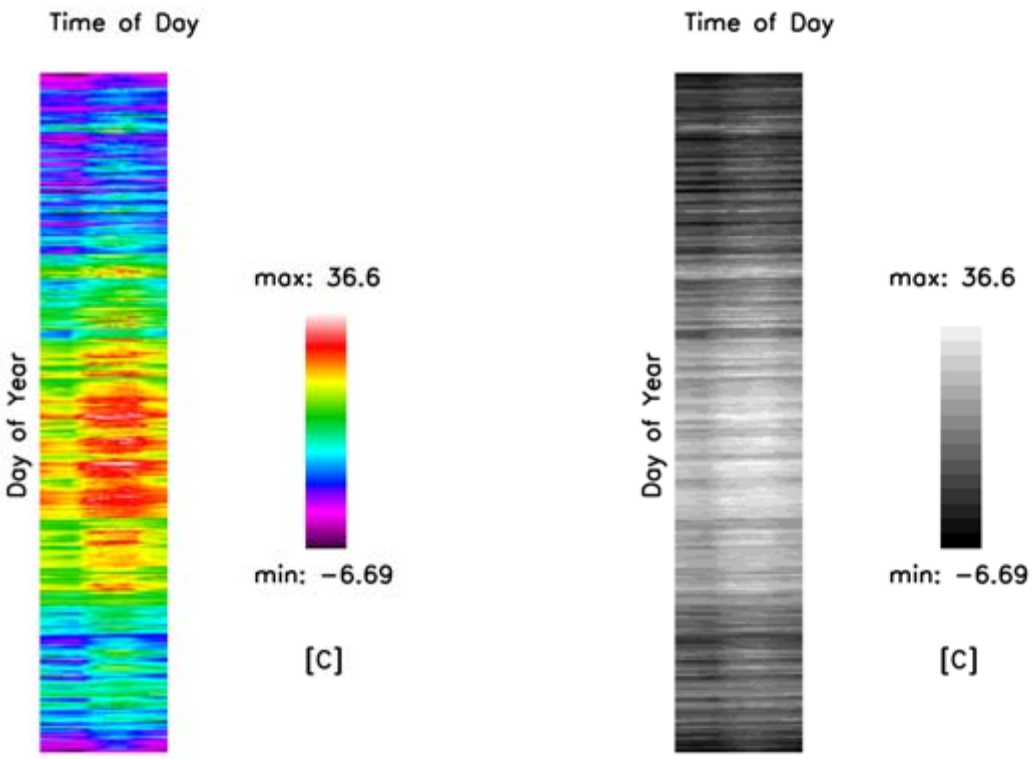


**(a)** **(b)**

**Figure C-1** **Time map of outdoor air dry-bulb temperature (°C) in (a) color and (b) gray-scale**

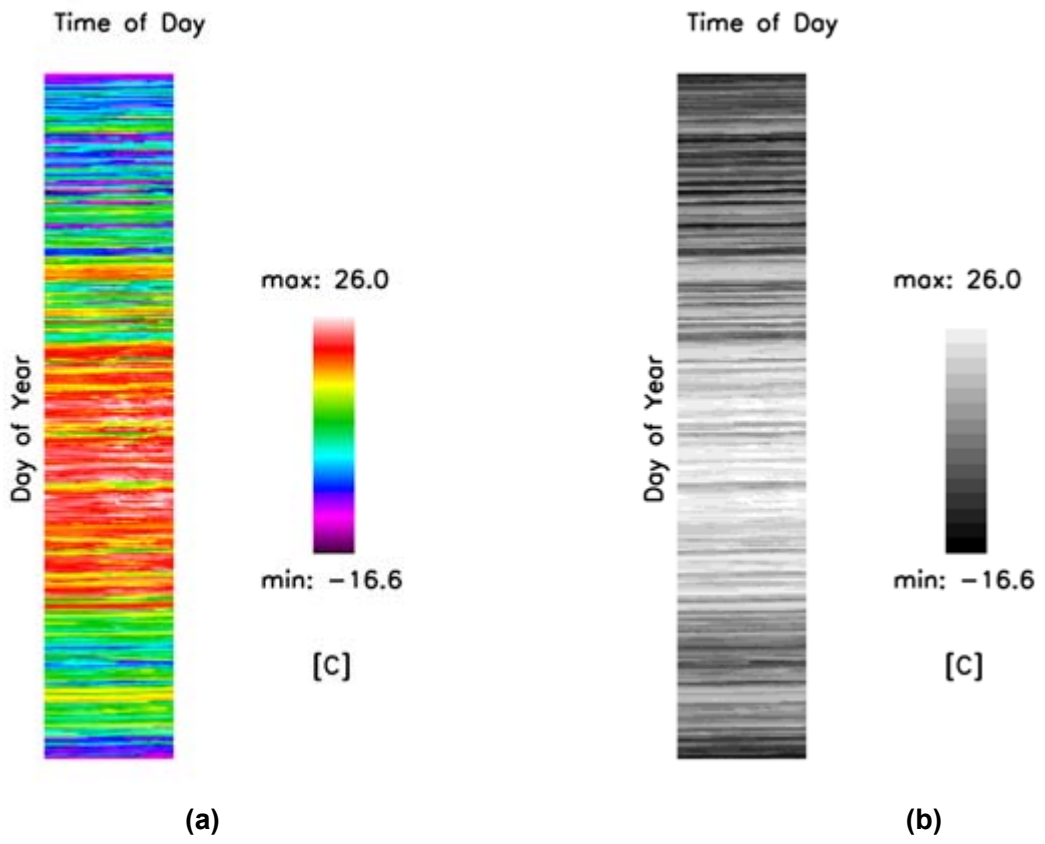


**Figure C-2** **Time map of outdoor air dew-point temperature (°C) in (a) color and (b) gray-scale**

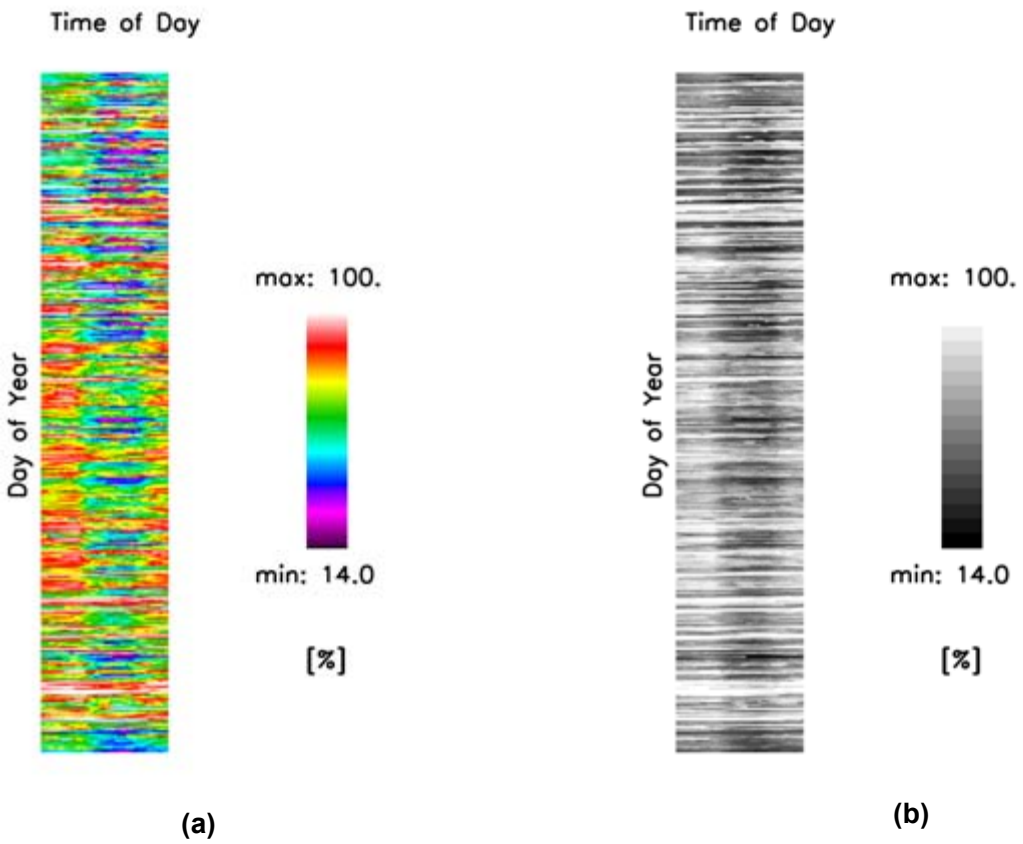


**Figure C-3** **Time map of outdoor air relative humidity (%) in (a) color and (b) gray-scale**

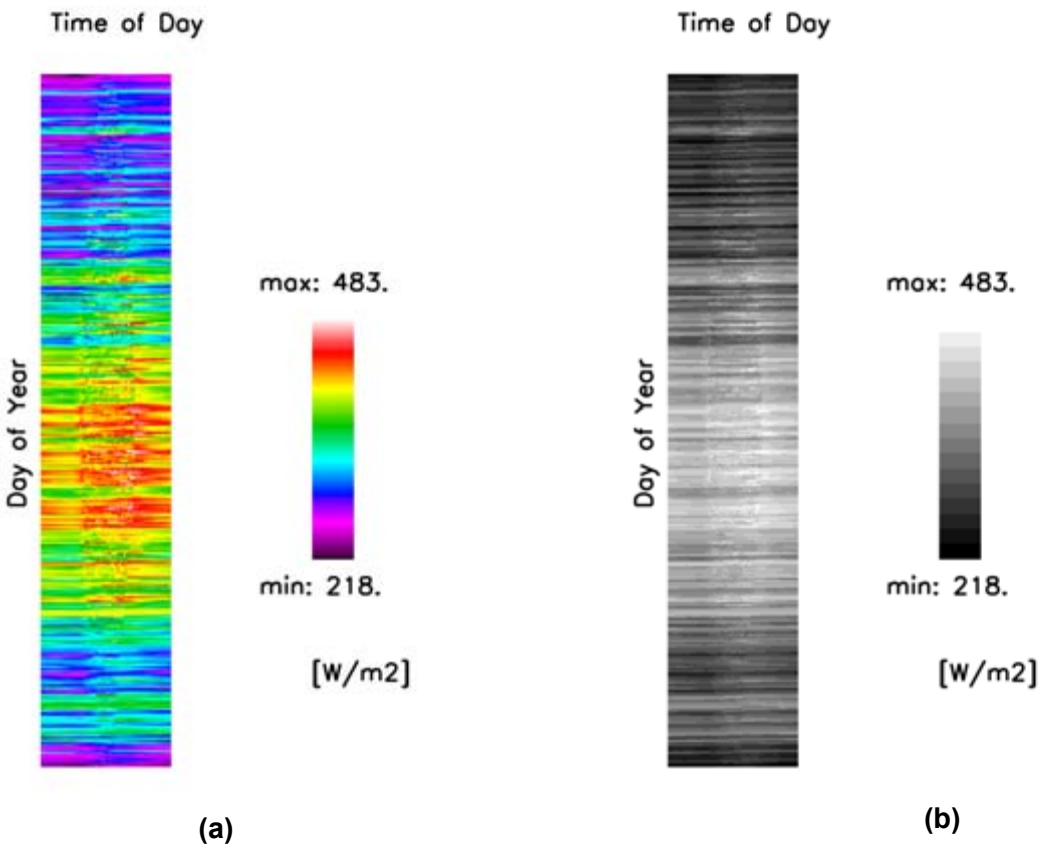


**Figure C-4** **Time map of horizontal infrared radiation (W/m$^2$) in (a) color and (b) gray-scale**

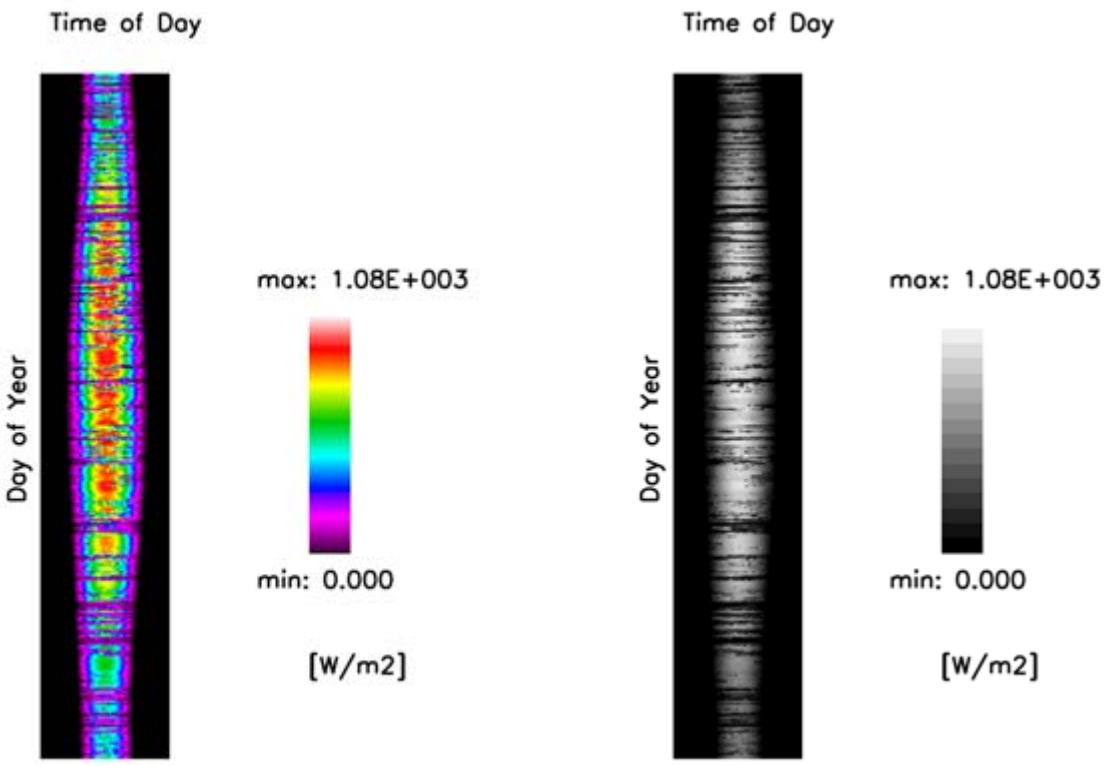


(a) (b)

**Figure C-5** **Time map of global horizontal solar radiation ($W/m^2$) in (a) color and (b) gray-scale**

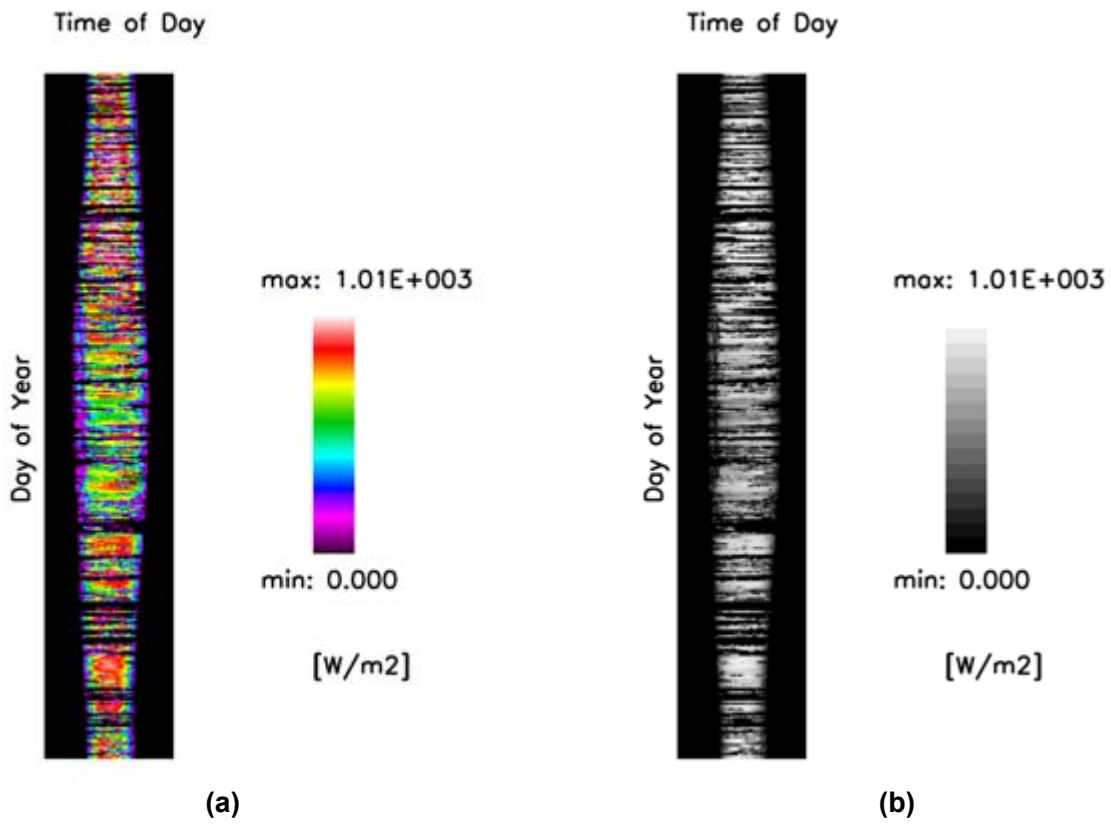


**Figure C-6** **Time map of direct normal solar radiation ($W/m^2$) in (a) color and (b) gray-scale**

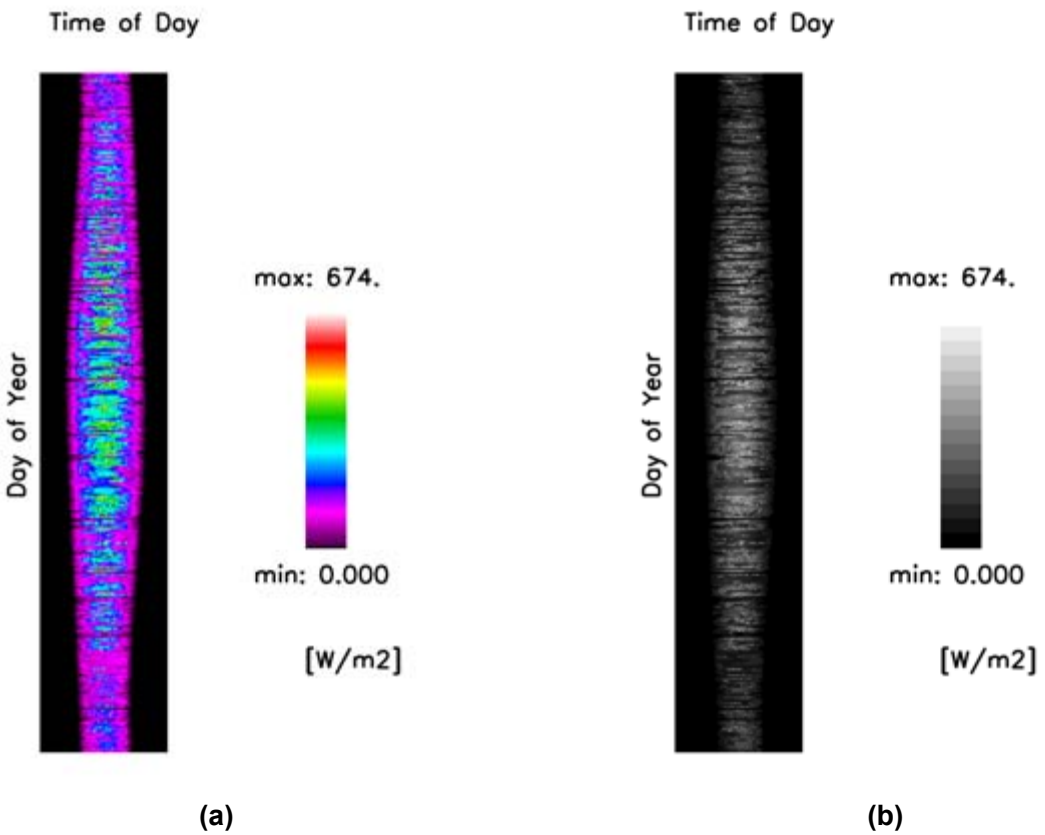


**Figure C-7 Time map of diffuse horizontal solar radiation (W/m$^2$) in (a) color and (b) gray-scale**

The maximum direct normal solar radiation and the maximum diffuse horizontal solar radiation shown in Figure C-6 and Figure C-7, respectively, appear high relative to the design data in the *ASHRAE Applications Handbook* (ASHRAE 2003b), Chapter 33, Figure 4. These values, however, are more acceptable when compared to weather data in the TMY2 format from other locations in the region. Table C-2 shows that the maximum direct normal solar radiation as measured at the Merrill Center is similar to other locations. The table also shows that the ASHRAE design value for maximum diffuse horizontal solar radiation is much lower than the weather data for this region.

**Table C-2 Comparison of Maximum Solar Radiation Values**

| Source or Location | Maximum Direct Normal Solar Radiation Btu/h·ft$^2$ (*W/m$^2$*) | Maximum Diffuse Horizontal Solar Radiation Btu/h·ft$^2$ (*W/m$^2$*) |
|---|---|---|
| *ASHRAE Applications* (ASHRAE 2003b) | 300 *(945)* | 40 *(126)* |
| Merrill Center (EnergyPlus weather file) | 322 *(1,013)* | 214 *(674)* |
| Baltimore International Airport, Maryland (TMY2) | 311 *(978)* | 152 *(480)* |
| Patuxent River Naval Air Test Center, Maryland (TMY2) | 264 *(833)* | 128 *(403)* |
| Washington-Dulles, Virginia (TMY2) | 312 *(983)* | 178 *(562)* |
| Wilmington, Delaware (TMY2) | 314 *(988)* | 163 *(513)* |
| Providence, Rhode Island (TMY2) | 308 *(971)* | 163 *(514)* |

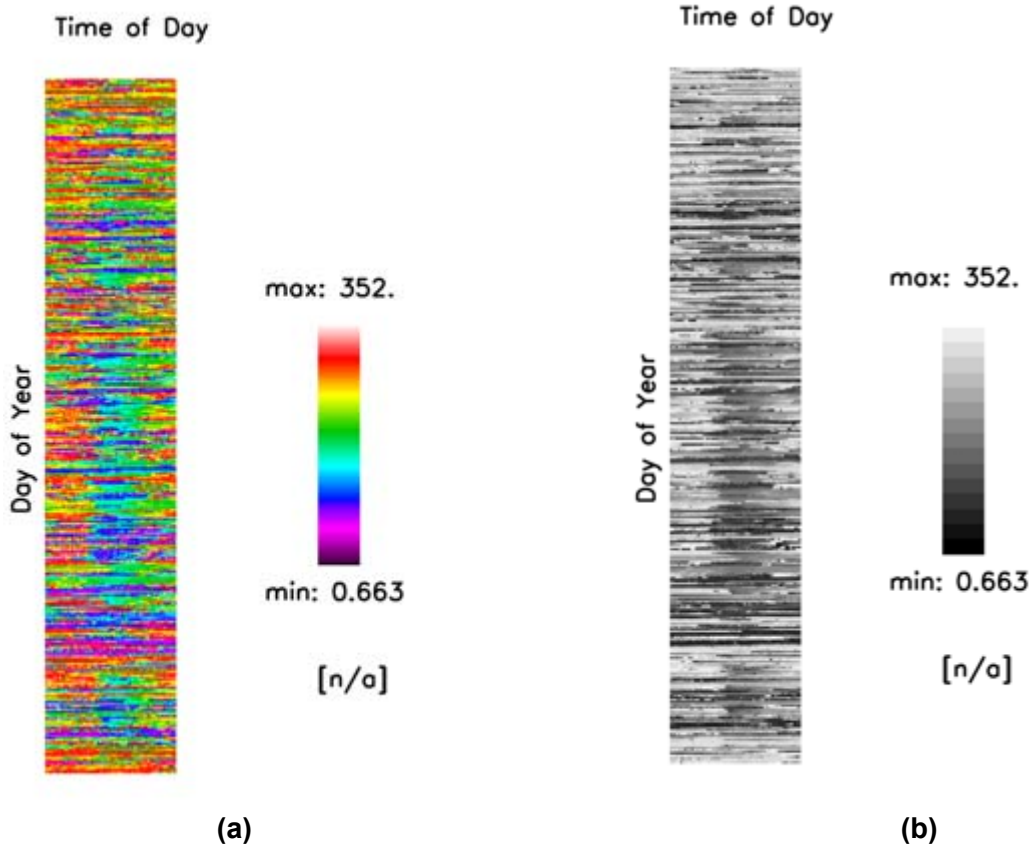


**Figure C-8 Time map of wind direction (clockwise degrees from North) in (a) color and (b) gray-scale**

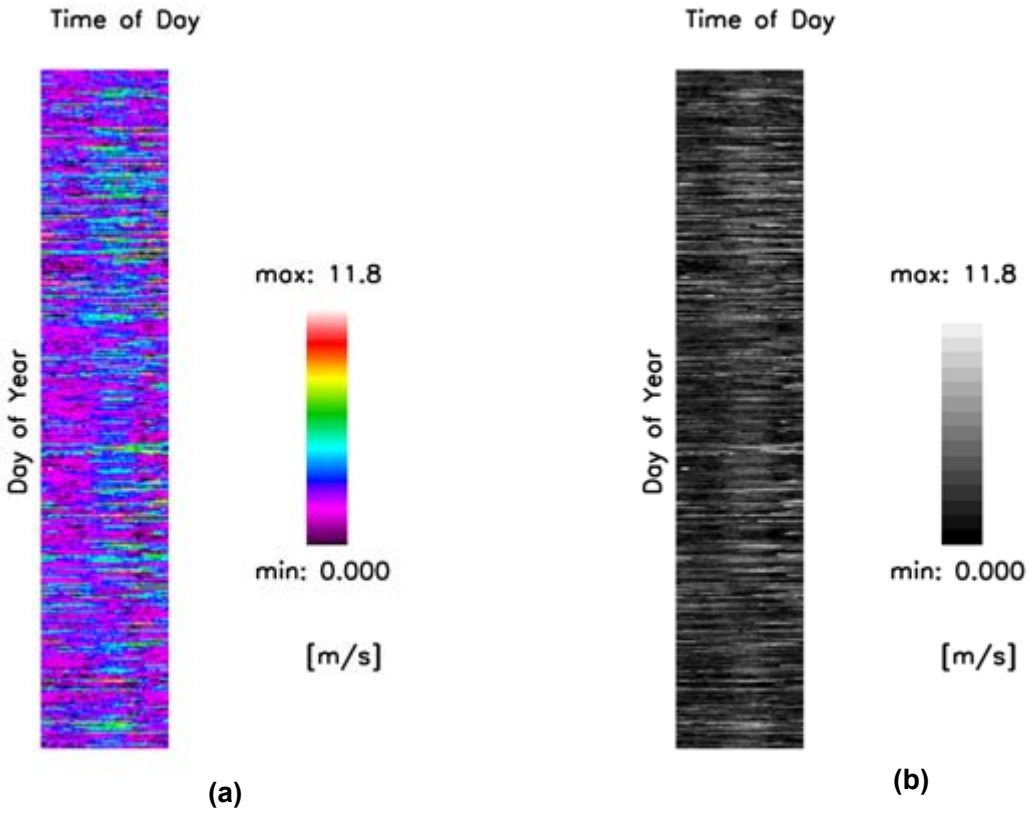


**Figure C-9 Time map of wind speed (m/s) in (a) color and (b) gray-scale**

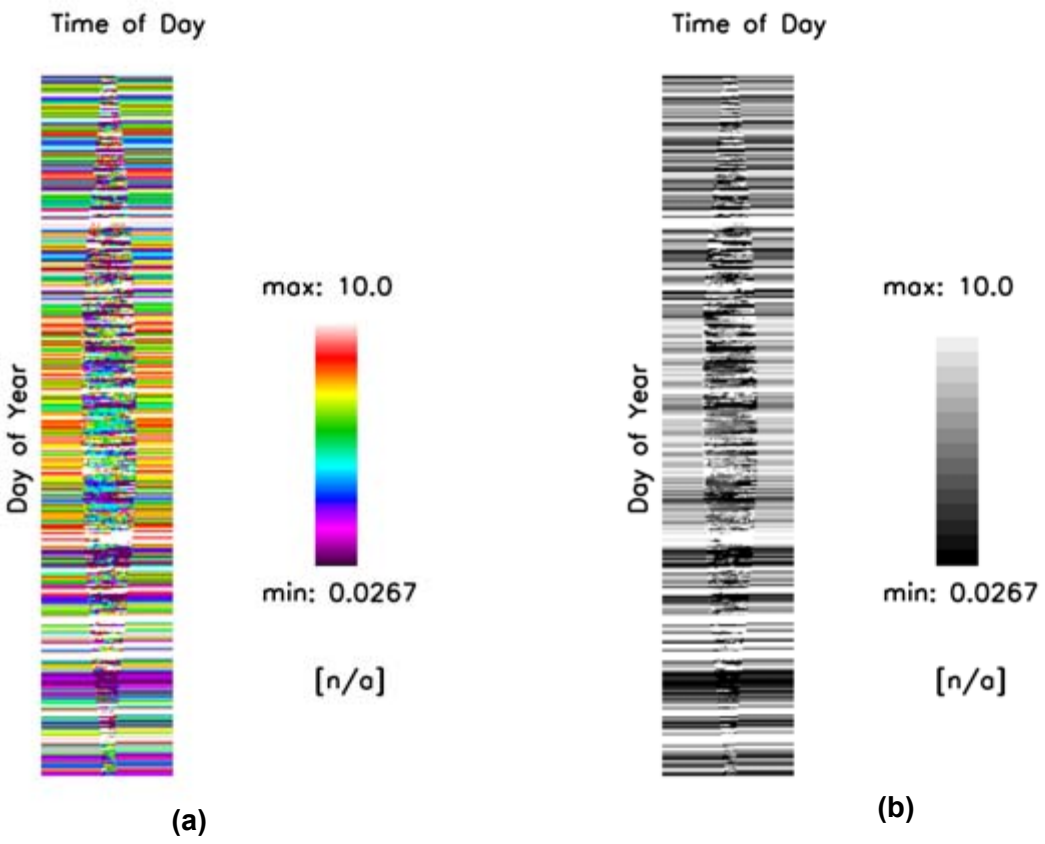


**Figure C-10** **Time map of total and opaque sky cover (tenths of coverage) in (a) color and (b) gray-scale**

## Appendix D Calibration Schedules for EnergyPlus Modeling

This appendix provides time map figures that show the calibration schedules created for use with EnergyPlus. These were derived from 15-minute measurements and totaled to create hourly schedules for the entire modeling/analysis year. Data were rearranged to start on January 1 and end on December 31. Appendix A describes the time map figure art.

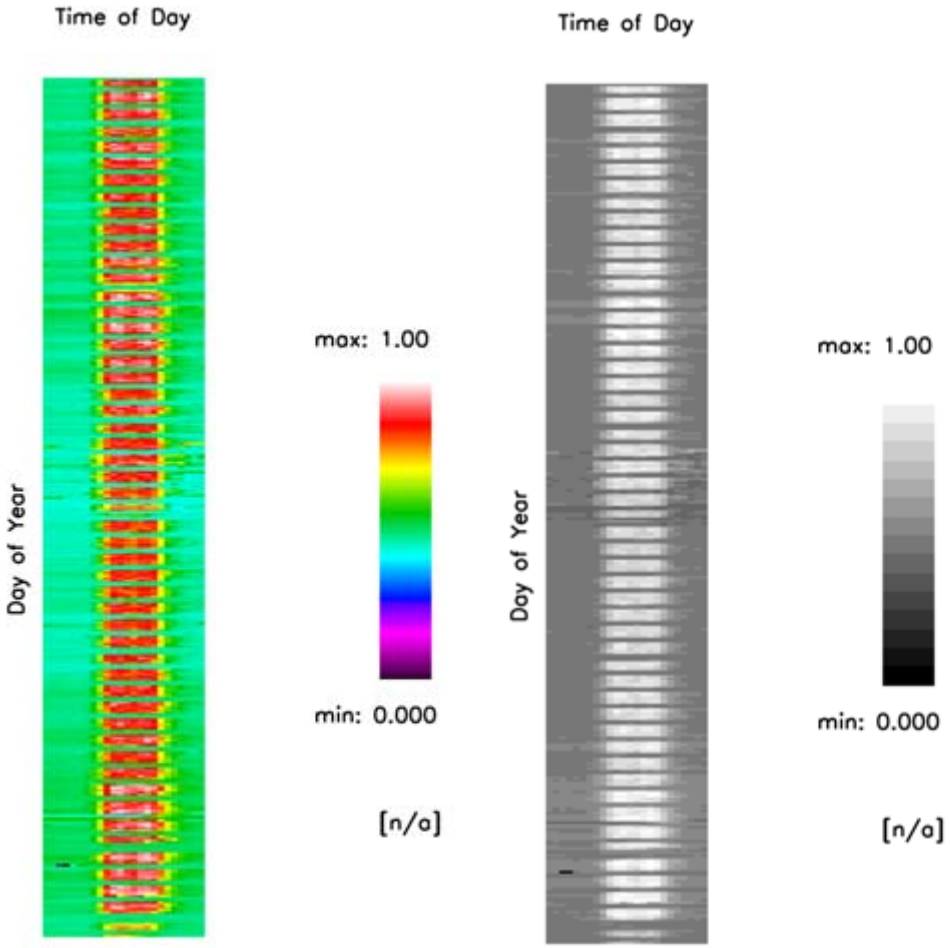


(a) (b)

**Figure D-1 Time map of calibration schedule for first-floor receptacles loads, normalized factors in (a) color and (b) gray-scale**

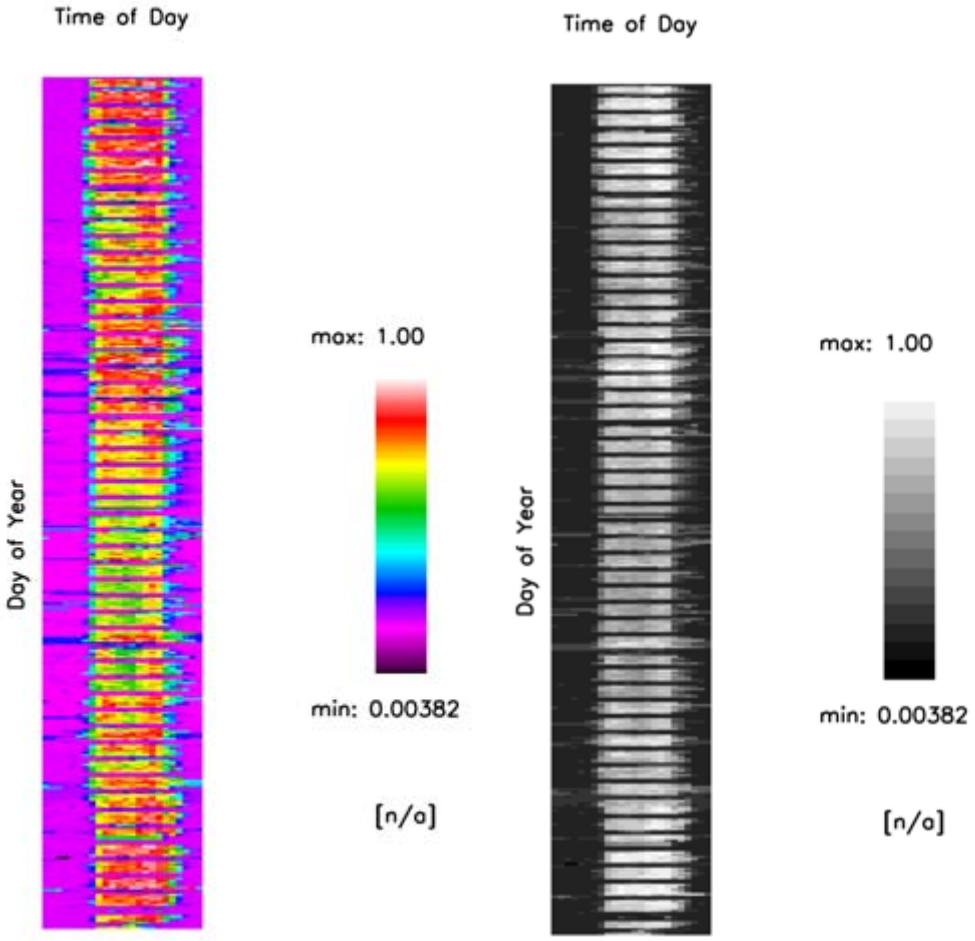


(a) (b)

**Figure D-2** **Time map of calibration schedule for first-floor lighting loads, normalized factors in (a) color and (b) gray-scale**

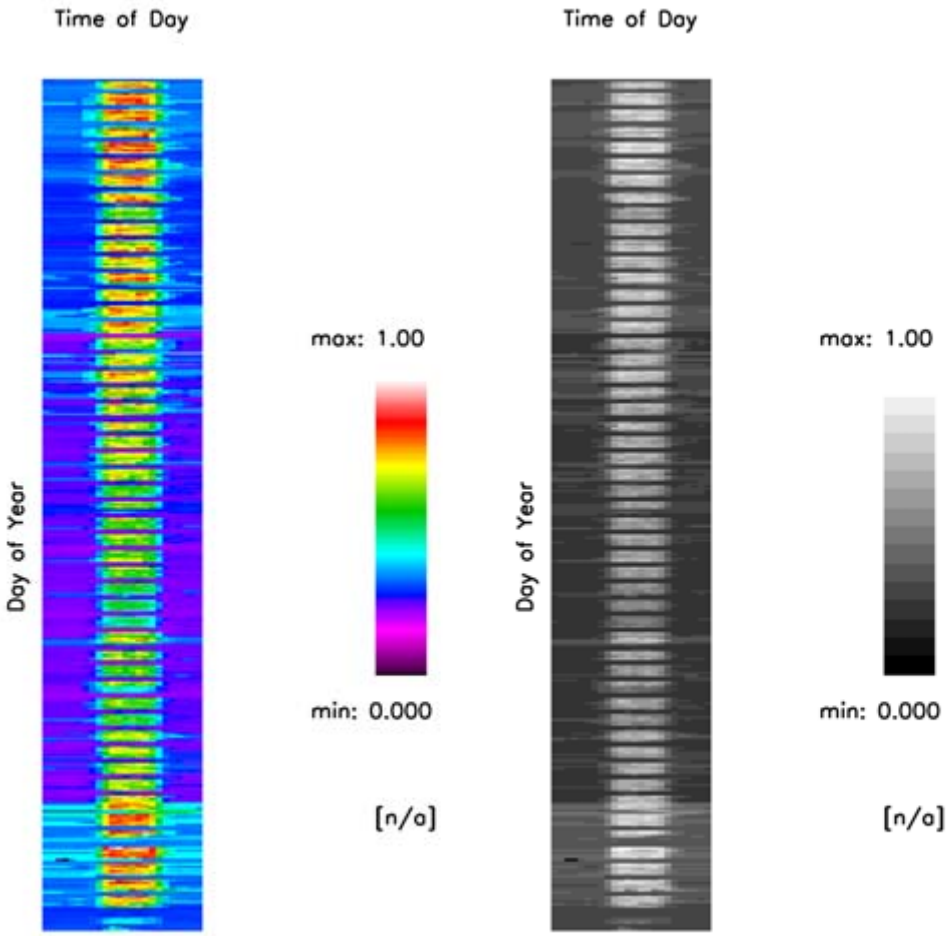


(a) (b)

**Figure D-3 Time map of calibration schedule for second-floor receptacle loads, normalized factors in (a) color and (b) gray-scale**

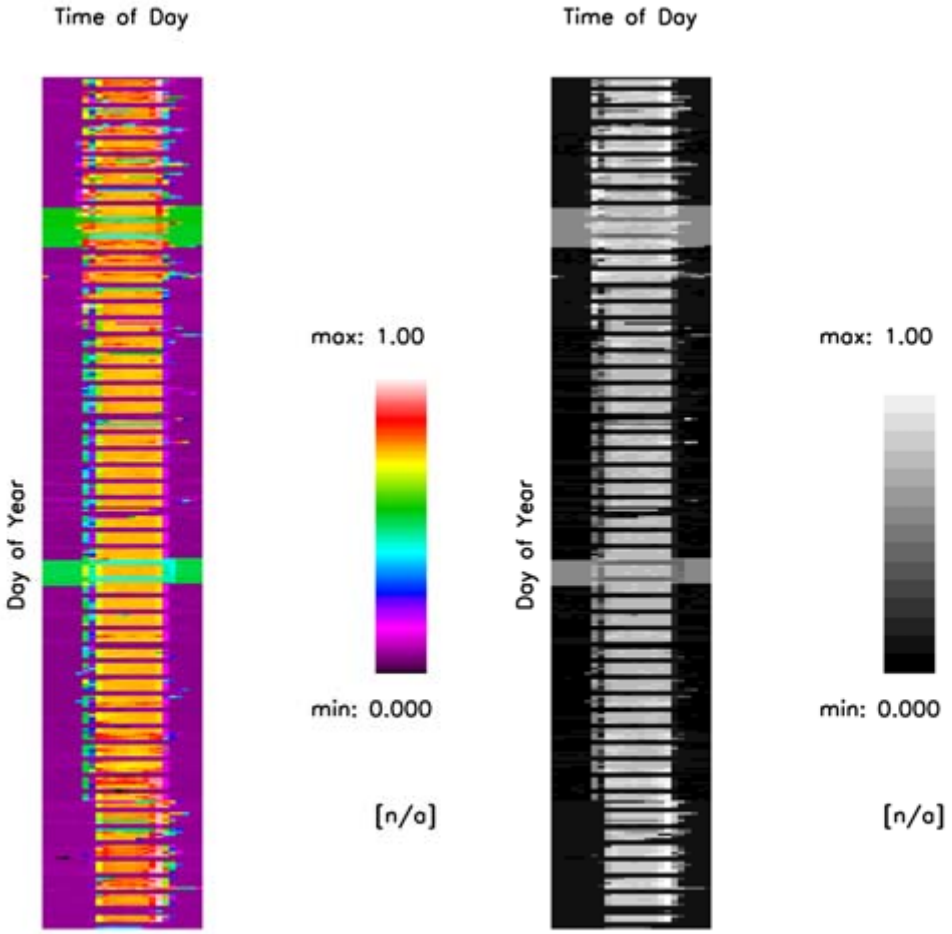


(a) (b)

**Figure D-4 Time map of calibration schedule for second-floor lighting loads, normalized factors in (a) color and (b) gray-scale**

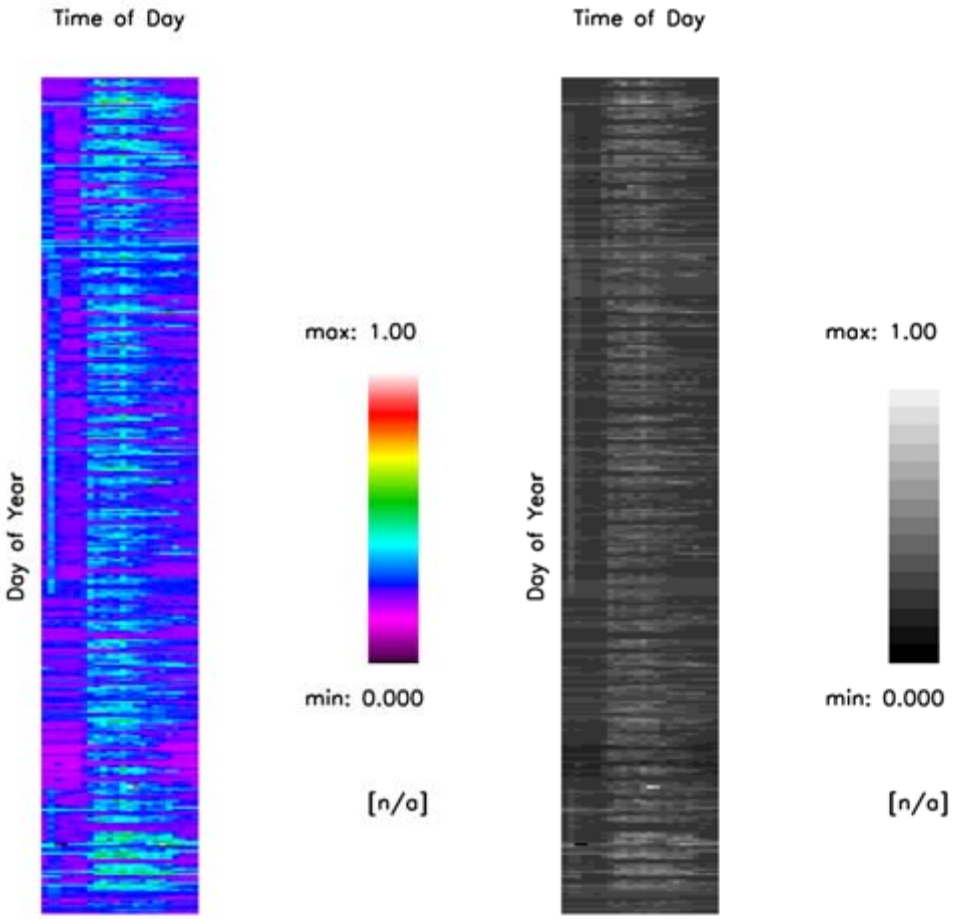


(a) (b)

**Figure D-5** **Time map of calibration schedule for conference pavilion receptacle and lighting loads, normalized factors in (a) color and (b) gray-scale**

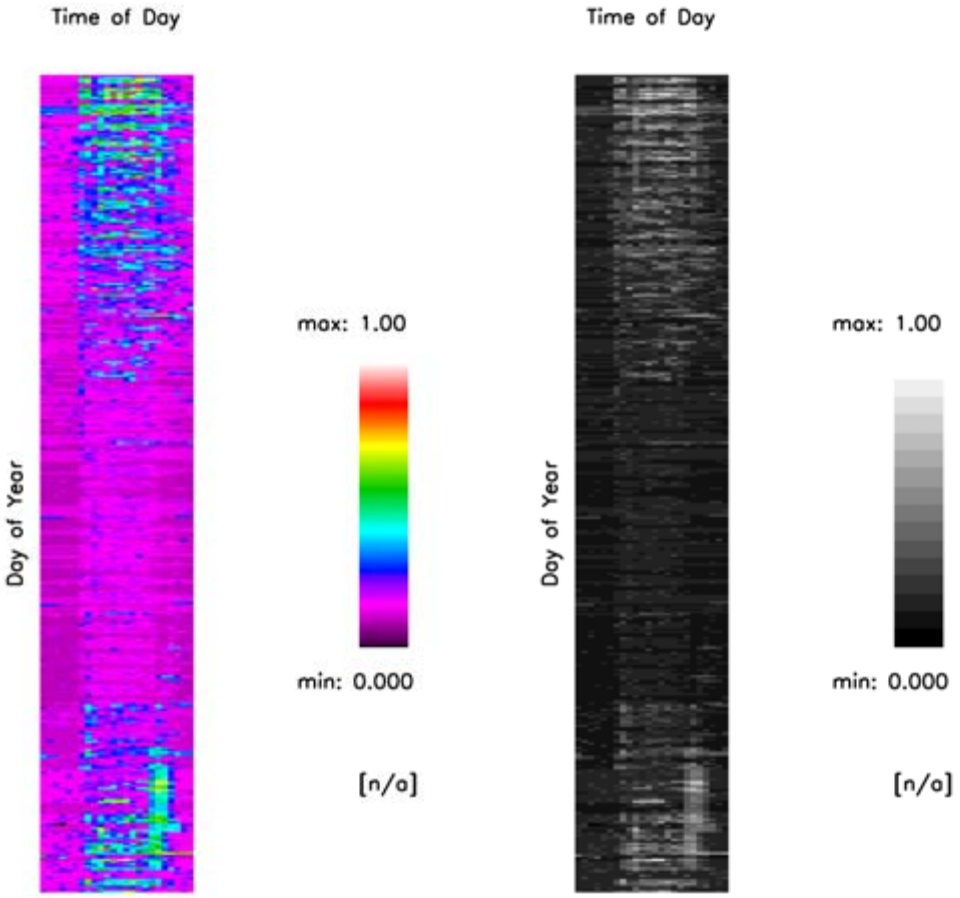


(a) (b)

**Figure D-6** **Time map of calibration schedule for miscellaneous loads (elevator, exterior lighting, mechanical room receptacles), normalized factors in (a) color and (b) gray-scale**

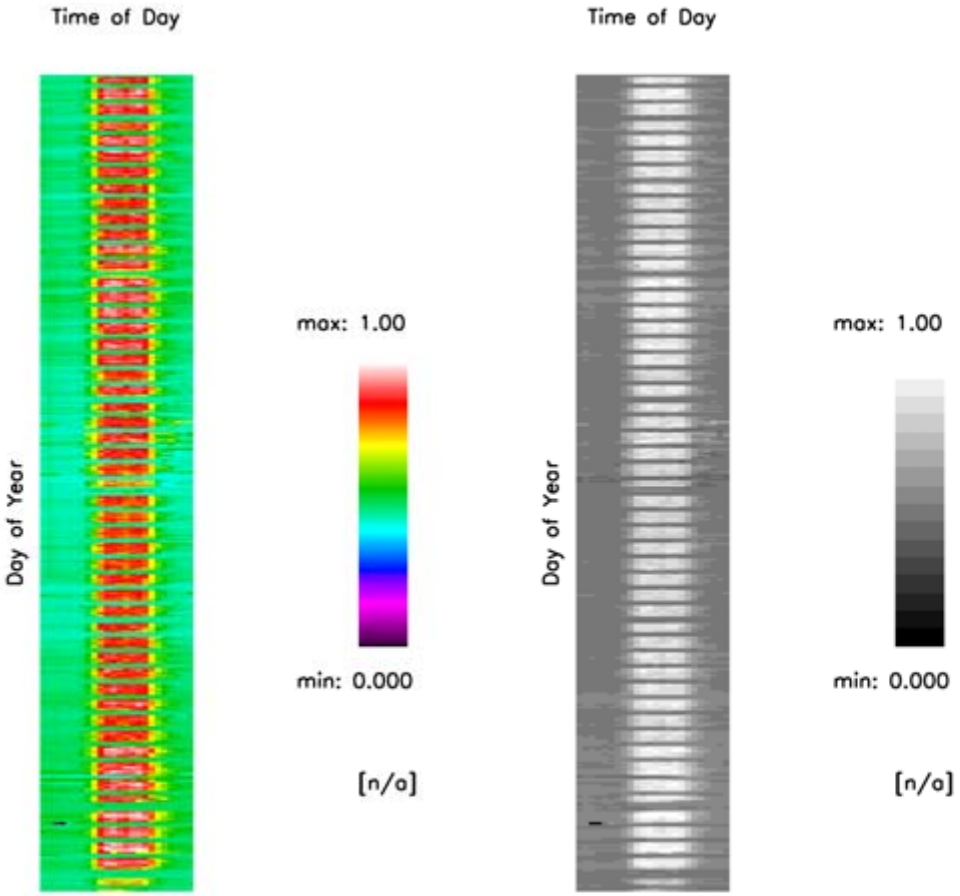


(a) (b)

**Figure D-7** **Time map of calibration schedule for blended (first floor plus 18.4% of conference pavilion) first receptacle loads, normalized factors in (a) color and (b) gray-scale**

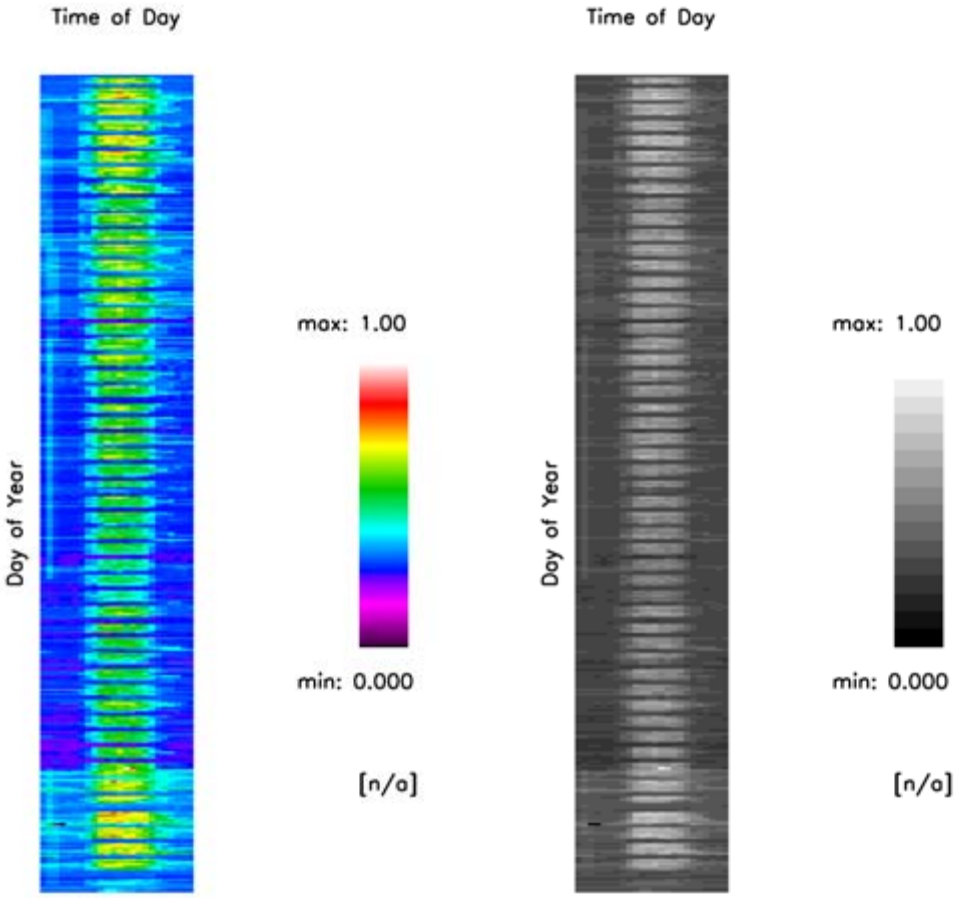


(a) (b)

**Figure D-8 Time map of calibration schedule for blended (second floor plus 81.6% of conference pavilion) second-floor receptacle loads, normalized factors in (a) color and (b) gray-scale**

The measured data can also be reduced to a form more useful for energy modeling. Table D-3 shows the magnitude of peak plug loads normalized by area for the first and second floors of the main building. The detailed schedules presented in Figure D-1 and Figure D-3 were combined to assemble average plug load profiles presented in Figure D-9. These were averaged.

**Table D-3 Peak plug loads from measurements**

| CBF Location | W/ft$^2$ | W/m$^2$ |
|---|---|---|
| first floor, main building | 1.4 | 14.9 |
| second floor, main building | 1.1 | 11.8 |

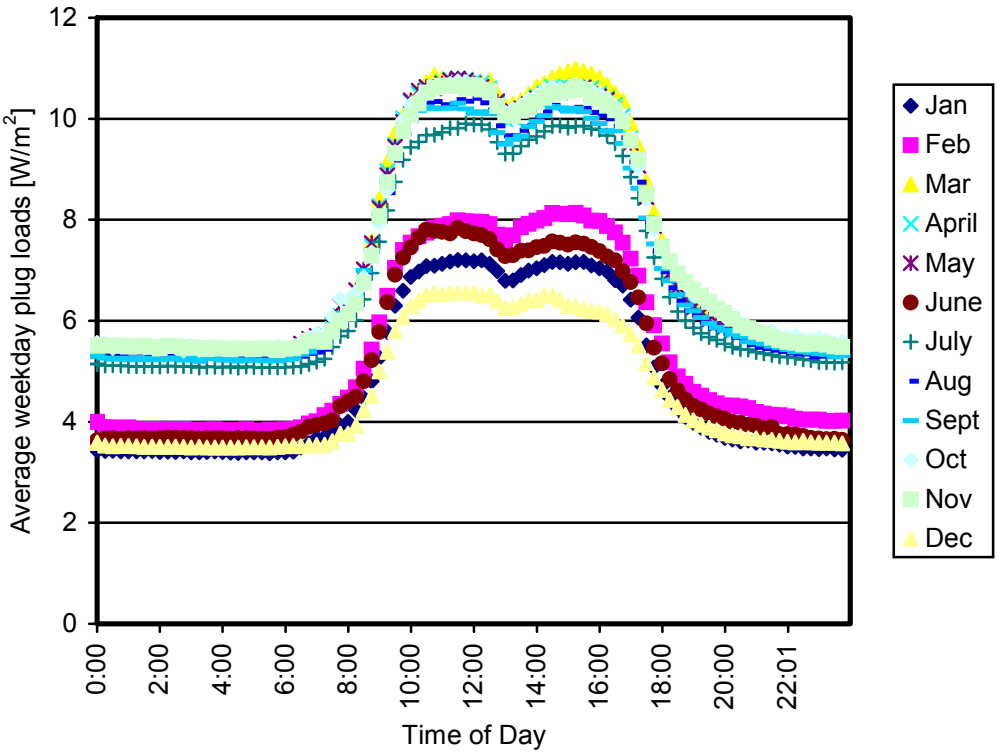


**Figure D-9** **Working weekday average plug load profiles by month for the first and second floors of the main building.**

## Appendix E Cloud Cover Modeling

Cloud cover is used to compute sky temperatures or horizontal infrared radiation intensity. EnergyPlus uses horizontal infrared radiation intensity to compute outside surface temperatures of surfaces exposed to the outside. Values for cloud cover are in tenths: 0 is clear and 10 is cloudy. Cloud cover was not observed directly and so was inferred from solar radiation measurements. A literature search did not produce a body of research on methods for directly modeling cloud cover from global horizontal solar measurements. (However, the reverse problem of generating radiation data from cloud cover data has been addressed (Maxwell et al. 1995, Perez et al. 2002).) The computer program TRNSYS (Klein et al. 1976) allows custom modules, and Auer has written a module called Type69 that models cloud cover and sky temperature. Unfortunately, a literature reference for Auer's method has not yet been determined. Using Auer's code for TRNSYS Type69, routines were developed for estimating horizontal infrared radiation intensity with the following five steps.

1. Combine direct horizontal, $B_h$, and diffuse horizontal, $D_h$, solar radiation to obtain global horizontal radiation, $G_h$. This value is a measured quantity since $D_h$ is determined by subtracting the Perez model result for $B_h$ from $G_h$.

$$G_h = B_h + D_h \tag{2}$$

2. Calculate cloud cover, $CC$, on a scale from 0 to 1 for $G_h > 0.0$ with:

$$CC = \left( MAX\left[ 0.001, 1.4286\frac{D_h}{G_h} - 0.3 \right] \right)^{0.5} \tag{3}$$

3. Fill low-sun angle and nighttime data based on neighboring acceptable data. The approach used here differs from Auer's because our processing was performed on all the time steps at once, whereas the TRNSYS routine was for use during a simulation where at a given time step only time history is available (and not the results from future time steps). For each time step, where solar zenith angle is greater than 65°, the calculated values for cloud cover are assumed inaccurate. For these times, data were artificially filled using an average of two results before and two results after the results were cut off because they were not reliable. The 65° cutoff angle was selected arbitrarily after separate trials with cutoff angles of 80°, 75°, and 70° failed to produce clear skies at night. For the beginning of the year, when averaging before and after was not possible, we used the data for the following morning; for the end of year, we used only the data from the preceding evening.
4. Multiply by a factor of 10.0 to convert to new scale with cloud cover in tenths.
5. Use the cloud cover data and the method documented by Walton (1983) and used in EnergyPlus to calculate horizontal infrared radiation intensity:

$$\varepsilon_{sky} = \left[ 0.787 + 0.764 \ln\left( \frac{T_{dewK}}{273.15} \right) \right] \left[ 1 + 0.0224CC - 0.0035\,CC^2 + 0.00028\,CC^3 \right] \tag{4}$$

$$G_{IR,h} = \varepsilon_{sky} \sigma T_{db}^4 \tag{5}$$

# Appendix F Baseline Energy Model Error Analysis

This appendix presents details of the methods used to develop estimates for uncertainty in the model predictions for baseline energy use.

## F.1 Geometry

This section describes the geometry of the baseline building models. Figure F-1 shows the three baseline buildings that were modeled. In all cases, the models have the same number of floors and a floor area of 26,000 $ft^2$ (2,414 $m^2$). The three methods of specifying geometry for baseline models are:

- A square solar neutral footprint, referred to as a *box w aspect ratio 1.0*.
- A rectangular footprint with an aspect ratio similar to the Merrill Center referred to as a *box w aspect ratio 4.4*.
- The actual geometry of the Merrill Center referred to as *same as built*.

The aspect ratio 1.0 box represents a solar neutral building. The aspect ratio 4.4 box represents a building footprint similar to the Merrill Center if its conference pavilion were attached to one end of the main building. In addition, error analysis efforts modeled perturbations in aspect ratio because there is no consensus for how to combine the pavilion and main building. For baseline modeling, the building is modeled four times with orientation rotated through the four cardinal directions and results averaged.

The box geometries use a default rectangular geometry. Aspect ratio is used here to indicate the east-west length of the building divided by the north-south length. This building geometry is a simple square or rectangular footprint with equal floor area on each floor and windows extending as a continuous band on each façade with a uniform height. Box buildings bear little resemblance to the Merrill Center, but they are meant to represent a typical low-cost market commercial office building. The box buildings are developed based on the following assumptions:

- Rectangular floor plan
- Uniform floor-to-floor heights
- Uniform plenum heights
- Ten zones per floor, including four perimeter zones, one core zone, and five return plenums (in a drop ceiling), no windows in plenum, and equal distribution of windows (based on glazing fraction or window-to-wall ratio) on all facades and floors.

Computer routines were developed to automatically generate model inputs for EnergyPlus based on the following parameters:

- Total building area
- Number of floors
- Aspect ratio
- Floor-to-floor height
- Return plenum height
- Depth of perimeter zones

- Glazing sill height
- Glazing area fraction
- Glazing edge offset.

The same-as-built geometry matches the first and second floors of the Merrill Center. Figure F-1 shows the thermal zones and floor plan for the same as-built baseline model. The envelope materials match the minimum requirements of ASHRAE 90.1-2001 outlined in Table 5-11. Shading surfaces are also not present.

The current study modeled all three geometries with the intent of understanding the differences in results and the contribution of geometry to their uncertainty. Which method of determining baseline geometry is the most appropriate for rating purposes? The answer to this question is still being debated. Proponents of modeling the same geometry as the proposed (or in this case as-built) building argue that such an approach is better because:

- Site requirements dictate footprint.
- Problems would otherwise arise with differing ratios of exposed envelope area and interior volume.
- Having just one geometrical representation reduces the effort required to do the modeling.

Proponents of modeling box-type geometries argue that baseline performance should be independent from an actual design. This approach provides credits when orientation and aspect ratio are used to improve building performance and conversely, penalizes building designs that make poor judgments related to orientation.

( a )

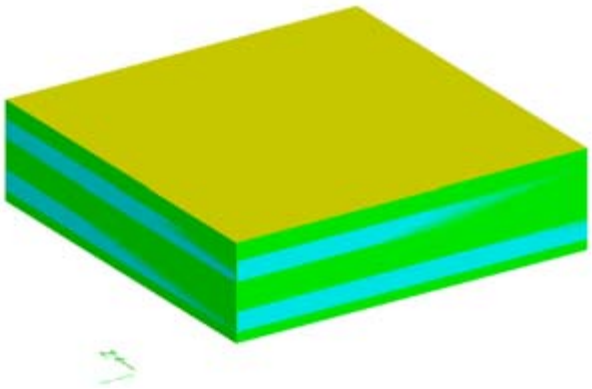

( b )

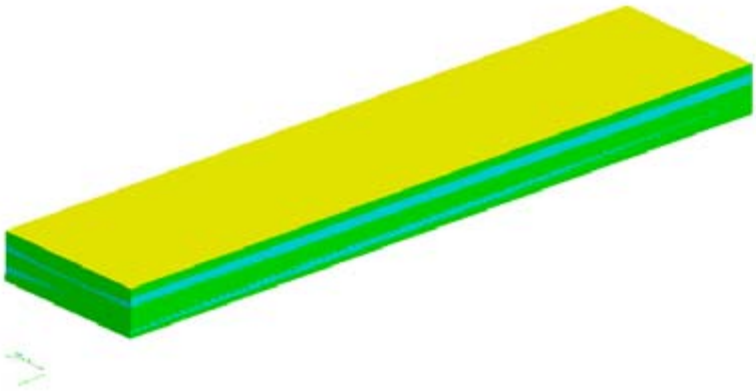

( c )

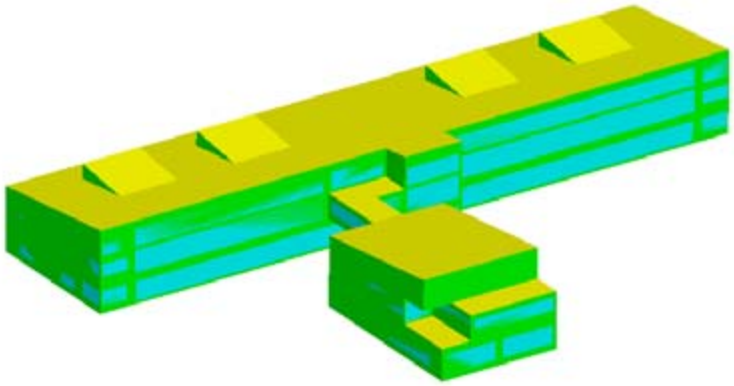

**Figure F-1** **Baseline building model geometries, (a) box with aspect ratio 1.0, (b) box with aspect ratio 4.4, and (c) same as built**

This section lists results for annual energy performance for the three baseline geometries. Various performance indices and end uses are included to meet the interests of different readers. Section 5.3.3 provides a more concise presentation of the results.

Table F-1 lists the results for site energy use for three baseline geometries, Table F-2 lists the results for source energy, and Table F-3 lists energy costs. The methods are all considered valid. Therefore, the mean was calculated by giving equal weight to each result. Linear deviations were recorded and were considered sources of error in the analysis. The results indicate that choosing between a square footprint (aspect ratio of 1), a rectangular footprint (with aspect ratio similar to the Merrill Center of 4.4), and the actual geometry of the Merrill Center has about a 3% effect on results. The large variation in fan energy results from the as-built geometry, which leads to higher solar loads, and therefore, higher design airflow rates in sizing calculations for the constant volume fans.

**Table F-1 Baseline Energy Model Results for Site Energy Use**

| **Geometry** | **Lights** MWh/yr | **Plugs** MWh/yr | **Misc.** MWh/yr | **Fans** MWh/yr | **Cooling** MWh/yr | **Heating** MWh/yr | **Total Site** MWh/yr | **Intensity** kBtu/ft$^2$·yr *(kWh/m$^2$·yr)* |
|---|---|---|---|---|---|---|---|---|
| Aspect Ratio 1.0 | 131.1 | 154.1 | 30.6 | 40.7 | 59.7 | 50.3 | 466.5 | 51.3 *(162.0)* |
| Aspect Ratio 4.4 | 131.1 | 154.1 | 30.6 | 47.7 | 68.0 | 56.8 | 488.3 | 53.7 *(169.6)* |
| Same as As-Built | 122.6 | 153.9 | 30.7 | 67.9 | 73.1 | 48.3 | 496.6 | 54.7 *(172.4)* |
| Mean | 128.3 | 154.0 | 30.6 | 52.1 | 66.9 | 51.8 | 483.8 | 53.2 *(168.0)* |
| ± Geom. err. est. | 3.3% | 0.1% | 0.2% | 26.1% | 10.0% | 8.2% | 3.1% | 3.1% |

**Table F-2 Baseline Energy Model Results for Source Energy Use**

| **Geometry** | **Lights** MWh/yr | **Plugs** MWh/yr | **Misc.** MWh/yr | **Fans** MWh/yr | **Cooling** MWh/yr | **Heating** MWh/yr | **Total Source** MWh/yr | **Intensity** kBtu/ft$^2$·yr *(MJ/m$^2$·yr)* |
|---|---|---|---|---|---|---|---|---|
| Aspect Ratio 1.0 | 422.8 | 497.2 | 98.9 | 131 | 193 | 54.2 | 1,397 | 154 *(1,746)* |
| Aspect Ratio 4.4 | 422.8 | 497.2 | 98.9 | 154 | 219 | 61.1 | 1,453 | 160 *(1,816)* |
| Same as As-Built | 395.6 | 496.4 | 99.2 | 219 | 236 | 51.9 | 1,498 | 165 *(1,873)* |
| Mean | 413.6 | 496.9 | 98.9 | 168 | 216 | 55.8 | 1,449 | 159 *(1,811)* |
| ± Geom. err. est. | 3.3% | 0.1% | 0.1% | 26.1% | 10.0% | 8.2% | 3.5% | 3.5% |

**Table F-3 Baseline Energy Model Results for Energy Costs**

| Geometry | Lights $/yr | Plugs $/yr | Misc. $/yr | Fans $/yr | Cooling $/yr | Heating $/yr | Demand Charges $/yr | Total Site $/yr | Intensity $/ft$^2$·yr *($/m$^2$·yr)* |
|---|---|---|---|---|---|---|---|---|---|
| Aspect Ratio 1.0 | 5,946 | 6,635 | 1,296 | 1,839 | 3,034 | 2,258 | 13,600 | 34,608 | 1.12 *(12.0)* |
| Aspect Ratio 4.4 | 5,946 | 6,635 | 1,296 | 2,153 | 3,451 | 2,551 | 14,405 | 36,437 | 1.18 *(12.7)* |
| Same as As-Built | 5,555 | 6,628 | 1,301 | 3,127 | 3,877 | 2,172 | 17,355 | 40,014 | 1.29 *(13.9)* |
| Mean | 5,816 | 6,633 | 1,298 | 2,373 | 3,454 | 2,327 | 15,120 | 37,019 | 1.20 *(12.87)* |
| ± Geom. err. est. | 3.4% | 0.1% | 0.2% | 27.1% | 12.2% | 8.1% | 12.4% | 7.3% | 7.4% |

## F.2 Input Perturbation Methods for Error Analysis

This section provides a summary of efforts to estimate the accuracy of computer modeling results based on sensitivity analysis of uncertainty in input. This report uses two complementary methods of modeling uncertainty that were first presented by Lomas and Eppel (1992):

- Differential sensitivity analysis (DSA), which provides information on the contribution of individual sources of error
- Monte Carlo analysis (MCA), which provides a better method of capturing nonsuperimposable interactions between individual sources of input error.

These sensitivity analyses are used to model uncertainty and are not rigorous treatments of error propagation. Both methods have the advantage that the core simulation program (EnergyPlus in this case) is treated as a black-box function. As a result, the error analysis is separable from the program, the program does not need to be modified, and it is assumed valid. Systematic errors may not be captured, but these methods do address problems that stem from bad input. Although both methods require considerable computing, DSA and MCA are more practical to implement than propagating error throughout the numerous computations in EnergyPlus and the post-processing routines. MacDonald (2002) used affine polynomials to propagate error through the ESP-r program. The baseline model with box geometry and an aspect ratio of 4.4 was selected for most of the analysis in this section.

The first step in both DSA and MCA analyses is to identify the input parameters to be analyzed and their respective uncertainty characteristics. Estimating the uncertainty in energy modeling is not common practice and there are no standardized methods for characterizing input errors. Therefore, we had to make numerous assumptions for which input parameters should be included and which level of uncertainty should be assigned to them. Table F-4 lists the input parameters and their uncertainties used in this study. We selected parameters that are not clearly specified in ASHRAE 90.1-2001 or 90.1 Appendix G, with the exception of lighting levels, which are specified, but were varied anyway. The selection of input parameters was limited because each had to be implemented in preprocessor routines used to automatically prepare input files. Floor area is included as a variable because there is uncertainty in the floor area of the actual building. Aspect ratio is included as a variable because there is uncertainty in how well the selection of 4.4 would represent a building that combined the conference pavilion. Because of limitations on the amount of effort available for programming preprocessors, only a portion of the vast amount of input for an EnergyPlus model has been included in such routines. In this study, the

uncertainty in a particular value is modeled as 2.33 times the standard deviation (*s*), which leads to a 98% probability that the value lies within +2.33s and –2.33s of the mean. For MCA analysis, it is also necessary to characterize the probability distribution function associated with a particular input value. Following the research of MacDonald (2002), the current study implemented uniform, normal, log-normal, and triangle probability distributions for MCA analysis.

**Table F-4 Input Parameters Included in DSA and MCA and Uncertainties**

| Parameter | Units | Mean and/or Mode | Minimum | Maximum | Standard Deviation | Probability Distribution |
|---|---|---|---|---|---|---|
| Floor Area | [$m^2$] | 2,414.4 | 2,293.7 | 2,535.1 | 51.8 | normal |
| Aspect Ratio | [ ] | 4.4 | 3.9 | 4.9 | 0.21 | normal |
| Floor-to-Floor Height | [m] | 4.572 | 4.072 | 5.072 | 0.22 | normal |
| Plenum Height | [m] | 0.914 | 0.614 | 1.214 | 0.13 | normal |
| Perimeter Zone Depth | [m] | 4.572 | 3.572 | 5.572 | 0.43 | normal |
| Glazing Sill Height | [m] | 1.0 | 0.8 | 1.2 | 0.086 | normal |
| Glazing Fraction | [m] | 0.4 | 0.35 | 0.45 | 0.021 | normal |
| Receptacle Intensity | [$W/m^2$] 1st<br>2nd | 14.91<br>15.49 | 14.16<br>14.72 | 15.66<br>16.26 | 0.32<br>0.33 | uniform |
| Lighting Intensity | [$W/m^2$] | 11.0 | 9.0 | 13.0 | 0.86 | triangle |
| Occupant Density | [People/ 100 $m^2$] | 9.0 | 6.0 | 12.0 | 1.28 | uniform |
| Infiltration Rate | [ACH] | 0.4 | 0.0 | 0.8 | 0.17 | normal |

The next step in error analysis was to implement a framework for performing DSA and MCA analysis using EnergyPlus as a black-box function. A computing framework (called EpInteface[7]) was developed to automate the following operations:

- Use either DSA or MCA to create a series of EnergyPlus input files.
- Execute EnergyPlus.
- Analyze EnergyPlus results.
- Record results from individual simulations.
- Compute error estimates.

[7] Similar to HPBAnalyzer, this application was written by Brent Griffith in an interpreted language called IDL by Research Systems Incorporated, Boulder, Colorado.

## F.3 Differential Sensitivity Analysis

For DSA analysis, 23 simulations were run to assess 11 input parameters (one for base case and two each for the input parameters). The input for each DSA model is varied one at a time. Results from DSA are given in Table F-5 for site energy uses, Table F-6 for source energy uses, and Table F-7 for energy costs.

An accepted method of combining a series of *n* independent sources of uncertainty, $\delta x_i$, is to sum them in quadrature as shown in Equation 6 (Taylor 1982; Lomas and Eppel 1992).

$$\delta q = \sqrt{(\delta x_1)^2 + (\delta x_2)^2 + (\delta x_3)^2 + \cdots + (\delta x_n)^2} \quad (6)$$

This method computes individual contributions of error in isolation and then combines them in a straightforward manner using Equation 6. As discussed by Lomas and Eppel (1992), quadrature addition requires one to assume that the modeling behaves as a roughly linear and superposable system.

**Table F-5 DSA of Uncertainty in Baseline Model Predictions: Annual Site Energy Use**

| Parameter | Input Error ± | Lights ± MWh/yr | Plugs ± MWh/yr | Fans ± MWh/yr | Cool ± MWh/yr | Heat ± MWh/yr | Total Site ± MWh/yr | Intensity ± kWh/m$^2$ | Intensity ± kBtu/ft$^2$ |
|---|---|---|---|---|---|---|---|---|---|
| Floor Area | 120 m$^2$ | 5.0 | 7.7 | 1.3 | 2.4 | 2.5 | 18.9 | 6.6 | 2.1 |
| Aspect Ratio | 0.5 | 0.0 | 0.0 | 0.2 | 0.8 | 0.9 | 2.0 | 0.7 | 0.2 |
| Floor-to-Floor Height | 0.5 m | 0.0 | 0.0 | 4.5 | 4.6 | 6.2 | 15.3 | 5.3 | 1.7 |
| Plenum Height | 0.3 m | 0.0 | 0.0 | 1.0 | 1.1 | 0.2 | 2.3 | 0.8 | 0.3 |
| Perimeter Zone Depth | 1.0 m | 0.0 | 0.0 | 0.8 | 0.5 | 1.4 | 2.7 | 0.9 | 0.3 |
| Glazing Sill Height | 0.2 m | 0.0 | 0.0 | 0.0 | 0.0 | 0.0 | 0.1 | 0.0 | 0.0 |
| Glazing Fraction | 0.05 m | 0.0 | 0.0 | 2.8 | 3.6 | 3.3 | 9.7 | 3.4 | 1.1 |
| Receptacle Intensity | 0.75 m | 0.0 | 7.7 | 0.0 | 1.0 | 1.7 | 10.4 | 3.6 | 1.1 |
| Lighting Intensity | 2.0 W/m$^2$ | 18.3 | 0.0 | 0.2 | 2.5 | 3.7 | 24.7 | 8.6 | 2.7 |
| Occupant Density | 3 People/ 100 m$^2$ | 0.0 | 0.0 | 0.6 | 0.2 | 14.8 | 15.4 | 5.4 | 1.7 |
| Infiltration Rate | 0.4 ACH | 0.0 | 0.0 | 2.3 | 1.0 | 10.3 | 11.5 | 4.0 | 1.3 |
| Combination in Quadrature | | 18.9 | 10.9 | 6.1 | 7.1 | 20.0 | 50.3 | 17.5 | 5.5 |

**Table F-6 DSA of Uncertainty in Baseline Model Predictions: Annual Source Energy Use**

| Parameter | Input Error ± | Lights ± GJ/yr | Plugs ± GJ/yr | Fans ± GJ/yr | Cool ± GJ/yr | Heat ± GJ/yr | Total Source ± GJ/yr | Intensity ± MJ/m$^2$ | Intensity ± kBtu/ft$^2$ |
|---|---|---|---|---|---|---|---|---|---|
| Floor Area | 120 m$^2$ | 58.3 | 89.5 | 15.5 | 27.3 | 9.7 | 200.3 | 69.6 | 6.1 |
| Aspect Ratio | 0.5 | 0.0 | 0.0 | 2.6 | 9.6 | 3.6 | 15.8 | 5.5 | 0.5 |
| Floor-to-Floor Height | 0.5 m | 0.0 | 0.0 | 52.0 | 53.6 | 24.0 | 129.6 | 45.0 | 4.0 |
| Plenum Height | 0.3 m | 0.0 | 0.0 | 11.7 | 13.3 | 0.7 | 25.7 | 8.9 | 0.8 |
| Perimeter Zone Depth | 1.0 m | 0.0 | 0.0 | 9.6 | 5.8 | 5.3 | 20.7 | 7.2 | 0.6 |
| Glazing Sill Height | 0.2 m | 0.0 | 0.0 | 0.2 | 0.4 | 0.1 | 0.6 | 0.2 | 0.0 |
| Glazing Fraction | 0.05 m | 0.0 | 0.0 | 32.2 | 42.2 | 12.8 | 87.2 | 30.3 | 2.7 |
| Receptacle Intensity | 0.75 m | 0.0 | 89.5 | 0.2 | 11.5 | 6.6 | 107.7 | 37.4 | 3.3 |
| Lighting Intensity | 2.0 W/m$^2$ | 212.0 | 0.0 | 2.8 | 29.0 | 14.5 | 258.3 | 89.7 | 7.9 |
| Occupant Density | 3 People/ 100 m$^2$ | 0.0 | 0.0 | 6.6 | 2.3 | 57.4 | 66.4 | 23.0 | 2.0 |
| Infiltration Rate | 0.4 ACH | 0.0 | 0.0 | 26.3 | 11.3 | 39.7 | 77.4 | 26.9 | 2.4 |
| Combination in Quadrature | | 219.9 | 126.6 | 70.4 | 82.5 | 77.5 | 577.0 | 200.3 | 17.6 |

**Table F-7 DSA of Uncertainty in Baseline Model Predictions: Annual Energy Cost**

| Parameter | Input Error ± | Light ± $/yr | Plug ± $/yr | Fans ± $/yr | Cool ± $/yr | Heat ± $/yr | Demand ± $/yr | Total Site ± $/yr | Intensity ± $/m$^2$ | Intensity ± $/ft$^2$ |
|---|---|---|---|---|---|---|---|---|---|---|
| Floor Area | 120 m$^2$ | 233 | 332 | 61 | 120 | 112 | 543 | 1,401 | 0.49 | 0.05 |
| Aspect Ratio | 0.5 | 0 | 0 | 10 | 41 | 41 | 57 | 149 | 0.05 | 0.00 |
| Floor-to-Floor Height | 0.5 m | 0 | 0 | 199 | 232 | 279 | 478 | 1,187 | 0.41 | 0.04 |
| Plenum Height | 0.3 m | 0 | 0 | 46 | 56 | 8 | 125 | 219 | 0.08 | 0.01 |
| Perimeter Zone Depth | 1.0 m | 0 | 0 | 35 | 22 | 62 | 51 | 170 | 0.06 | 0.01 |
| Glazing Sill Height | 0.2 m | 0 | 0 | 1 | 1 | 1 | 1 | 3 | 0.00 | 0.00 |
| Glazing Fraction | 0.05 m | 0 | 0 | 121 | 177 | 149 | 301 | 748 | 0.26 | 0.02 |
| Receptacle Intensity | 0.75 W/m$^2$ | 0 | 332 | 1 | 46 | 76 | 202 | 504 | 0.17 | 0.02 |
| Lighting Intensity | 2.0 W/m$^2$ | 845 | 0 | 11 | 122 | 168 | 731 | 1,542 | 0.54 | 0.05 |
| Occupant Density | 3 People/ 100 m$^2$ | 0 | 0 | 26 | 19 | 667 | 123 | 835 | 0.29 | 0.03 |
| Infiltration Rate | 0.4 ACH | 0 | 0 | 99 | 21 | 461 | 194 | 733 | 0.25 | 0.02 |
| Combination in Quadrature | | 876 | 469 | 268 | 349 | 899 | 1,124 | 2,810 | 0.98 | 0.09 |

## F.4 Monte Carlo Analysis

For MCA, each input file has all the parameterized input varied according to the probability distribution for each input parameter. The number of separate simulations in MCA is independent of the number of input parameters with Lomas and Eppel (1992); adequate results can be obtained after 60 simulations. The full set of simulations was processed to compute mean results and standard deviations, *s*, for various metrics. Our findings supported using 60 simulations for MCA error analysis, but the results do not appear to be very sensitive to the selection of this number. The contributions of individual input parameters are combined and cannot be separated as in DSA. (MCA also provides mean results that warrant some attention as a possible alternative method of computing baseline performance.) Table F-8 lists results from MCA analysis for site energy use, Table F-9 lists results for source energy use, and Table F-10 lists results for energy cost.

**Table F-8 MCA of Uncertainty in Baseline Model Predictions: Annual Site Energy Use**

| | Lights MWh/yr | Plugs MWh/yr | Fans MWh/yr | Cool MWh/yr | Heat MWh/yr | Total Site MWh/yr | Intensity kWh/m$^2$ | Intensity kBtu/ft$^2$ |
|---|---|---|---|---|---|---|---|---|
| Average | 129 | 153 | 37 | 62 | 58 | 471 | 163.4 | 51.8 |
| ±2.3 *s* | 26.9 | 9.2 | 8.1 | 7.2 | 26.8 | 63.0 | 21.9 | 6.9 |
| ±% | 20.8 | 6.0 | 21.7 | 11.6 | 46.4 | 13.4 | 13.4 | 13.4 |

**Table F-9 MCA of Uncertainty in Baseline Model Predictions: Annual Source Energy Use**

| | Lights GJ/yr | Plugs ± GJ/yr | Fans ± GJ/yr | Cool ± GJ/yr | Heat ± GJ/yr | Total Source ± GJ/yr | Intensity ± MJ/m$^2$ | Intensity ± kBtu/ft$^2$ |
|---|---|---|---|---|---|---|---|---|
| Average | 1,503 | 1,779 | 435 | 723 | 224 | 5,019 | 1,743 | 154 |
| ±2.3 *s* | 312 | 107 | 95 | 84 | 104 | 524 | 182 | 16 |
| ±% | 20.8 | 6.0 | 21.7 | 11.6 | 46.4 | 10.4 | 10.4 | 10.4 |

**Table F-10 MCA of Uncertainty in Baseline Model Predictions: Annual Energy Cost**

| | Lights $/yr | Plugs $/yr | Fans $/yr | Cool $/yr | Heat $/yr | Demand $/yr | Total Site $/yr | Intensity $/m$^2$ | Intensity $/ft$^2$ |
|---|---|---|---|---|---|---|---|---|---|
| Average | 5,870 | 6,597 | 1,691 | 3,150 | 2,594 | 13,551 | 34,802 | 12.1 | 1.12 |
| ±2.3 *s* | 1,243 | 396 | 356 | 374 | 1,204 | 1,531 | 4,294 | 1.5 | 0.14 |
| ±% | 21.2 | 6.0 | 21.1 | 11.9 | 46.4 | 11.3 | 12.3 | 12.3 | 2.3 |

## F.5 Weather Data Sensitivity

Weather data are handled separately from the other model input data because of fundamental differences in how the data are entered and used in the simulation program. Weather data were measured by instruments situated on top of the building, so many of the usual problems with weather data in energy modeling are avoided. (Weather stations are often located at airports far from building sites and have differing microclimates.) However, measurement inaccuracies and modeling/processing of the data, especially sky models and cloud cover estimates, lead to uncertainties in the data. The three baseline geometries were repeated with both the high and low versions of the weather file in a separate differential sensitivity exercise. The simpler method of using high and low weather files was selected because a more rigorous application of DSA and/or MCA to perturb individual elements of the time series data would be too involved.

The results were processed to show the errors associated with weather for different end uses. Table F-11 shows the uncertainty in site energy, Table F-12 shows the uncertainty in source energy, and Table F-13

shows the uncertainty in energy cost associated with the upper and lower bounds on weather data. Except for the solar neutral baseline with aspect ratio 1.0, the models were each run at four different cardinal rotations and three different weather files to determine the errors listed in these tables. The results from the three baseline geometries were combined by taking the largest to determine a final estimate of the error associated with inaccuracies in the weather data.

**Table F-11 Weather Data Error Analysis for Baseline Energy Model Results for Site Energy**

| Baseline Geometry | Fans ± MWh/yr | Cooling ± MWh/yr | Heating ± MWh/yr | Total Site ± MWh/y | Intensity ± kWh/ $m^2$·yr | Intensity ± kBtu/ $ft^2$·yr |
|---|---|---|---|---|---|---|
| Aspect Ratio 1.0 | 0.7 | 16.9 | 17.8 | 4.6 | 1.6 | 0.5 |
| Aspect Ratio 4.4 | 0.8 | 20.3 | 20.9 | 5.4 | 1.9 | 0.6 |
| Same as As-Built | 0 | 14.9 | 16.6 | 2.4 | 0.9 | 0.2 |
| Max | 0.8 | 20.3 | 20.9 | 5.4 | 1.9 | 0.6 |

**Table F-12 Weather Data Error Analysis for Baseline Energy Model Results for Source Energy**

| Baseline Geometry | Fans ± GJ/yr | Cooling ± GJ/yr | Heating ± GJ/yr | Total Source ± GJ/y | Intensity ± MJ/ $m^2$·yr | Intensity ± kBtu/ $ft^2$·yr |
|---|---|---|---|---|---|---|
| Aspect Ratio 1.0 | 49.5 | 265.8 | 61.7 | 248.7 | 86.4 | 7.6 |
| Aspect Ratio 4.4 | 9.8 | 235.6 | 81.0 | 157.4 | 54.7 | 4.8 |
| Same as As-Built | 0 | 172.5 | 64.0 | 108.5 | 37.5 | 3.5 |
| Max | 49.5 | 265.8 | 61.7 | 248.7 | 86.4 | 7.6 |

**Table F-13 Weather Data Error Analysis for Baseline Energy Model Results for Energy Costs**

| Baseline Geometry | Fans ± $/yr | Cooling ± $/yr | Heating ± $/yr | Demand Charges ± $/yr | Total Site ± $/yr | Intensity ± $/$m^2$·yr | Intensity ± $/$ft^2$·yr |
|---|---|---|---|---|---|---|---|
| Aspect Ratio 1.0 | 25.0 | 784.0 | 798.5 | 560.0 | 559.5 | 0.2 | 0.02 |
| Aspect Ratio 4.4 | 32.3 | 944.0 | 940.0 | 685.0 | 703.8 | 0.2 | 0.02 |
| Same as As-Built | 0 | 751.5 | 742.5 | 1082.5 | 1091.5 | 0.35 | 0.04 |
| Max | 32.3 | 944.0 | 940.0 | 1082.5 | 1091.5 | 0.35 | 0.04 |

## F.6 Overall Uncertainty Estimate

An overall assessment of the accuracy of baseline predictions is made by combining the separate sources of error. DSA and MCA are separate methods of determining the contributions of the same sources of input error, so these errors are not added together. Because MCA captures the interactions between deviations in model input parameters, it is considered more rigorous. However, were DSA to predict a higher combined uncertainty, it would be appropriate to use that instead of the result from MCA. Therefore, the methodology adopted here is to use the higher of the results from MCA and DSA to account for uncertainty in input data. Although MCA errors are usually higher, some of the errors in

overall source energy are higher from DSA. Errors associated with weather were also determined in a separate analysis and are considered independent. Finally, there is the contribution of uncertainty associated with the selection of building geometry (as-built or box with different aspect ratios). The mean of results from the three baseline geometries was determined to arrive at error estimates associated with the selection of baseline geometry (see Table F-11, Table F-12, and Table F-13).

Table F-14 lists the overall error estimates for model predictions of site energy use. Table F-15 lists the overall error estimates for source energy use. Table F-16 lists them for energy cost. The final estimates are determined by adding in quadrature the results for uncertainty from (1) DSA or MCA, (2) shape of the baseline building, and (3) weather data.

**Table F-14 Overall Error Analysis for Baseline Energy Model Results for Site Energy Use**

| Contribution to Error | Fans ± MWh/yr | Cooling ± MWh/yr | Heating ± MWh/yr | Total Site ± MWh/y | Intensity ± kWh/ $m^2$·yr | Intensity ± kBtu/ $ft^2$·yr |
|---|---|---|---|---|---|---|
| DSA | 6.1 | 7.1 | 20.0 | 50.3 | 17.5 | 5.5 |
| MCA | 8.1 | 7.2 | 26.8 | 63.0 | 21.9 | 6.9 |
| Max [DSA,MCA] | 8.1 | 7.2 | 26.8 | 63.0 | 21.9 | 6.9 |
| Weather | 0.8 | 20.3 | 20.9 | 5.4 | 1.9 | 0.6 |
| Geometry | 4.3 | 0.1 | 0.0 | 13.6 | 6.7 | 4.3 |
| Combination in Quadrature | 9.2 | 21.5 | 34.0 | 64.7 | 23.0 | 8.1 |

**Table F-15 Overall Error Analysis for Baseline Energy Model Results for Source Energy Use**

| Contribution to Error | Fans ± GJ/yr | Cooling ± GJ/yr | Heating ± GJ/yr | Total Source ± GJ/y | Intensity ± MJ/ $m^2$·yr | Intensity ± kBtu/ $ft^2$·yr |
|---|---|---|---|---|---|---|
| DSA | 70.4 | 82.5 | 77.5 | 577.0 | 200.3 | 17.6 |
| MCA | 95.0 | 84.0 | 104.0 | 524.0 | 182.0 | 16.0 |
| Max (DSA,MCA) | 95.0 | 84.0 | 104.0 | 577.0 | 200.3 | 17.6 |
| Weather | 49.5 | 265.8 | 61.7 | 248.7 | 86.4 | 7.6 |
| Geometry | 158.0 | 78.0 | 16.5 | 182.5 | 63.5 | 5.5 |
| Combination in Quadrature | 190.9 | 289.5 | 122.0 | 654.3 | 227.2 | 19.9 |

**Table F-16 Overall Error Analysis for Baseline Energy Model Results for Energy Costs**

| Contribution to Error | Fans ± $/yr | Cooling ± $/yr | Heating ± $/yr | Demand Charges ± $/yr | Total Site ± $/yr | Intensity ± $/m$^2$·yr | Intensity ± $/ft$^2$·yr |
|---|---|---|---|---|---|---|---|
| DSA | 268.0 | 349.0 | 899.0 | 1,124.0 | 2,810.0 | 0.98 | 0.09 |
| MCA | 356.0 | 374.0 | 1,204.0 | 1,531.0 | 4,294.0 | 1.5 | 0.14 |
| Max [DSA,MCA] | 356.0 | 374.0 | 1,204.0 | 1,531.0 | 4,294.0 | 1.5 | 0.14 |
| Weather | 32.3 | 944.0 | 940.0 | 1,082.5 | 1,091.5 | 0.35 | 0.04 |
| Geometry | 644.0 | 421.5 | 189.5 | 1,877.5 | 2,703.0 | 1.0 | 0.1 |
| Combination in Quadrature | 736.6 | 1,099.4 | 1,539.2 | 2,653.4 | 5,190.0 | 1.8 | 0.2 |

## Appendix G List of People Involved in Project

*Contracting Party:*
Geoff Oxnam
The Chesapeake Bay Foundation
Annapolis, MD

*General Contractor:*
Clark Construction Group
Bethesda, MD

*Mechanical Engineer:*
SmithGroup, Inc.
Washington, DC

*Building Control Systems:*
Siemens

*Postoccupancy Evaluation Team:*
National Renewable Energy Laboratory
Contact: Paul Torcellini
Golden, CO

*Building Operator:*
Roger Perry
The Chesapeake Bay Foundation
Annapolis, MD

*Structural Engineer:*
Shemro Engineering, Inc.
Bethesda, MD

*Architects/Engineers:*
Greg Mella
SmithGroup, Inc.
Washington, DC

*Landscape Architects:*
Karen Motivans
Shepherdstown, WV

*Civil Engineer:*
Greenman-Pedersen, Inc.
Laurel, MD

*LEED Coordinator:*
Janet Harrison
Annapolis, MD

# REPORT DOCUMENTATION PAGE

*Form Approved*
*OMB No. 0704-0188*



**PLEASE DO NOT RETURN YOUR FORM TO THE ABOVE ORGANIZATION.**

| 1. REPORT DATE *(DD-MM-YYYY)* | 2. REPORT TYPE | 3. DATES COVERED *(From - To)* |
|---|---|---|
| April 2005 | Technical Report | |

**4. TITLE AND SUBTITLE**
Analysis of the Energy Performance of the Chesapeake Bay Foundation's Philip Merrill Environmental Center

**5a. CONTRACT NUMBER**
DE-AC36-99-GO10337

**5b. GRANT NUMBER**

**5c. PROGRAM ELEMENT NUMBER**

**6. AUTHOR(S)**
B. Griffith, M. Deru, P. Torcellini, and P. Ellis

**5d. PROJECT NUMBER**
NREL/TP-550-34830

**5e. TASK NUMBER**
BEC3.1001

**5f. WORK UNIT NUMBER**

**7. PERFORMING ORGANIZATION NAME(S) AND ADDRESS(ES)**
National Renewable Energy Laboratory
1617 Cole Blvd.
Golden, CO 80401-3393

**8. PERFORMING ORGANIZATION REPORT NUMBER**
NREL/TP-550-34830

**9. SPONSORING/MONITORING AGENCY NAME(S) AND ADDRESS(ES)**

**10. SPONSOR/MONITOR'S ACRONYM(S)**
NREL

**11. SPONSORING/MONITORING AGENCY REPORT NUMBER**

**12. DISTRIBUTION AVAILABILITY STATEMENT**
National Technical Information Service
U.S. Department of Commerce
5285 Port Royal Road
Springfield, VA 22161

**13. SUPPLEMENTARY NOTES**

**14. ABSTRACT** *(Maximum 200 Words)*

The Chesapeake Bay Foundation designed their new headquarters building to minimize its environmental impact on the already highly polluted Chesapeake Bay by incorporating numerous high-performance energy saving features into the building design. CBF then contacted NREL to perform a nonbiased energy evaluation of the building. Because their building attracted much attention in the sustainable design community, an unbiased evaluation was necessary to help designers replicate successes and identify and correct problem areas. This report focuses on NREL's monitoring and analysis of the overall energy performance of the building.

**15. SUBJECT TERMS**
Chesapeake Bay; Chesapeake Bay Foundation; Philip Merrill Environmental Center; high-performance buildings; high performance; sustainable design; energy performance evaluation; energy analysis.

| 16. SECURITY CLASSIFICATION OF: | | | 17. LIMITATION OF ABSTRACT | 18. NUMBER OF PAGES | 19a. NAME OF RESPONSIBLE PERSON |
|---|---|---|---|---|---|
| a. REPORT | b. ABSTRACT | c. THIS PAGE | | | 19b. TELEPONE NUMBER (*Include area code)* |
| Unclassified | Unclassified | Unclassified | UL | | |